Slovenian Veterinary Research

Slovenski veterinarski zbornik

THE SCIENTIFIC JOURNAL OF THE VETERINARY FACULTY UNIVERSITY OF LJUBLJANA

ISSN 1580-4003

Slov Vet Res, Ljubljana, 2024, Volume 61, Number 4, Pages 221–306

Slovenian Veterinary Research

Slovenski veterinarski zbornik

THE SCIENTIFIC JOURNAL OF THE VETERINARY FACULTY UNIVERSITY OF LJUBLJANA

Volume 61, Number 4, Pages 221–306

The Scientific Journal of the Veterinary Faculty University of Ljubljana

Slovenian Veterinary Research

Slovenski veterinarski zbornik

Previously: RESEARCH REPORTS OF THE VETERINARY FACULTY UNIVERSITY OF LJUBLJANA
Prej: ZBORNIK VETERINARSKE FAKULTETE UNIVERZA V LJUBLJANI

4 issues per year / Izhaja štirikrat letno
Volume 61, Number 3 / Letnik 61, Številka 4

Published by / Založila	University of Ljubljana Press / Založba Univerze v Ljubljani
For the Publisher / Za založbo	Gregor Majdič, Rector of the University of Ljubljana / Rektor Univerze v Ljubljani
Issued by / Izdala	Veterinary Faculty University of Ljubljana / Veterinarska fakulteta Univerze v Ljubljani
For the Issuer / Za izdajatelja	Breda Jakovac Strajn, Dean of the Veterinary Faculty / Dekanja Veterinarske fakultete
Address	Veterinary Faculty, Gerbičeva 60, 1000 Ljubljana, Slovenia
Naslov	Veterinarska fakulteta, Gerbičeva 60, 1000 Ljubljana, Slovenija
Phone / Telefon	+386 (0)1 4779 100
E-mail	slovetres@vf.uni-lj.si
Sponsored by / Sofinancira	The Slovenian Research Agency / Javna agencija za raziskovalno dejavnost Republike Slovenije
Printed by / Tisk	DZS, d.d., Ljubljana, December/December 2024
Number of copies printed / Naklada	220
Indexed in / Indeksirano v	Agris, Biomedicina Slovenica, CAB Abstracts, IVSI Urlich's International Periodicals Directory, Science Citation Index Expanded, Journal Citation Reports – Science Edition
	https://www.slovetres.si/
	ISSN 1580-4003 2385-8761 (on-line)

The cover illustration by Pšenica Kovačič highlights how vulture feeding areas are frequently shared with corvids, which are particularly vulnerable to West Nile Virus. This artwork is inspired by the manuscript by Loureiro et al., featured in this issue, which reviews West Nile Virus in vultures across Europe.

Table of Content

Slov Vet Res
DOI 10.26873/SVR-2167-2024
UDC 303.446.3:355.233.1:611:66-089.853:636.09
Pages: 225–32

Teaching of Anatomy: Dissecting Dissection in Veterinary and Medical Education From a Historical Perspective Through to Today

Poučevanje anatomije: seciranje potrebe po sekciji v veterinarskem in medicinskem izobraževanju z zgodovinskega vidika do danes

Key words

anatomy;
dissection;
methodology;
syllabus;
technology

Accepted: 23 December 2024

Valentina Kubale[1]*, William Perez[2], Catrin S. Rutland[3]

[1]Veterinary faculty, University of Ljubljana, Slovenia, [2]National Research System and PEDECIBA, Montevideo, Urugvaj, [3]School of Veterinary Medicine and Science, University of Nottingham, Nottingham, United Kingdom. LE12 5RD

Co-Editor, Slovenian Veterinary Research, valentina.kubaledvojmoc@vf.uni-lj.si

As veterinary and human medicine education evolves, instructors can now incorporate a range of innovative anatomy tools, from low-fidelity models to high-fidelity simulators, 3D printing, dissection software, and augmented/virtual reality. However, cadaveric dissection in line with ethical animal use, guided by the 4Rs: replacement, reduction, refinement, and responsibility; still remains an important and critical teaching strategy. Dissection is the methodical isolation of the various parts of the cadaver to study their physical characteristics (colour, consistency, weight, dimensions, shape), location, and structure, as well as their irrigation and innervation. It enables a deeper understanding of anatomical structures through practical work. As a synonym of anatomy, dissection remains the main method to study, understand and research the body in veterinary and human medicine education. Students learn the key skills and core knowledge necessary for subsequent clinical work, including clinical examination, necropsies, and surgery. They also acquire the manual dexterity, pre-surgical techniques, and confidence vital for their future work. This paper investigates the advantages and disadvantages of using dissection and explores the contemporary, and often complimentary, methods used to teach anatomy. We should clarify that this discussion is about the dissection of

Z razvojem izobraževanja na področju veterinarske in humane medicine imajo asistenti in profesorji anatomije na voljo vedno več inovativnih orodij za poučevanje anatomije, od osnovnih modelov in naprednih simulatorjev do 3D-tiska, programske opreme za virtualno sekcijo ter navidezno in obogateno resničnost. Kljub tem napredkom pa disekcija kadavrov – izvedena v skladu z načeli etične uporabe živali, ki jih opredeljuje načelo 4R: zamenjava, zmanjšanje, izboljšanje in odgovornost – ostaja ključna in nepogrešljiva metoda poučevanja. Disekcija omogoča metodično preučevanje struktur telesa, vključno s preučevanjem njegovih fizičnih lastnosti, kot so barva, konsistenca, teža, mere, oblika in lokacija. Poleg tega razkriva njegovo strukturo, ožiljenost in inervacijo ter s tem omogoča poglobljeno razumevanje anatomskih struktur skozi praktično delo. Ta praktični pristop študentom ponuja poglobljeno razumevanje anatomskih značilnosti in razvija veščine, ki so nujne za nadaljnje klinično delo, skupaj s preiskavami, obdukcijami in kirurškimi posegi. Poleg tega disekcija prispeva k razvoju ročnih spretnosti, predkirurških tehnik in samozavesti, ki so bistvene za prihodnjo poklicno pot študentov. Članek analizira prednosti in izzive disekcije ter raziskuje sodobne, pogosto neinvazivne alternative za poučevanje anatomije. Pomembno je poudariti, da se razprava osredotoča na seciranje kadavrov in s tem povezane etične vidike, ne pa na

cadavers (including the associated ethical considerations), rather than the largely outdated practice of vivisection.

The history of dissection, in teaching and researching anatomy and medicine, spans millennia. In ancient Mesopotamia, often called the 'oldest known cradle of civilization', rudimentary animal dissections were performed and observations were made from human wounds, these helped form words for internal anatomical structures such as blood vessels (1). Mesopotamian clay liver models dating back to 2000 BC still survive today (2). We also know that in ancient Egypt (circa 3000 BC), embalmers had developed detailed knowledge of human anatomy, but this was initially more for religious than medical purposes (3). There is no doubt that by 1850 BC this work had accumulated into rigorous medical and scientific knowledge regarding anatomy, surgery, medicine, disease and healing. Much knowledge was gained during this time about the cardiovascular and reproductive systems, the brain, and even tumours (3). This work continued and Aristotle (384–322 BCE) and Erasistratus (304–258 BCE) were known to be dissecting animals to understand anatomy and physiology (4). Systematic human dissection was also recorded to be in use in the 3rd century BC by the Greek anatomists Herophilus and Erasistratus in Alexandria (Egypt) (5). Dissection has gone through many complex cultural taboos, during these times animal dissection was often permitted, with Greek anatomists and physicians such as Hippocrates (460–370 BCE) and Galen (129–216 CE) gaining anatomical knowledge through this practice (6, 7). During the Medieval period in Europe dissection was culturally taboo however Islamic physician Avicenna (980–1037 CE) from Percia, and Al-Zahrawi (936–1013 CE) an Arab surgeon, amongst others continued to add to the wealth of knowledge known about the body during the 'Golden Age of Islam' (8, 9). During the 14th–17th centuries, there was a resurgence of acceptance in the practice of dissection in Europe, yet the centuries to follow had several times of turmoil due to religious beliefs, laws and unethical practices (10). Despite this, dissection was one of the primary methods to teach anatomy (11, 12).

Detailed and meticulous dissection requires patience and time, as well as the motivation and knowledge necessary to perform it, and is therefore a rigorous and active method of study. Animals are three-dimensional beings, and it is in dissection that students build up their ideas and mental images of the structures of the animal body, a process that is carried out gradually with experience. Another objective of dissection is to introduce the concept of biological, specific, and interspecific variability. In anatomy, variability is a constant, there are variations between individuals, and those caused by age, physiological state, sex, breed, disease, injury, and other factors. An additional benefit of anatomical dissection in teaching is that cadavers can also be reused in many cases for other uses. These may include using components towards research projects both at undergraduate levels and beyond – another method of teaching widely used to support anatomical teaching (13). The

vivisekcijo, ki je v današnjem času že večinoma opuščena praksa.

Disekcija kot metoda za preučevanje anatomije in medicine ima večtisočletno zgodovino. V starodavni Mezopotamiji, poznani kot »zibelka civilizacije«, so izvajali preproste disekcije živali in opazovali človeške rane, kar je privedlo do prvega oblikovanja terminologije za notranje anatomske strukture, vključno s krvnimi žilami (1). Ohranjeni glineni modeli jeter iz Mezopotamije, ki datirajo v leto 2000 pr. n. št., pričajo o zgodnjih prizadevanjih za razumevanje anatomije in so se ohranili do danes (2). V starem Egiptu (približno 3000 pr. n. št.) so balzamerji razvili podrobno znanje o človeški anatomiji, ki je bilo sprva povezano z verskimi obredi. Do leta 1850 pr. n. št. je to znanje postalo pomemben del medicinskega in znanstvenega razumevanja anatomije, kirurgije, bolezni in zdravljenja. Takrat so že poznali osnovne koncepte kardiovaskularnega in reproduktivnega sistema, možganov ter celo tumorjev (3). Zgodovinski zapisi kažejo, da sta Aristotel (384–322 pr. n. št.) in Erasistrat (304–258 pr. n. št.) secirala živali za razumevanje anatomije in fiziologije (4). V 3. stoletju pr. n. št. sta grška anatoma Herofil in Erasistrat v Aleksandriji izvajala sistematično disekcijo človeških trupel (5). Čeprav je disekcija pogosto naletela na kulturne in verske tabuje, je bil njen pomen v raziskovanju anatomije neizpodbiten. V grški tradiciji so zdravniki, kot sta Hipokrat (460–370 pr. n. št.) in Galen (129–216 n. št.), anatomska spoznanja pridobivali predvsem z disekcijo živali (6, 7). Medtem ko so disekcijo v srednjeveški Evropi kulturno in versko zavračali, sta islamska učenjaka Avicenna (980–1037 n. št.) in Al-Zahrawi (936–1013 n. št.) v »zlati dobi islama« znatno prispevala k razvoju anatomskega znanja (8, 9). V obdobju renesanse, od 14. do 17. stoletja, je disekcija ponovno postala sprejeta v Evropi, čeprav so verska prepričanja, zakonske omejitve in etični pomisleki še dolgo vplivali na njeno izvajanje (10). Kljub zgodovinskim izzivom je disekcija vse do danes ostala ena ključnih metod poučevanja anatomije, saj je temelj za razumevanje človeškega telesa in njegovo raziskovanje (11, 12).

Natančna izvedba disekcije zahteva potrpežljivost, čas, motivacijo in ustrezno znanje, kar jo uvršča med temeljite, dosledne in aktivne metode študija. Živali so tridimenzionalna bitja, zato študentje skozi proces disekcije postopoma gradijo svoje miselne podobe in razumevanje struktur živalskega telesa, kar je proces, ki se razvija z izkušnjami. Disekcija ima tudi pomembno vlogo pri uvajanju koncepta biološke, specifične in medvrstne raznolikosti. V anatomiji je spremenljivost stalnica, ker so anatomske razlike prisotne tako med posamezniki, po drugi strani pa jih povzročajo dejavniki, kot so starost, spol, pasma, fiziološko stanje, bolezni, poškodbe in drugi. Dodatna prednost anatomske disekcije kot metode pri poučevanju je njena vsestranskost, saj je kadavre mogoče pogosto uporabiti tudi za druge namene, na primer pri raziskovalnih projektih na dodiplomski ali podiplomski ravni (13). Poleg tega omogočajo pripravo vsebin za dodatna učna orodja, kot so fotografije, rentgenski posnetki, računalniška tomografija (CT), ultrazvok, magnetna

cadavers used for dissection may be used (before or after) to create opportunities for creating content for complimentary teaching tools. For example, taking photographs, conducting X-rays, computed tomography (CT), ultrasound, and magnetic resonance imaging (MRI) scans, creating prosections (observation of dissection or prepared preparations), developing models including 3D printing, and making histology and histopathology slides (14). These in turn can be used to develop multimedia, virtual and physical museums and in addition to content for reference textbooks and research papers and student assignments. The cadavers used in dissection also often provide valuable opportunities to help create images and tissues in preparation for student practical examinations to test knowledge gained. Although many of these tools are relatively new, we know models for example, as well as dissection, have been used for centuries. Anna Morandi Manzolini (1714-74) was selling her wax models based upon her dissections throughout the world (15). Ultimately, these tools can be used alongside dissection to create a more clinically integrated curriculum, which has proved to be a popular with learners (16-18).

Dissection involves the meticulous work of removing the connective tissue that surrounds the various structures and organs and involves gradually uncovering the structures that make up each region of the body and their relationships, all of which are lost with virtual anatomy or the use of anatomical models. Some may argue that this approach takes more time, with less time often given when teaching using non-dissection techniques (19). Another relevant topic acquired in the dissection room is the varied interactions with the student. Educators in the dissection room teach students how to communicate effectively, access information, interact with their peers and learn teamwork, which may additionally help students manage the stress of college/university, especially in the early years. These interactions may also provide enjoyable collaboration times for students, and provides a hands-on approach to learning anatomy (20). It should be noted that integrated teaching using prosections and other teaching tools can also be teacher led and include collaborative and teacher-learner interaction time. For example, in a spiral curriculum investigating both dissection and prosection teaching, alongside clinical skills, students overwhelmingly valued and enjoyed both dissection and prosection learning (20, 21). Importantly these students also reported motivation to learn anatomy in this system and appreciated linking clinical aspects to anatomical learning.

Given the benefits and long history of anatomical dissection for medical and scientific courses (22), what are the challenges facing anatomists in the use of this technique? Many universities and colleges, and of course our students and the public, consider the ethics behind using cadavers. Universities choose to invest time and money into collecting cadavers in the most ethical manner, with all required permits and with owner consent. This may be via body donation programmes or via local clinics, shelters, zoos and

resonanca (MR), pripravo histoloških ali histopatoloških preparatov, prosekcijo (opazovanje disekcije ali že pripravljenih preparatov) in tudi razvoj modelov za 3D-tiskanje (14). Hkrati so materiali uporabni še za izdelavo multimedijskih, virtualnih in klasičnih muzejev ter služijo kot dopolnitev referenčnim učbenikom, raziskovalnim nalogam in študentskim projektom. Kadavri, uporabljeni pri disekciji, so pogosto ključni za pripravo praktičnih delov študentskih izpitov, saj nudijo priložnosti za ustvarjanje slikovnega gradiva in tkiv ter kot taki služijo za preverjanje pridobljenega znanja. Medtem ko so sodobna učna orodja relativno nova, je uporaba modelov, prav tako kot sekcije, v anatomiji dolgotrajna tradicija. Na primer, Anna Morandi Manzolini (1714–1774) je ustvarjala in prodajala natančne voščene anatomske modele, izdelane na podlagi svojih disekcij, kar je pripomoglo k razvoju poučevanja anatomije po vsem svetu (15). Sodobno poučevanje anatomije vse bolj vključuje uporabo različnih učnih orodij v kombinaciji z disekcijo, kar omogoča razvoj kurikuluma predmeta in tako dodatno vključuje še klinični pomen poznavanja anatomije. Pristop, ki povezuje praktično delo z razumevanjem kliničnih primerov, je med študenti izjemno priljubljen in se je izkazal za zelo učinkovitega pri krepitvi znanja in veščin, za katere želimo, da jih študenti osvojijo (16–18).

Disekcija zahteva natančno odstranjevanje vezivnega tkiva, ki obdaja različne strukture in organe, ter omogoča postopno odkrivanje anatomskih struktur in njihovih medsebojnih povezav. Te ključne informacije se pri uporabi virtualne anatomije ali anatomskih modelov pogosto izgubijo. Čeprav nekateri trdijo, da poučevanje z alternativnimi metodami brez disekcije zahteva manj časa, je pri teh tehnikah pogosto zanemarjena poglobljena obravnava anatomskih odnosov med strukturami (19). Poleg spoznavanja anatomskih struktur disekcija omogoča raznolike interakcije med študenti in predavatelji. V secirnici se študenti naučijo učinkovite komunikacije, dostopanja do informacij in sodelovanja z vrstniki, timskega dela, kar jim lahko pomaga pri obvladovanju stresa, zlasti v zgodnjih letih študija. Te interakcije ponujajo tudi priložnost za prijetnejše sodelovanje in praktičen pristop k učenju anatomije (20). Celostno poučevanje, ki vključuje disekcijo, prosekcije in druge učne metode, ustvarja prostor za sodelovanje in interakcijo med učitelji in študenti. Na primer, t. i. spiralni kurikulum, ki združuje disekcijo, prosekcije in osnove osvajanja kliničnih veščin, je med študenti izjemno cenjen. Študenti poročajo o večji motivaciji za učenje anatomije, saj pristop učinkovito povezuje anatomsko izobraževanje s kliničnimi primeri (20, 21). Disekcija tako ostaja nepogrešljivo orodje za poglobljeno razumevanje anatomije, ker ponuja ne le tehnične in klinične veščine, temveč tudi pomembne izkušnje sodelovanja, komunikacije in praktičnega učenja.

Kaj so številni izzivi kljub dolgi tradiciji in mnogoterim prednostim anatomske disekcije za medicinska in znanstvena izobraževanja (22), s katerimi se anatomi soočamo pri uporabi te tehnike? Eden ključnih izzivov, s katerim se sooča veliko univerz in fakultet, je obravnava etičnosti uporabe kadavrov, kar vključuje spoštovanje do lastnikov, ki svoje živali darujejo,

farmers. This ensures animals are not bred or euthanised specifically for dissection. It also helps students, and the public, understand that ethical routes are used to procure cadavers. These ethical considerations are often discussed openly with students and accreditation boards, and cadaver use policies are often formed following consultations with stakeholders. It is also widely recognised that anatomical dissection can be expensive. It takes academic and technical time to prepare specimens, teach the classes, prepare examinations and manage the specimens. Naturally there is also a cost to the specialist equipment and space needed to conduct these classes (including chemicals, refrigeration, tables, lighting, instruments, room ventilation, health and safety consumables and equipment, owning appropriate transport). It should be noted that alternative methods of teaching also require time, teachers and money, but possible at a lower cost due to their reuse and sharing of multimedia resources between universities. Increasingly health and safety laws and local rules look at the use of chemicals such as commonly used fixatives. Monitoring and adhering to these regulations, and adapting to new regulations, can require specialist equipment, time, changes in practice and complexities in finding appropriate chemicals. Implementing these all have cost and time implications of course, but also require the skills to navigate new laws and regulations. These regulations are all designed to maximise health and safety of all technicians, academics and of course students, in addition to any others potentially impacted such as housekeeping staff. Frequently universities provide occupational health to support staff frequently working in these areas too. It should also be noted that whilst students often report the value of dissection classes and may benefit from time working together and with teachers, this learning style may in itself be stressful for some students (23). While students may find anatomical dissection challenging, there is limited research comparing their experiences in clinical situations when dissection has not been part of their university training.

Dissection of cadavers has been used in human and veterinary medical education since the 16th century and was documented to be in use for research well before this (14, 24, 25). However, since the 1980's, some universities reduced or even ceased using this form of teaching (10, 26). Interestingly, many of the medical schools that ceased dissection reinstated it following research into decreasing pedagogical skills and a negative impact on surgical skills resulting in reduced patient safety (10, 27-29). Others increased the levels of dissection teaching in postgraduate courses to compensate for reductions at an undergraduate level (29, 30), but notably this was reported in human medicine. This difference is essential as veterinary medicine graduates do not enter a period of compulsory supervised post-graduate study, therefore these vital skills must be achieved within the undergraduate curriculum. Many schools offering modern curricula have integrated dissection within clinical contexts and settings, and have added complimentary techniques, as opposed to anatomy and

in transparentnost pri pridobivanju vzorcev. Univerze vlagajo čas in sredstva v zagotavljanje, da so kadavri pridobljeni na etičen način, z vsemi dovoljenji in izrecnim soglasjem lastnika. Takšna darovanja kadavrov ter sodelovanje z lokalnimi klinikami, zavetišči, živalskimi vrtovi in kmeti zagotavljajo, da živali niso vzrejene ali evtanazirane izključno za disekcijo. Take etične prakse študentom in javnosti pomagajo razumeti pomen odgovornega pridobivanja kadavrov, hkrati pa so pogosto predmet odprtih razprav z različnimi komisijami, akreditacijskimi odbori in drugimi zainteresiranimi stranmi. Oblikujejo se politike uporabe kadavrov, ki temeljijo na posvetovanjih in transparentnosti. Številne univerze in visoke šole ter seveda naši študenti in javnost upoštevajo etičnost uporabe kadavrov. Drug pomemben izziv so visoki stroški anatomske disekcije. Priprava vzorcev, organizacija predavanj, praktičnih vaj in izpitov zahtevata znaten akademski in tehnični čas. Prav tako so potrebne finance, povezane z nabavo specializirane opreme in infrastrukture, vključno s kemikalijami, hlajenjem, razsvetljavo, mizami, orodji, prezračevalnimi sistemi in varnostno opremo. Poleg tega zakonodaja o zdravju in varnosti, skupaj z lokalnimi predpisi, ureja uporabo fiksativov, kar lahko povzroči dodatne stroške in potrebo po prilagoditvah v praksi. Prilagajanje tem regulacijam zahteva čas, opremo in spretnosti, vendar so ti predpisi namenjeni zagotavljanju zdravja in varnosti za vse vpletene – od tehnikov in asistentov, profesorjev do študentov in drugega sodelujočega podpornega osebja. Mnogo univerz zagotavlja tudi dodatno zdravstveno podporo osebju, ki redno dela v takšnih okoljih. Kljub številnim prednostim disekcije nekateri študenti poročajo, da je ta metoda učenja lahko stresna (23). Čeprav se študentom anatomska disekcija včasih zdi zahtevna, obstaja le malo raziskav, ki bi primerjale njihove izkušnje v klinični praksi z izkušnjami tistih, ki med univerzitetnim izobraževanjem niso opravljali disekcije.

Disekcija kadavrov se v humani in veterinarski medicinski izobrazbi uporablja že od 16. stoletja, njena uporaba v raziskovalne namene pa je dokumentirana že veliko prej (14, 24, 25). Vendar pa so v osemdesetih letih prejšnjega stoletja nekatere univerze zmanjšale ali celo prenehale uporabljati to obliko poučevanja (10, 26). Zanimivo je, da so številne medicinske šole, ki so opustile to metodo, ponovno uvedle disekcijo po ugotovitvah raziskav, ki so pokazale negativne posledice za poznavanje anatomije in kasneje za sposobnost izvajanja kirurških postopkov, saj je pomanjkanje praktičnih veščin vplivalo na varnost pacientov (10, 27–29). Nekatere institucije so povečale obseg poučevanja z uporabo disekcije na ravni podiplomskega izobraževanja, da bi nadomestile zmanjšan obseg na ravni dodiplomskega izobraževanja (29, 30). Ta pristop je bil pogostejši v humani medicini, kjer diplomanti po zaključenem dodiplomskem izobraževanju vstopajo v obvezna obdobja nadzorovanega podiplomskega študija. Veterinarska medicina pa tega ne predvideva, zato morajo študenti ključne veščine pridobiti že med dodiplomskim študijem. Sodobni učni načrti vključujejo disekcije v kliničnem kontekstu in jih dopolnjujejo s tehnološko podprtimi metodami, namesto da bi bila anatomija s sekcijo samostojen predmet (28, 31, 32). Poleg disekcije obstajajo številna

dissection being standalone subjects (28, 31, 32). There are many tools used to compliment dissection based anatomical learning. In cases where universities have ceased dissection these will, or would have been, the only resources available to students. Prosections or plastinated products are final products, where the dissection work has already been done usually by academic or technical staff or on occasion by students themselves. Non tissue models of organs/systems/cells, formalin fixed tissues and models originally derived from animal tissues such as corrosion casts and preserved tissue sections are also commonly used in teaching and share many features common to prosections and plastinated samples. When using technological resources and multimedia resources, such as different types of virtual anatomy software (even further from reality from prosections), many are based on images, videos or scans (such as MRI, computed tomography, X-ray). In some cases, these are based on a single animal, from one species, which may be considered the same or worse than using plastinated preparations given the lack of specimen variation. As time passes, many of the resources are increasing the variety of animals used in their resources though.

These types of anatomical models, or methods of learning anatomy, do not generally enable the experience of hands-on dissecting by the student. By removing the connective tissue surrounding the organs, all structures are immediately exposed to the learner. When using the non-dissection teaching tools mentioned, there is no dissection or discovery of structures, this may provide less appreciation of anatomical variability for the learner. The student does not learn key pre-surgical skills such as working with scalpels, cutting tissue or a experiencing the emotions related to working with a cadaver. The structures are often presented to the student in non- dissection-based methods, rather than a true exploration of structures as is often the case in dissection learning. In dissection there are usually no answers readily available as to the name of each structure. In contrast, and both a strength and a weakness, other learning tools such as videos, books, models, online tools, virtual reality, augmented reality and others, may provide labelled structures. Although dissection costs are generally relatively large, a great deal of expertise and time is also often required to create these non-dissection teaching tools, and frequently some of the cost is covered by reusing cadaver material from anatomical dissection. Some non-dissection techniques still require the use of chemicals and time from experts (e.g. plastination). Other non-dissection techniques may need investments in appropriate software and accompanying hardware devices such as headsets for virtual reality, or the purchase of a virtual reality dissection 'anatomy table' (33).

Many of these non-dissection tools will have been developed over many years and despite some disadvantages, their benefits are vast. Indeed, the authors of this article have been involved in creating many learning tools for their students, and those further afield, to compliment dissection

orodja, ki podpirajo učenje anatomije. V primerih, ko so univerze opustile disekcijo, so ta orodja pogosto postala ali pa bodo postala edini vir, ki je na voljo študentom. Prosekcije in plastinirani preparati so končni izdelki, pri katerih je disekcijo izvedlo strokovno osebje ali včasih študentje sami. Pri poučevanju se pogosto uporabljajo tudi netkivni modeli organov/sistemov/celic, tkiv, fiksiranih s formalinom, in modeli, prvotno pridobljeni iz živalskih tkiv, kot so korozijski odlitki in ohranjeni deli tkiva. Ti imajo veliko skupnih značilnosti s prosekcijami in plastiniranimi vzorci. Tehnološki viri, kot so programske opreme za virtualno anatomijo, ponujajo dodatne možnosti. Te platforme temeljijo na slikah, videoposnetkih ali skeniranju, kot so MR, CT in rentgenske slike. Vendar pa so takšni viri v nekaterih primerih omejeni na eno samo živalsko vrsto, kar se lahko šteje za enako ali slabše od uporabe plastiniranih preparatov glede na pomanjkanje vzorcev različnih živalskih vrst. Sčasoma se pri mnogih virih povečuje raznolikost živali, ki se uporabljajo. Postopoma se sicer povečuje število vrst, ki so vključene v te vire, vendar ti pogosto ostajajo dopolnilna orodja, ki ne morejo v celoti nadomestiti praktičnih izkušenj disekcije.

Alternativne metode učenja anatomije, kot so modeli ali multimedijska orodja, študentom običajno ne omogočajo praktične izkušnje seciranja. Pri uporabi teh pristopov so vezivna tkiva, ki obdajajo organe, že odstranjena, kar pomeni, da so vse strukture takoj izpostavljene študentu. Tak način študija onemogoča proces postopnega odkrivanja anatomskih struktur, ki je osnova disekcije, zato lahko študent manj ceni anatomsko variabilnost. Poleg tega študentje pri teh metodah ne pridobijo ključnih predkliničnih veščin, povezanih s kirurgijo, kot je natančno delo s skalpelom, pravilno rezanje tkiva ali obvladovanje čustev, povezanih z delom s kadavri. Pri alternativnih metodah so strukture običajno predstavljene kot že prepoznane in označene, kar lahko omeji sposobnost študentov za samostojno raziskovanje in identifikacijo anatomskih struktur. Nasprotno je pri disekciji pogosto potrebno aktivno raziskovanje, saj odgovori, kot so imena posameznih struktur, niso takoj na voljo. To spodbuja bolj poglobljeno učenje in razumevanje anatomije. Čeprav so stroški izvajanja disekcije pogosto visoki, tudi ustvarjanje učnih orodij brez disekcije zahteva ogromno strokovnega znanja in časa. Paradoksalno je, da se veliko teh virov še vedno opira na material iz disekcije, kar vključuje pripravo vzorcev za plastinacijo ali druge tehnike. Nekatere metode brez seciranja, kot je plastinacija, prav tako zahtevajo uporabo kemikalij in dodatnega strokovnega časa. Poleg tega so za naprednejše tehnike brez disekcije, kot so virtualna resničnost (VR), obogatena resničnost (AR) ali uporaba anatomske mize za navidezno seciranje, potrebne visoke finančne naložbe v programsko in strojno opremo. To vključuje tudi nakup očal VR ali drugih naprav, kar lahko predstavlja dodatno finančno obremenitev (33).

Kljub določenim omejitvam imajo alternativna učna orodja brez disekcije številne prednosti in velik potencial za nadaljnji razvoj. Avtorji tega članka so bili dejavni pri ustvarjanju takšnih orodij, ki dopolnjujejo učne ure disekcije, tako za

lessons. Appropriate laboratory spaces are required to create models and prosections, as are chemicals, waste disposal and technician and academic time, but this is usually on smaller scale than compared to dissection classes, and specimens often last longer and digital assets can be used indefinitely (if they are updated and supported by the correct technology). Increasingly, 3D methods are emerging which add to the user experience when learning anatomy. These resources may be accessible outside of the dissection room, are easy to provide to students without staff interaction, can be less expensive, and indeed many are developed by anatomists themselves. As these tools advance, they are frequently adding more specimens and combining information from a variety of sources. This may give the learner access to species they may not encounter regularly in person, for example more exotic species. These tools are widely accepted, enjoyed, and appreciated by students and educators alike but are not seen by them as a replacement for cadaver dissection (33-36).

Anatomy has always been taught by dissection, but nowadays the frequently reported reduction in experienced teaching staff, reductions in anatomy teaching time, and difficulties in obtaining cadavers have reduced in some cases reduced the availability of dissection (26). There is an alarming trend away from time spent in dissection with little evidence-based research on the overall impact on learning and skills, both as a student and during later careers (26). Research into learner outcomes tends to be based on whether anatomical structures can be named by learners in examinations (for example following dissection vs. non-dissection-based teaching), and not on other key skills potentially gained such as confidence and surgical competence. This is true for all types of learning at undergraduate level and is a known limitation in researching long term skills and knowledge related to any of these teaching and learning tools.

Some research into dissection based learning versus digital learning indicated better retention of information and more student satisfaction when learning through dissection , whilst other studies show better outcomes following dissection based teaching (37). The abandonment of dissection in some areas may have reduced anatomical knowledge or skills, but this reduction may take many decades to observe and is complex to quantify. Research in human medicine has shown the complexities involved in removing dissection, which ultimately meant an increase in postgraduate levels or reinstating dissection in undergraduate studies. In human medicine the longer term outcomes of reduced dissection or temporary removal of dissection (usually reinstated following problems in later or clinical years) has taught our profession many valuable lessons, especially in terms of information and skills lost when dissection is not utilised (28). At the same time, people have been noting a noticeable reduction in the number of qualified instructors and therefore researchers (10). Decision makers working in disciplines far away from anatomy may not understand the

lastne študente kot za širšo strokovno javnost. Za izdelavo teh modelov in sekcij so potrebni laboratorijski prostori, kemikalije, tehnični in akademski čas ter ustrezno odstranjevanje odpadkov. Vendar so te zahteve pogosto manj obsežne v primerjavi z zahtevami fakultet, ki pri študiju vključujejo disekcijo. Ustvarjeni preparati so dolgotrajni, digitalna sredstva na drugi strani pa omogočajo praktično neomejeno uporabo, če so ustrezno posodobljena in podprta s primerno tehnologijo. Sodobne 3D-metode so vse bolj vključene v poučevanje anatomije, saj izboljšujejo uporabniško izkušnjo in ponujajo nove možnosti za učenje. Prednosti teh virov so v njihovi dostopnosti izven učilnic, enostavni distribuciji brez potrebe po sodelovanju osebja in pogosto nižjih stroških. Veliko takšnih orodij anatomi razvijejo sami, kar omogoča prilagoditev potrebam posameznih študentov in programov. Napredovanje teh tehnologij prinaša vključevanje več primerkov in združevanje informacij iz različnih virov, kar omogoča dostop do vrst, s katerimi se študentje redkeje srečujejo v praksi, kot so na primer bolj eksotične vrste. Taka raznolikost povečuje vrednost učnih orodij, saj študentje pridobijo širši vpogled v anatomske razlike. Študentje in učitelji ta orodja splošno sprejemajo, uživajo v njihovi uporabi in jih cenijo, vendar jih večina ne dojema kot nadomestek za disekcijo trupel, temveč kot dopolnilo h klasični metodi učenja s pomočjo disekcije (33–36).

Disekcija je tradicionalno veljala za temelj poučevanja anatomije, vendar se sodobni izobraževalni sistemi pogosto soočajo z izzivi, kot so pomanjkanje izkušenega učiteljskega osebja, skrajševanje časa, namenjenega anatomiji, in težave pri pridobivanju kadavrov, kar je v številnih primerih privedlo do zmanjšane razpoložljivosti disekcije (26). Pojavlja se še skrb vzbujajoč trend skrajševanja časa, namenjenega disekciji, pri čemer primanjkuje raziskav, ki bi temeljile na dokazih in bi celovito analizirale vpliv skrajšanja na učenje ter razvoj ključnih veščin, tako med študijem kot v kasnejši karieri (26). Študije pogosto ocenjujejo učne rezultate na podlagi sposobnosti študentov, da na izpitih prepoznajo in poimenujejo anatomske strukture, vendar redko vključujejo oceno drugih ključnih veščin, pridobljenih z disekcijo, kot sta samozavest in spretnost dela s skalpelom in pinceto. Ta omejitev je značilna za vse vrste dodiplomskega izobraževanja in opozarja na potrebo po boljšem raziskovanju dolgoročnih vplivov različnih metod poučevanja na znanje in veščine, ki jih študenti pridobijo. Razumevanje teh učinkov bi lahko pomembno prispevalo k izboljšanju učnih načrtov in oblikovanju učinkovitejšega poučevanja anatomije.

Raziskave primerjave disekcije in digitalnega učenja nakazujejo, da učenje, ki temelji na disekciji, pogosto prinaša boljše ohranjanje informacij in večje zadovoljstvo študentov. Nekatere študije poročajo tudi o boljših rezultatih po poučevanju z uporabo disekcije (37). Kljub temu lahko opustitev disekcije na nekaterih področjih vodi do zmanjšanja osnovnega anatomskega znanja ali praktičnih spretnosti, čeprav lahko traja desetletja, da se te spremembe v celoti razkrijejo in kvantificirajo. V humani medicini so posledice zmanjšane uporabe disekcije ali njenega

importance of dissection, especially if they are not anatomists, but it is recognised that one concern they may have relates to the economics of this teaching method.

Although technological resources and anatomical models are very useful and enhance and complement the learning experience, we believe that they cannot fully replace dissection in the veterinary and human anatomy teaching. Gummery and coauthors (21) highlighted perceptions of students in later years, and those of recent graduates, who emphasised the importance of the skills and techniques they learnt in dissection. Although anatomy is traditionally considered a basic science, anatomical learning, including dissection, increasingly integrates and links clinical techniques and skills, especially in spiral and vertically integrated curricula. Clinical (or applied) anatomy is often described as the practical application of anatomical knowledge to diagnosis and treatment. Veterinary medicine curricular are increasingly teaching clinical anatomy. The American Association of Clinical Anatomists defines clinical anatomy as "anatomy in all its aspects - gross, histologic, developmental and neurologic as applied to clinical practice, the application of anatomic principles to the solution of clinical problems and/or the application of clinical observations to expand anatomic knowledge" (38). Meanwhile the World Association of Veterinary Anatomists (WAVA) promotes and represents veterinary anatomy, by "encouraging research, promoting the use of modern teaching methods and better knowledge of anatomy in applied science, and encouraging the exchange of information" (39).

Together, curriculum revisions, introduction of novel innovative techniques, and the introduction of clinical skills courses in the early years have led to reduction and even elimination of animal cadaver dissection from some anatomy courses. We believe that modern teaching methods need not shy away from well-established techniques such as dissection. Instead, they should integrate the valuable skills and information gained from dissection with other complementary anatomical learning techniques. This can be done in a clinically relevant manner within thoughtfully designed curricula, incorporating blended learning opportunities that enhance learner motivation and engagement.

začasnega umika pogosto zahtevale povečanje podiplomskih programov ali ponovno uvedbo disekcije v dodiplomske kurikulume. Dolgoročni rezultati so razkrili izgube v znanju in spretnostih, ki so pomembno vplivale na klinično prakso, kar je prineslo dragocene lekcije za anatomsko izobraževanje (28). Hkrati pa se soočamo še z opaznim upadom števila usposobljenih inštruktorjev, kar negativno vpliva tudi na raziskovalno dejavnost na področju anatomije (10). Odločevalci, ki niso specializirani za anatomijo, pogosto ne razumejo ključnega pomena disekcije, kar je še posebej očitno, ko gre za presojo ekonomičnosti te metode poučevanja. Vendar je treba priznati, da disekcija prinaša nenadomestljive pedagoške in klinične koristi, ki jih alternativne metode ne morejo v celoti posnemati.

Čeprav so tehnološki viri in anatomski modeli izjemno koristni ter pomembno prispevajo k izboljšanju in dopolnjevanju učnega procesa, menimo, da ne morejo povsem nadomestiti disekcije kot temeljne metode pri poučevanju veterinarske in humane anatomije. Gummery in sod. (21) so poudarili perspektive študentov višjih letnikov in nedavnih diplomantov, ki so izpostavili pomen poznavanja tehnik in spretnosti, pridobljenih z disekcijo. Tradicionalno je bila anatomija obravnavana kot temeljna znanost, vendar se anatomsko učenje, vključno z disekcijo, vedno bolj prepleta s kliničnimi tehnikami in praktičnimi veščinami. To je še posebej opazno v spiralnih in vertikalno integriranih učnih načrtih, kjer klinična anatomija predstavlja povezavo med teoretičnim znanjem in njegovo praktično uporabo. Klinična anatomija, opredeljena kot praktična uporaba anatomskega znanja pri diagnozi in zdravljenju, pridobiva vse večji pomen v veterinarskih učnih načrtih. Ameriško združenje kliničnih anatomov jo opisuje kot interdisciplinarno področje, ki združuje različne vidike anatomije, kot so makroskopska, mikroskopska, razvojna in nevrološka anatomija, ter njihovo uporabo v klinični praksi (38). Svetovno združenje veterinarskih anatomov (WAVA; iz angl. *Word Association of Veterinary Anatomists*) pa promovira veterinarsko anatomijo z raziskavami, sodobnimi učnimi metodami in širjenjem znanja, da bi izboljšali razumevanje anatomije kot uporabne znanosti (39). Združevanje disekcije in dopolnilnih učnih orodij je zato ključno za ohranjanje visokih standardov izobraževanja in pripravo študentov na praktične izzive v kliničnem okolju.

Spremembe kurikulumov, uvedba inovativnih tehnik in vključitev poučevanja kliničnih veščin v zgodnjih letih študija so privedle do zmanjšanja ali celo opustitve seciranja živalskih kadavrov v nekaterih anatomskih programih. Vendar menimo, da sodobne učne metode ne bi smele izključevati dobro uveljavljenih tehnik, kot je sekcija. Nasprotno, k dragocenim veščinam in znanju, pridobljenem z disekcijo, je treba vključiti še druge komplementarne anatomske učne pristope. To lahko dosežemo na klinično relevanten način z oblikovanjem premišljenih kurikulumov, ki združujejo različne učne metode in spodbujajo motivacijo ter aktivno sodelovanje študentov.

References

1. Wysiadecki G, Varga I, Klejbor I, et al. The most ancient sources of anatomic knowledge. Transl Res Anat 2024; 35: 100295. doi: 10.1016/j.tria.2024.100295
2. Cavalcanti de AMA, Martins C. History of liver anatomy: Mesopotamian liver clay models. HPB (Oxford) 2013; 15(4): 322-3. doi: 10.1111/j.1477-2574.2012.00555.x
3. Loukas M, Hanna M, Alsaiegh N, Shoja MM, Tubbs RS. Clinical anatomy as practiced by ancient Egyptians. Clin Anat 2011; 24(4): 409-15. doi: 10.1002/ca.21155
4. Loew FM, Cohen BJ. Chapter 1 - Laboratory animal medicine: historical erspectives. In: J. G. Fox, eds. Laboratory Animal Medicine. 2nd ed. Burlington: Academic Press, 2002; 1-17. doi: 10.1016/B978-012263951-7/50004-1
5. Bay NS, Bay BH. Greek anatomist herophilus: the father of anatomy. Anat Cell Biol 2010; 43(4): 280-3. doi: 10.5115/acb.2010.43.4.280
6. Ganz JC. Chapter four - Hippocrates (ca 460 BC to ca 370 BC). In: Ganz JC, ed. Progress in brain research. Amsterdam: Elsevier, 2024; 284: 31-48. doi: 10.1016/bs.pbr.2024.02.004
7. Ganz JC. Chapter seven - Rome-Galen (129 to ca. 216). In: Ganz JC, ed. Progress in brain research. Amsterdam: Elsevier, 2024; 284: 65-86. doi: 10.1016/bs.pbr.2024.02.007
8. Zarrintan S, Tubbs RS, Najjarian F, Aslanabadi S, Shahnaee A , Abu Al-Qasim Al-Zahrawi (936-1013 CE), icon of medieval surgery. Ann Vasc Surg 2020; 69: 437-40. doi: 10.1016/j.avsg.2020.07.012
9. Taheri-Targhi S, Gjedde A, Araj-Khodaei M, et al. Avicenna (980–1037 CE) and his early description and classification of dementia. J Alzheimer Disease 2019, 71(4): 1093-8. doi: 10.3233/JAD-190345
10. Ghosh SK. Human cadaveric dissection: a historical account from ancient Greece to the modern era. Anat Cell Biol 2015; 48(3): 153-69. doi: 10.5115/acb.2015.48.3.153
11. Magee R. Art macabre: resurrectionists and anatomists. ANZ J Surg 2001; 71(6): 377-80.
12. Papa V, Varotto E, Vaccarezza M, Ballestriero R, Tafuri D, Galassi FM. The teaching of anatomy throughout the centuries: from Herophilus to plastination and beyond. Medicina Histor 2019; 3(2): 69-77.
13. Jeyapalan JN, James V, Gardner DS, Lothion-Roy JH, Mongan NP, Rutland, CS. Impact of COVID-19 on student attainment and pedagogical needs when undertaking independent scientific research. Anatom Histol Embryol 2023; 52(1): 93-100. doi: 10.1111/ahe.12842
14. Kubale V, Cousins E, Bailey C, El-Gendy SAA, Rutland CS. Introductory chapter: veterinary anatomy and physiology. In: Sian Rutland K, eds. Veterinary anatomy and physiology. Rijeka: IntechOpen, 2019. doi: 10.5772/intechopen.82412
15. Messbarger R. The lady anatomist: the life and work of anna morandi manzolini. Chicago: University of Chicago Press, 2010.
16. Brown B, Adhikari S, Marx J, Lander L, Todd GL. Introduction of ultrasound into gross anatomy curriculum: perceptions of medical students. J Emerg Med 2012; 43(6): 1098-102. doi: 10.1016/j.jemermed.2012.01.041
17. Ivanusic J, Cowie B, Barrington M. Undergraduate student perceptions of the use of ultrasonography in the study of "living anatomy". Anat Sci Educ 2010. 3(6): 318-22. doi: 10.1002/ase.180
18. Fitzpatrick CM, Kolesari GL, Brasel KJ. Teaching anatomy with surgeons' tools: use of the laparoscope in clinical anatomy. Clin Anat 2001; 14(5): 349-53. doi: 10.1002/ca.1062
19. McLachlan JC, Bligh J, Bradley P, Searle J. Teaching anatomy without cadavers. Med Educ 2004; 38(4): 418-24. doi: 10.1046/j.1365-2923.2004.01795.x
20. Rajeh NA, Badroun LE, Alqarni AK, et al. Cadaver dissection: a positive experience among Saudi female medical students. J Taibah Univ Med Sci 2017; 12(3): 268-72. doi: 10.1016/j.jtumed.2016.07.005
21. Gummery E, Cobb KA, Mossop LH, Cobb MA. Student perceptions of veterinary anatomy practical classes: a longitudinal study. J Vet Med Educ 2018; 45(2): 163-76. doi: 10.3138/jvme.0816-132r1
22. Varner C, Dixon L, Simons MC. The past, present, and future: a discussion of cadaver use in medical and veterinary education. Front Vet Sci 2021; 8: 720740. doi: 10.3389/fvets.2021.720740
23. Clement SM, Ubben TA, Yates DT. Cadaveric prosections prepared by qualified instructional staff were more efficient and effective teaching modalities for veterinary gross anatomy than in-class dissections by students. J Vet Med Educ 2024; 51(5): 593-609. doi: 10.3138/jvme-2024-0031
24. von Staden H. The discovery of the body: human dissection and its cultural contexts in ancient Greece. Yale J Biol Med 1992; 65(3): 223-41.
25. Rath G., Garg K. Inception of cadaver dissection and its relevance in present day scenario of medical education. J Indian Med Assoc 2006; 104(6): 331-3.
26. Smith CF, Freeman SK, Heylings D, Finn GM, Davies DC. Anatomy education for medical students in the United Kingdom and Republic of Ireland in 2019: a 20-year follow-up. Anat Sci Educ 2022; 15(6): 993-1006. doi: 10.1002/ase.2126
27. Patel KM, Moxham BJ. Attitudes of professional anatomists to curricular change. Clin Anat 2006; 19(2): 132-41. doi: 10.1002/ca.20249
28. 28. Rizzolo LJ, Stewart WB. Should we continue teaching anatomy by dissection when ...? Anat Rec B New Anat 2006; 289(6): 215-8. doi: 10.1002/ar.b.20117
29. Warner JH, Rizzolo LJ. Anatomical instruction and training for professionalism from the 19th to the 21st centuries. Clin Anat 2006; 19(5): 403-14. doi: 10.1002/ca.20290
30. Stringer MD, Lyall P. Design, implementation, and evaluation of a postgraduate Diploma in Surgical Anatomy. Anat Sci Educ 2012; 5(1): 48-54. doi: 10.1002/ase.1253
31. Huitt TW, Killins A, Brooks WS. Team-based learning in the gross anatomy laboratory improves academic performance and students' attitudes toward teamwork. Anat Sci Educ 2015; 8(2): 95-103. doi: 10.1002/ase.1460
32. Memon I. Cadaver dissection is obsolete in medical training! a misinterpreted notion. Med Princip Pract 2018; 27(3): 201-10. doi: 10.1159/000488320
33. Little WB, Artemiou E, Fuentealba C, Conan A, Sparks C. Veterinary students and faculty partner in developing a virtual three-dimensional (3d) interactive touch screen canine anatomy table. Med Sci Educ 2019; 29(1): 223-31. doi: 10.1007/s40670-018-00675-0
34. Little WB, Artemiou E, Conan A, Sparks C. Computer assisted learning: assessment of the Veterinary Virtual Anatomy Education Software IVALA™. Vet Sci 2018; 5(2): 58. doi: 10.3390/vetsci5020058
35. Theoret CL, Carmel EN. Bernier S. Why dissection videos should not replace cadaver prosections in the gross veterinary anatomy curriculum: results from a comparative study. J Vet Med Educ 2007; 34(2): 151-6. doi: 10.3138/jvme.34.2.151
36. Ryan MT, Baird AW, Mulholland CW, Irwin JA. Practical classes: a platform for deep learning? Overall context in the first-year veterinary curriculum. J Vet Med Educ 2009; 36(2): 180-5. doi: 10.3138/jvme.36.2.180
37. Previdelli RL, Boardman E, Frill M, Frean S, Channon SB. Supporting collaborative dissection through the development of an online wiki positively impacts the learning of veterinary anatomy. Anat Sci Educ 2024; 17(1): 88-101. doi: 10.1002/ase.2324
38. AACA. LaGrange: American Association of Clinical Anatomists, 2024. https://clinical-anatomy.org/ (15. 12. 2024)
39. WAVA. Oslo: World Association of Veterinary Anatomists, 2024. https://www.wava-amav.org/. (15. 12. 2024)

Slov Vet Res
DOI 10.26873/SVR-1923-2024
UDC 578:616-036.22:616.993:639.128(4)
Pages: 233–44

Review Article

West Nile Virus in Vultures From Europe – a Sight Among Other Raptors

Key words

epidemiology;
Europe;
scavengers;
vultures;
West Nile virus;
zoonotic

Filipa Loureiro[1,2]*, Luís Cardoso[2,3], Ana Matos[4,5], Manuela Matos[6], Ana Cláudia Coelho[2,3]

[1]Wildlife Rehabilitation Centre (CRAS), Veterinary Teaching Hospital (HVUTAD), University of Trás-os-Montes e Alto Douro (UTAD), 5000-801 Vila Real, [2]Animal and Veterinary Research Centre (CECAV), Associate Laboratory for Animal and Veterinary Sciences (AL4AnimalS), UTAD, Vila Real, [3]Department of Veterinary Sciences, School of Agrarian and Veterinary Sciences (ECAV), UTAD, 5000-801 Vila Real, [4]Research Centre for Natural Resources, Environment and Society (CERNAS), Polytechnic Institute of Castelo Branco; 6001-909 Castelo Branco, [5]Quality of Life in the Rural World (Q-RURAL), Polytechnic Institute of Castelo Branco, 6001-909 Castelo Branco, [6]Centre for the Research and Technology of Agro-Environmental and Biological Sciences (CITAB), UTAD, 5000-801 Vila Real, Portugal

*__Corresponding author:__ filipal@utad.pt

Abstract: The West Nile virus (WNV) is an arbovirus mainly transmitted by *Culex* spp. and the causative agent of a zoonotic disease that is present worldwide. This pathogen is endemically maintained in a life cycle with birds acting as reservoirs, and humans and horses as accidental and dead-end hosts. Sporadic WNV outbreaks have been reported in Europe, and the potential impact of WNV infection on populations of threatened or endangered birds of prey is considerable. Surveillance programs are needed for early detection of this virus. All four species of vultures present in Europe are considered protected species. As scavengers, vultures are at the top of the food chain, and can be susceptible to, and negatively affected by, pathogens like WNV. In a conservation perspective, the impact of WNV in European vultures, alone or concomitantly with other factors, should be addressed. This review of documented cases can be considered a starting point.

Received: 30 December 2023
Accepted: 21 September 2024

Introduction

Vultures are the biggest European bird scavengers, performing an essential role in the environment. Information and awareness-raising are needed to change the paradigm of the bad reputation they are given. Vultures are often seen as sinister and death-dealing, being spotted with their large wings wide spread, gliding in circles. And even in literature, comics or cinema, they usually appear as a forewarning of bad things to come, a sort of bad omen. This negative image may be due to their threatening appearance and the fact that they are scavengers. However, vultures provide an important service to the ecosystem by cleaning up and recycling carcasses of dead animals. They can quickly eliminate large amounts of flesh, in different stages of decomposition, that may potentially host pathogenic microorganisms, thus removing this potential source of infection from the environment. Furthermore, thanks to its extremely acidic gastric pH and stable intestinal microbiome with remarkable anti-microbial activity, they can neutralize pathogens that pass through their gastrointestinal tract, limiting the spread of diseases (1-4). This majestic group of raptors also proves to be of great socioeconomic value to local communities. Bird-watching of scavenging birds has been yielding economic benefits to rural economies within developing regions (5).

Four species of vulture are found in Europe: the bearded vulture (*Gypaetus barbatus*), the cinereous vulture (*Aegypius monachus*), the griffon vulture (*Gyps fulvus*) and the Egyptian vulture (*Neophron percnopterus*). Two hundred years ago, these species of vultures were among the most common breeding bird species in the mountains of central and southern Europe. Yet, the decreasing availability

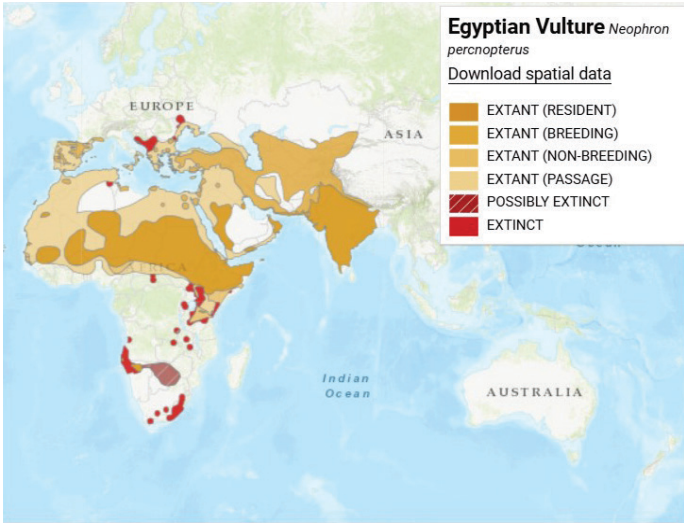

Figure 1: Distribution map of Egyptian vulture (*Neophron percnopterus*). Reproduced with permission from BirdLife International and Handbook of the Birds of the World 2021. *Neophron percnopterus*. The IUCN Red List of Threatened Species. Version 2022-2. (6)

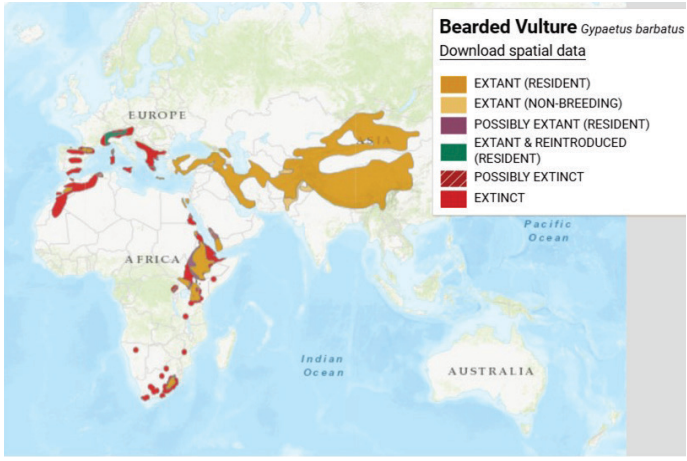

Figure 2: Distribution map of bearded vulture (*Gypaetus barbatus*), Reproduced with permission from BirdLife International and Handbook of the Birds of the World 2021. *Gypaetus barbatus*. The IUCN Red List of Threatened Species. Version 2022-2. (6)

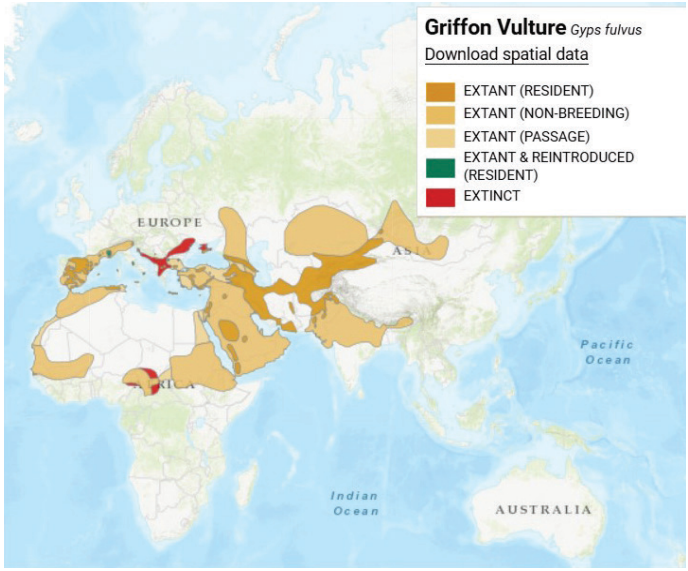

Figure 3: Distribution map of griffon vulture (*Gyps fulvus*), Reproduced with permission from BirdLife International and Handbook of the Birds of the World 2021. *Gyps fulvus*. The IUCN Red List of Threatened Species. Version 2022-2. (6)

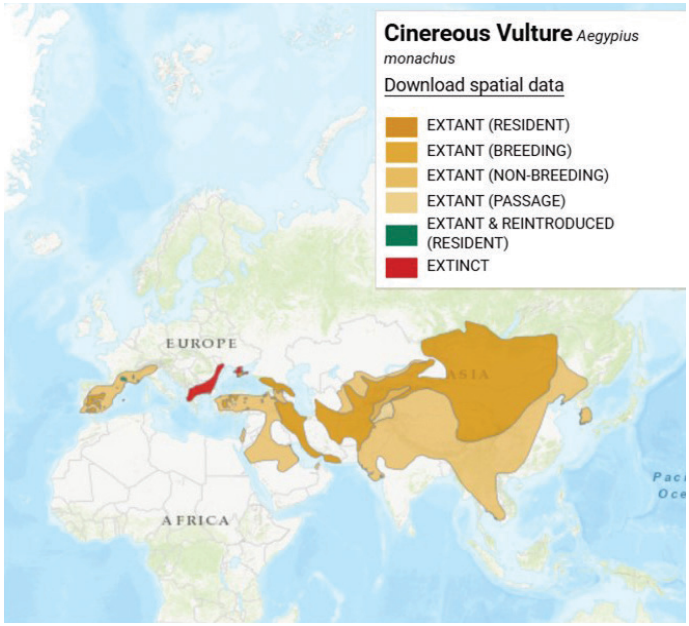

Figure 4: Distribution map of cinereous vulture (*Aegypius monachus*), Reproduced with permission from BirdLife International and Handbook of the Birds of the World 2021. *Aegypius monachus*. The IUCN Red List of Threatened Species. Version 2022-2. (6)

of food, coupled with habitat loss, persecution and poisoning, made vultures disappear from most of their European range, with populations considerably smaller and increasingly isolated by the 1960s. Many conservation efforts have been and are being made; as a result, European vulture populations are steadily recovering.

In 2007 the Egyptian vulture was declared globally 'Endangered' by the International Union for the Conservation of Nature (IUCN) Red List (6). The majority of its European population is found in the Iberian Peninsula with an estimated 1,300–1,500 couples. This species is a long-distance migratory bird of prey, spending its winters in sub-Saharan Africa and returning in March to reproduce in Europe (Figure 1). It faces many threats, mostly electrocution and poisoning.

The bearded vulture's population drastically decreased at the beginning of the 20th century, and was driven to extinction throughout most of its former range. Nowadays, it is the rarest vulture in Europe, and its presence is limited to the Alps, Pyrenees and Andalusia, with isolated populations in Crete and the Corsica islands (Figure 2). It is considered 'Near Threatened' by IUCN Red List (6). This vulture has a unique feeding habit: its diet consists of a huge percentage of bleached carcass bones (7). In the wild, they rub themselves with ferric oxides, which turns their plumage rusty

Table 1: Reported causes of free-living vulture morbidity and mortality (adapted from the review by Ives *et al*., 2022).

Species	IUCN global status[a]	Toxic	Trauma	Infectious	Idiopathic	Metabolic	Inflammatory	Total[b]
A. monachus	NT	9 (485)	1 (9)	6 (46)	1 (1)	2 (16)	1 (1)	20 (558)
G. barbatus	NT	8 (61)	7 (80)	1 (3)	2 (2)	0	1 (1)	19 (147)
G. fulvus	LC	18 (615)	12 (978)	5 (73)	1 (5)	1 (51)	0	37 (1722)
N. percnopterus	EN	15 (500)	13 (176)	3 (38)	0	0	0	31 (714)

[a] LC – Least concern; NT – Near threatened; EN – Endangered. [b] Number of studies (number of affected individual vultures reported).

orange. Major threats are changes in farming practices and direct persecution (8-10).

Griffon vultures are the most social of European vultures, with gregarious and competitive habits, breeding in large colonies. They feed in groups and can penetrate animal carcasses to feed on the softer tissues, such as muscles and viscera (11-12). Following a decline in the 20th century, as a result of wildlife poisoning, hunting and decreasing of food supplies (13), in recent years the species has significantly increased in some areas, particularly in France and in the Iberian Peninsula (Figure 3), and has an extremely large range in Europe, being now considered 'Least concern' by IUCN (6,12).

The cinereous vulture is the biggest raptor in Europe, with a wingspan almost reaching 3 meters. Its conservation status is listed as 'Near Threatened' by IUCN's red list and as 'Critically Endangered' in Portugal (6,14). Over the last century, the population of this species has decreased across its distribution area in Europe, and it is now extinct in many European countries (namely in Italy, Austria, Poland, Slovakia and Romania) (Figure 4) (6). Major threats to the viability of the species include habitat destruction by increasing forest fires, illegal use of poisons, limited food availability due to health restrictions and reduced wild herbivore populations, consumption of food resources contaminated by veterinary drugs or lead (from hunting ammunition), human disturbance during the breeding season and death by collision with/electrocution on power lines (14).

The most frequently reported cause of free-living vulture death and disease worldwide (Table 1) was due to toxic agents, with special emphasis on lead and pesticides. Regarding traumatic causes of morbidity and mortality, the second highest prevalence, the most reported are of anthropogenic origin: collision with and electrocution by power lines, gunshot, and direct persecution, among others (15). It is not uncommon for the main cause of vulture admission at wildlife rehabilitation centres and the cause of subsequent death, when it occurs, to remain unknown (16).

Vultures are considered to be resistant to certain microorganisms, such as *Bacillus anthracis* (17) or *Clostridium botulinum*, due to having naturally occurring antibodies against the toxins of these bacteria, coming from previous exposure to these pathogens (18). However, vultures can be susceptible to and negatively affected by other pathogens. The effects of infectious diseases have not been thoroughly investigated for most vulture species, obligate scavengers. Some pathogens should be seen as a potential threat to vulture conservation because they can cause disease in individual birds, and potentially jeopardize vulture health when associated with other menaces, such as contaminants and intentional poisoning (5). Highly virulent avian influenza virus, for instance, has caused a significant impact on griffon vultures in France and may have dramatic effects on the populations around the world, especially in the most critically endangered species (19). Attention should be paid to other viruses.

Far beyond the need for conservation, it makes perfect sense to use vulture and other raptor research and monitoring to a One Health approach, which brings together environmental, human and animal health. Vultures can be used to provide information relevant to public health (20). In this case, the scope can be the detection and monitoring of the spread of a recently emerged viral zoonosis in Europe such as WNV (21). The aim of this study is to bring together all the information on the WNV in vultures and highlight the need for further studies on the expression of the agent in this group of birds. We consider it is a topic highly relevant to animal and public health.

West Nile Virus

West Nile virus (WNV), lying within the genus Flavivirus and family Flaviviridae, is one of the most widespread arboviruses (22-23). The cycle of the WNV is maintained between birds (as reservoirs) and mainly mosquitos of the genus *Culex* (as vectors). Spread occurs when infected mosquitoes bite mammals. Horses and humans can be accidental dead-end hosts, along with other mammals (24-25). WNV has recently emerged as a major public health concern in Europe. The infection numbers have recently increased in European countries, while some remarkable socio-economic and environmental changes were noticed, including an economic crisis (in part due to the COVID-19 pandemic) and the occurrence of very high temperatures (26-27).

WNV strains have been grouped into nine genetic lineages, by phylogenetic analysis, being lineages 1 and 2 the most relevant (28-29). Both lineages 1 and 2 have been shown to cause severe disease in birds, horses and humans (30-32).

In humans, the severity of infections can range from asymptomatic to serious or fatal hemorrhagic fever or neurological disease. Most people (around 80%) with WNV infections remain asymptomatic. Among those who develop symptoms and clinical signs, the most common presentation is febrile illness (fever) accompanied by an acute syndrome, and less than 1% develop encephalitis or other forms of neuroinvasive disease (33-35).

As the key vertebrate hosts in WNV transmission cycle, avian species are the focus of surveillance worldwide (36). The information on the role of the birds of prey as reservoirs, spreaders, or sentinels of WNV is not yet clearly described, and specially the information available on the influence of vulture species on the epidemiology of WNV remains scarce (37-38).

For birds of prey, the pathogen is usually detected in the carcasses of birds found dead or moribund through wild-life surveillance programs or raptors admitted to wild-life rehabilitation centres (39). Three modes of WNV infection may be considered: mosquito-borne transmission, contact transmission and oral transmission (38). Variations in the prevalence of WNV infection between different species and populations of birds of prey can be explained by differences in exposure, based on infection prevalence values of prey species, differences in roosting habitat and exposure to the ornithophilic mosquito (40-42).

WNV infection in raptors appears to act as a multisystemic disease, affecting different organs, depending on the host species and also individuals. The disease can be fatal in most raptors, with an acute onset of illness a few days after infection occurs (43). On the other hand, the infection can also originate a debilitating and chronic disease, predisposing the affected animals to concurrent pathological conditions. In these cases, non-specific signs often occur, like depression, dehydration and severe weight loss (40,44-45). The WNV is neurotropic and, consequently, neurological signs are a very common outcome of infection, such as alterations in the mental status, head tilt, tremors, leg paresis or paralysis, among others. Ocular disorders often occur as well (32,46-48). The most common abnormalities in haematology screening are anaemia and leukocytosis (49), accompanied by splenomegaly, which can be seen in the ventrodorsal and laterolateral radiographic projections (50). Long-term sequelae have been detected in raptors, among which the recurrence of neurologic signs, feather pulp abnormalities and abnormal molt can persist for long periods of time, and may have a negative impact on the longevity of these species (37,43).

WNV infections can be diagnosed by isolating the virus, detecting viral antigens or RNA, or using serological methods. Research on avian immunity has focused on humoral immunity and there is still lack of information on cellular immunity. Humoral immunity against WNV is determined by the presence of antibodies in the blood of animals. This can be measured by a range of serological assays, being the virus neutralization test (VNT) considered the gold standard in flaviviruses serology, which detects serum neutralizing antibodies and more accurately detects protective antibodies, being more specific than other serological techniques (38). The main alternative is the capture enzyme-linked immunoassay (ELISA), which detects antibodies directed against the virus envelope protein. There are class-specific ELISAs for the detection of immunoglobulin (Ig) Y (the avian equivalent of IgG in mammals) or IgM against WNV. In adult birds, antibodies are developed following exposure and infection with WNV (38,51). In juveniles, presence of maternal antibodies can be detected (52). The long-term stability of antibodies confirmed in several species of raptors suggests that humoral immunity to WNV may be long-lasting in most individuals that survive infection (53). That is why positive serological results from ELISA suggest that a bird has been exposed to WNV, but generally do not indicate when the infection occurred (54). It is highly recommended to use VNTs to confirm WNV in all positive and doubtful samples detected by ELISA, in order to increase the accuracy of estimated seroprevalences in wild birds. The use of VNT will be especially important in areas where co-circulation of related flaviviruses exists (51).

The molecular diagnosis of WNV infection can be made using specific RT-PCR. Fresh brain samples, cloacal, and choanal swabs can be tested for this virus, as well as other organs where the virus is commonly found in raptors (heart, spleen, liver, kidney, adrenal gland and intestine). West Nile virus can also be detected in serum samples. Immunohistochemistry (IHC) also can be useful to detect WNV antigens in affected tissues from both living and dead birds (44,46,55-56).

There is still no specific treatment for WNV infection in raptors. In spite of the supportive treatment and anti-inflammatory drugs, to minimize the effects caused by infection, the majority of affected birds end up dying (57-58). There are still no vaccines specifically available for use in birds (38,45,48) or humans (24).

West Nile Virus in vultures Literature review

We have reviewed the scientific literature retrieved from PubMed and ScienceDirect databases, using general searches with the following terms: 'West Nile Virus' AND 'Vultures'. We performed other searches using different combinations of the following relevant terms: 'Scaveng* bird' AND 'flaviviruses'. We filtered our search based on the

Table 2: Diagnosed cases of WNV infection in European vultures

Species	WNV diagnosis (positives/sample size)	Geographical area	Year	Study
G. barbatus	ELISA; VNT (10/12; 2/3)	Austria	NM	Wodak *et al.*, 2011
G. barbatus	RT-PCR (1/1)	Austria	2008	Bakonyi *et al.*, 2013
A. monachus *N. percnopterus*	ELISA (2/8 – wild; 0/1 – captive) (1/9 – wild; 1/17 – captive)	Spain	2006-2009	García-Bocanegra *et al.*, 2011
G. barbatus	ELISA; SNT 14; 2	Spain	2017	Busquets *et al.* 2019
N. percnopterus	ELISA; MNT (2/2; 2/2)	Iran	2017-2018	Bakhshi *et al.*, 2021
A. monachus *G. fulvus*	ELISA; VNT; RT-PCR (19/20; 4/19; 0/0) (45/110; 20/45; 1/5)	Spain	2017-2019	Bravo-Barriga *et al.*, 2021
G. fulvus	RT-PCR 4/25a	Serbia	2018-2022	Marinković *et al.*, 2023

ELISA – enzyme-linked immunosorbent assay; MNT – microneutralization test; NM – not mentioned; RT-PCR – reverse transcription polymerase chain reaction; SNT – serum neutralization test (=VNT); VNT – virus neutralization test. [a]The authors report that 4 of the 25 tested positive for infectious agents, including WNV, among others. It is not mentioned how many of the 4 were in fact positive for WNV.

geographical location where the studies were performed, focusing on Europe and European species of vultures (Table 2). Eight reports were found that reported WNV infections in European vulture species, in Russia, Serbia, Austria and Spain, plus one in Iran.

Between 2008 and 2009 outbreaks of WNV infection occurred in central Europe, with an unexpected spread of a lineage 2 WNV strain. In 2011, a study from Austria described a WNV outbreak in birds of prey in 2008 and 2009 in the eastern part of the country. Samples were collected from birds nearby the location of the first detected infections and from poultry houses at the Research Institute of Wildlife Ecology in Vienna. ELISA positive results were found in 10 bearded vultures among other species of birds. 66% of the positive ELISA reactions could be confirmed with VNT, including two out of three vultures tested (59). One wild bearded vulture was confirmed by RT-PCR and IHC as positive for WNV, also in Austria (60).

In 2011 the first report of flaviviruses circulation in Egyptian vulture was published in Spain. Between 2006 and 2009 serum samples were obtained from several bird species in Andalusia, southern Spain, among free-ranging and captive animals held in rehabilitation centres. Two cinereous vultures and two Egyptian vultures tested positive on competitive enzyme-linked immunosorbent assay (cELISA) for WNV. As the used ELISA kit has been designed to detect anti-bodies directed against the envelope protein (pr-E) of WNV, which contains an epitope common to Japanese encephalitis virus (JEV) antigen, the VNT was further performed as a confirmation and more specific test for the positive samples on ELISA (61).

In 2017, the WNV was detected in one bearded vulture in Lleida, Northeastern Spain. The animal had been admitted to a local wildlife rehabilitation centre, and evidenced neurological signs. Serum samples were analysed and the results were positive on cELISA and negative on VNT. One month later, antibodies against WNV were detected on VNT. Thirteen additional vultures of the same species tested positive for cELISA, from which two were confirmed for VNT (titres between 1/20 and 1/40) (62).

Among samples collected in 2017-2018, two Egyptian vultures tested positive with micro-VNT, after a positive result on ELISA in Iran (63). This species is estival migratory in the European continent, and migrates to the African Sahelian region in the winter (64). Birds from Western Europe usually winter in Western Africa, and birds from Eastern Europe winter in Eastern Africa or the Arabian Peninsula (65). They are the same birds that return to Europe, a reason for mentioning this study, despite the fact that it is based on another continent.

From October 2017 to December 2019, almost 400 wild birds were sampled in the Cáceres and Badajoz provinces, Western Spain, in collaboration with two local rehabilitation centres. Analysis by RT-PCR in sick birds confirmed the presence of WNV line-age 1 RNA in a griffon vulture and specific antibodies against WNV in juvenile birds were detected in specimens of griffon vulture and cinereous vulture (66).

In the period between 2018 and 2022 in Serbia, 25 dead griffon vultures from the wild were submitted to macroscopical and histopathological examination, followed by different diagnostic screening. Infectious agents were detected in

4/25 animals, obtaining PCR confirmation of a WNV infection, with lymphoplasmacytic encephalitis (67).

WNV emerged in the United States of America (USA) in 1999 (68) and has since spread throughout much of the American continent. The WNV was identified as the primary cause of death in one nestling wild California condor (*Gymnogyps californianus*). The infection was diagnosed by IHC on the heart in conjunction with compatible lesions. In the USA, the WNV infection is an emerging mortality factor for young, wild-hatched birds and vaccination is required at nest sites where the WNV is prevalent (69). Other New World vulture species, such as the black vulture (*Coragyps atratus*) and theTurkey vulture (*Cathartes aura*), were confirmed to have WNV infection (49,53,70), as well as the Lappet-faced vulture (*Torgos tracheliotus*), an Old World vulture not present in Europe (57).

Epidemiology of WNV in vulture populations

The probability of a WNV case being reported depends on many factors, which can be divided in two main groups: factors related to the probability of infection itself, and those related to the probability of its detection. As with other birds of prey, the probability of infection in vultures depends on the blood feeding preferences of the main vector species, the animal species they bite, and the intrinsic susceptibility of the host animal species. The probability of detection will be affected by the intensity and specificity of clinical signs exhibited by the host, the location and distance in relation to a wildlife rehabilitation centre, and the size of the population of that species. The larger the population, the more likely the infection will be detected (38). The estimated population of mature Egyptian vultures is around 12,400-36,000, but on a downward trend; the bearded vulture population is between 1,675-6,700 mature individuals, and that of the cinereous vulture is around 16,800-22,800 mature birds. Only the griffon vulture population, counting with 80,000-90,0000 individuals worldwide, is currently tending to increase (71). These circumstances mean that these are not very large populations, making the task of identifying WNV infections more difficult and raising concerns that the WNV could jeopardize the conservation of these species.

One pertinent question is 'how do vultures acquire WNV infection?'. Most of the WNV infections in the Palearctic region have origin in a bird-mosquito cycle and the main WNV transmission mode to birds of prey is through mosquito bites (40). Mosquitoes are considered the main biological vectors of the WNV and, in Europe, two species are pointed out as key to transmission: *Culex pipiens* (Linnaeus), biotypes *pipiens* and *molestus*, and *Culex modestus* (Ficalbi). In fact, it is reported that *C. pipiens* mosquitoes do feed on vultures in the wild. In Switzerland, Egyptian vultures were found to be a host species for blood-fed mosquitoes (72).

In susceptible birds, besides inducing a viremic phase sufficient to infect additional mosquitoes and enhancing its transmission, the WNV can also be shed orally and through the cloaca (73-74), which represent alternative transmission mechanisms beyond vectors (75). Oral transmission by consumption of infected prey or carrion has also been described in birds of prey, and experimentally documented (40,43,74). Infection through feeding on WNV-infected preys may be more common in species like the Northern goshawk (*Accipiter gentilis*), which predates smaller birds (38), or in species that consume small mammals, potential reservoirs of WNV in both cases (40,76), but should not be excluded in vultures.

Vultures of the genus Gyps are obligatory scavengers, usually feeding in large groups on a resource that is random and unpredictable in space and time (77). This feeding behaviour, with several birds huddled together to feed on the same carcass, creates the opportunity of oral transmission of the virus among them, if the carcass has been contaminated by an infected bird. Typically, the griffon vulture's diet is based on carcasses of medium and large ungulates, whereas the Egyptian vulture largely consumes small and medium-sized vertebrates, and garbage, despite also feeding on large carcasses (78). From the year 2000 onwards, following the bovine spongiform encephalopathy crisis, government legislation has been introduced across Europe, imposing the removal and disposal of the carcasses of dead livestock. Farmers have been forbidden to leave carcasses in the field, and the food availability for scavengers dramatically decreased. Further European Union (EU) legislation included the maintenance of some feeding stations (commonly known as 'vulture restaurants'), in the scope of vulture conservation, but food remained scarce. This has triggered considerable changes in the diet composition of the griffon vulture, which started to consume small vertebrates, like rabbits, and to explore garbage dumps (79). The garbage consumption can bring direct consequences, such as ingestion of foreign bodies and poisoning (80), and indirect problems, like immunosuppression. Furthermore, corvids are commonly seen in dumps (81) and, as birds in this family are very susceptible to the WNV infection (40,82-83), they can be an important source of transmission for vultures.

Early detection of pathogens, like the WNV, will allow the establishment of effective measures to prevent or mitigate the effect of the virus on human populations, as well as to protect susceptible endangered species.

Discussion and Conclusion

Zoonotic emerging infectious diseases represent a rising and important threat to public health, and vector-borne diseases were responsible for almost a quarter of the documented emerging infectious diseases events in the first decade of the 21st century (84).

The West Nile virus (WNV) was first reported in Uganda in 1937 (85) and was subsequently isolated from patients, birds, and mosquitoes from the early 1950s (86). The virus became endemic in several parts of the African continent (87) and the first outbreak of WNV in Europe was reported in 1962 in the French Camargue region (88). Since 1996, after a high rate of confirmed cases in Eastern Europe (Romania) (89), several outbreaks have been often reported in the European continent, with a noticeable seasonal pattern, during the warmer weather (July to October) (90). Birds of prey are especially susceptible to the WNV (38). Upon the species and individuals, WNV infection can cause acute death, a fatal outcome several weeks after infection, or birds can eventually survive to chronic infections (43,57-58). Both in Europe and North America, raptors are among the birds described as more frequently infected during WNV outbreaks (50,60). Identifying target species is important for developing an efficient surveillance and monitoring program, a reason why targeting specific raptor species as disease sentinels may be beneficial.

The role of Palearctic-African migratory birds in the introduction of the WNV to Europe has long been the subject of debate (22-23,91). The suspicion that migratory birds could be the main introductory hosts of the WNV in new regions was based on the following: the majority of outbreaks in temperate regions occurred during late summer or early fall, when migratory birds and mosquitoes coexist in a large scale (86,90,92); the principal vectors from which the virus has been isolated are mainly ornithophilic mosquitoes (93-94); circulating antibodies against the WNV have been found in many migratory bird species, and long-distance migrants in Europe (in particular, species wintering south of the Sahara) are exposed during their migratory journeys and/or their winter stay in Africa to higher levels of WNV circulation (or a closely antigenically related Flavivirus), when compared with the levels found in their breeding grounds (95) and, finally, migratory birds have been linked to transporting related viruses in the Western Hemisphere (96). It is difficult to define a population geographically, especially for migratory birds the WNV has been isolated from some actively migrating species of birds (e.g., the White stork (Ciconia ciconia) (97) and the Turtle dove (Streptopelia turtur) (98). Migratory birds play an essential role in the long-distance movement of JEV serocomplex flaviviruses. When migrations between enzootic and areas free of WNV occur, birds that become infected prior to or during migration can actively transport the virus in their blood or tissues and infect mosquitoes and/or their predators (95). The establishment and maintenance of vector populations and the associated threat of vector-borne pathogen transmission in northern latitudes may be facilitated by global environmental change (98-99). Even non-migratory vultures make large dispersal movements and have a large foraging range (100), which explains why they can possibly help spread pathogens around.

The West Nile virus (WNV) poses a threat to endangered species around the world, such as the Iberian imperial eagle (Aquila adalberti) (101). The Egyptian vulture is a long-distance migratory species, as mentioned above (6), and therefore may be even more susceptible to contracting a WNV infection.

A successful introduction of the WNV in destination territories depends on the conditions for local maintenance, such as ecological key factors, which promote the virus maintenance and transmission, like presence and abundance of competent birds (hosts) and mosquitoes (vectors), and favorable abiotic conditions (102-103). Temperature is the most frequently used environmental condition regarding the WNV and/or its vectors, followed by precipitation (102). Mediterranean savannahs, in Spanish known as 'dehesas' and in Portuguese 'montados', are found in regions with mild, rainy winters and very hot, dry summers occupied by an agro-silvopastoral landscape in the Southwest of the Iberian Peninsula. These areas are threatened by climate change and the abandonment of traditional uses, and are therefore protected under the European Habitats Directive (104-105). Mediterranean 'dehesas' or 'montados' hold a very important fraction of the European populations of some endangered avian scavengers such as cinereous and Egyptian vultures, as well as other endemic globally endangered top predators. Foraging griffon vultures from different populations located across Western Europe make long trips into these regions of the Iberian Peninsula, suggesting that these areas have a beneficial added value for griffon vultures and other avian species, also providing the main habitat for wintering bird species that come from Northerly latitudes (104,106). According to Casades-Martí (103), this continental Mediterranean territory, with wildlife–livestock interaction, is favorable to the circulation on the WNV and other flaviviruses. Interactions between wild birds and farm animals are more likely to occur here, resulting in a higher probability of exposure to flaviviruses (107). Although mosquitoes are considered the main vectors of WNV, this agent has occasionally been isolated from other hematophagous arthropods, namely argasid and amblyommine ticks (93). As other soaring bird species, griffon vultures perform long-scale movements (106,108) and are considered a partial migratory species, with juveniles (especially in the first year of live) crossing the Strait of Gibraltar to Africa during fall and returning to Europe in the following years (109).

The abundance of vectors is a relevant parameter for pathogen transmission. Those habitats more suitable to the expansion of Culex mosquitoes during peak times of the WNV transmission represent the highest risk for the potential spillover of WNV into human populations (110).

In spite of some ticks (soft ticks) being considered resident and sedentary (111), that does not mean they have a limited role in the circulation of infectious agents. Pathogens transmitted by these ticks can be spread into new areas taking advantage of the large foraging movements or migration of

its hosts, namely griffon vultures (106,108-109). Although ticks can be alternative vectors, a recent study in the Pyrenees (Northeastern Spain), flavivirus was detected in all seven vultures' blood samples by the generic qRT-PCR, but all analyzed ticks were negative for flavivirus detection, which reinforces the potential involvement of other more common arthropod vectors, like mosquitoes, in the transmission of the virus (112-113).

Scavengers are susceptible to be infected by consuming WNV-infected carcasses (40,83). The WNV activity is far more likely to be detected in urban areas than in rural areas, suggesting that human density and associated factors should be considered when interpreting dead wild bird surveillance for the WNV (83). Long-lived avian scavengers are affected by the habitat where they live, anthropized landscapes being considered a more stressful habitat. Birds that live there generally present poor body condition and are more vulnerable to disease. Foraging in more anthropized areas can bring both advantages and disadvantages in terms of energy balance and stress. In these territories, availability and predictability of food is likely higher, but data suggest, on the other hand, that the food quality is not so good, leading to a poor nutritional status (114), which contributes to higher levels of circulating glucocorticoids. Concurrent factors that lead to lower immunity must be taken in consideration, such as the risk of lead accumulation, ingested from hunting ammunition, or severe competition in a high density and challenging environment, especially in highly social species, like griffon vultures, or less capable species, for example Egyptian vultures (115). It is known that the WNV has killed many thousands of birds around the world, but it is difficult to measure the long-term impact of the disease on wildlife populations.

Deforestation, besides being a major cause of biodiversity loss by itself and causing a negative impact on human health (116-117), is linked to the emergence of zoonotic and vector-borne diseases, like the WNV. Deforestation can increase contact between vectors and avian reservoirs. Forest loss may facilitate exchanges between human and zoonotic cycles, as open areas favor the human presence and settlement (116). The relationship between deforestation and the occurrence of zoonotic outbreaks has already been suggested (90,117), and should be further investigated for WNV.

There are relatively few reports of infectious diseases as a direct and primary cause of mortality in avian scavengers, and it has been a neglected topic of research so far. Given the current decline in scavenging bird populations, baseline information on exposure to infectious agents will be helpful for monitoring population health and investigating future disease-related epidemics, thus helping to guide conservation efforts. Although WNV infections have been registered in numerous species of birds of prey in Europe and North America, actual rates of morbidity and mortality associated with the WNV in wild raptors' populations remain unknown. The implementation of a collaborative international, holistic and multi-disciplinary One Health action is crucial to allow a more accurate risk assessment and an early response to the WNV and other emerging zoonotic pathogens. The presence of the WNV in vultures may therefore have public health and wildlife conservation implications and deserves further investigation.

References

1. Houston DC, Cooper JE. The digestive tract of the whiteback griffon vulture and its role in disease transmission among wild ungulates. J Wildl Dis 1975; 11: 306–13.
2. Moleón M, Sánchez-Zapata JA, Margalida A, Carrete M, Owen-Smith N, Donázar JA. Humans and scavengers: the evolution of interactions and ecosystem services, BioScience 2014; 64(5): 394–403. doi: 10.1093/biosci/biu034
3. Arbulu S, Jiménez JJ, Gútiez L, et al. Evaluation of bacteriocinogenic activity, safety traits and biotechnological potential of fecal lactic acid bacteria (LAB), isolated from Griffon Vultures (Gyps fulvus subsp. fulvus). BMC Microbiol 2016; 16(1): 228. doi: 10.1186/s12866-016-0840-2
4. Blumstein DT, Rangchi TN, Briggs T, De Andrade FS, Natterson-Horowitz B. A systematic review of carrion eaters' adaptations to avoid sickness. J Wildl Dis 2017; 53(3): 577–81. doi: 10.7589/2016-07-162
5. Plaza P, Blanco G, Lambertucci S. Implications of bacterial, viral and mycotic microorganisms in vultures for wildlife conservation, ecosystem services and public health. Ibis 2020; 162(4): 1109-–24. doi: 10.1111/ibi.12865
6. BirdLife International and Handbook of the Birds of the World 2021. The IUCN Red List of Threatened Species, Version 2022–2. https://www.iucnredlist.org/ (27. 9. 2023).
7. Hiraldo F, Delibes M . El quebrantahuesos Gypaetus barbatus (L.). sistemática, taxonomía, biología, distribución y protección. Madrid: Instituto para la Conservación de la Naturaleza, 1979.
8. Donázar JA, Palacios CJ, Gangoso L, Ceballos O, González MJ, Hiraldo F. Conservation status and limiting factors in the endangered population of Egyptian vulture (Neophron percnopterus) in the Canary Islands. Biol Conserv 2002; 107; 89–97. doi: 10.1016/S0006-3207(02)00049-6
9. Thiollay J-M. The decline of raptors in West Africa: long-term assessment and the role of protected areas. Ibis 2006; 148(2): 240–54. doi: 10.1111/j.1474-919X.2006.00531.x
10. Angelov I, Hashim I, Oppel S. Persistent electrocution mortality of Egyptian Vultures Neophron percnopterus over 28 years in East Africa. Bird Conserv Int 2013; 23(1): 1–6. doi: 10.1017/S0959270912000123
11. Cortés-Avizanda A, Jovani R, Carrete M, Donázar JA. Resource unpredictability promotes species diversity and coexistence in an avian scavenger guild: a field experiment. Ecology 2012; 93(12): 2570–9. doi: 10.1890/12-0221.1
12. Pirastru M, Mereu P, Manca L, Bebbere D, Naitana S, Leoni GG. Anthropogenic drivers leading to population decline and genetic preservation of the Eurasian griffon vulture (Gyps fulvus). Life (Basel) 2021; 11(10): 1038. doi: 10.3390/life11101038
13. Virani MZ, Kendall C, Njoroge P, Thomsett S. Major declines in the abundance of vultures and other scavenging raptors in and around the Masai Mara ecosystem, Kenya. Biol Conserv 2011; 144(2): 746–52. doi: 10.1016/j.biocon.2010.10.024

14. Cabral MJ, Almeida J, Almeida PR, et al. Livro Vermelho dos Vertebrados de Portugal. Lisboa: Instituto da Conservação da Natureza, 2005: 215–6.

15. Ives AM, Brenn-White M, Buckley JY, Kendall CJ, Wilton S, Deem SL. A global review of causes of morbidity and mortality in free-living vultures. EcoHealth 2022; 19(1): 40–54. doi: 10.1007/s10393-021-01573-5

16. Garcês A, Pires I, Sargo R, Sousa L, Prada J, Silva F. Admission causes, morbidity, and outcomes in scavenger birds in the North of Portugal (2005–2022). Animals (Basel) 2023; 13(13): 2093. doi: 10.3390/ani13132093

17. Hugh-Jones ME, De Vos V. Anthrax and wildlife. Rev Sci Tech 2002; 21(2): 359–83. doi: 10.20506/rst.21.2.1336

18. Ohishi I, Sakaguchi G, Riemann H, Behymer D, Hurvell B. Antibodies to Clostridium botulinum toxins in free-living birds and mammals. J Wildl Dis 1979; 15(1): 3–9. doi: 10.7589/0090-3558-15.1.3

19. Duriez O, Sassi Y, Le Gall-Ladevèze C, et al. Highly pathogenic avian influenza affects vultures' movements and breeding output. Curr Biol 2023; 33(17): 3766–74.e3. doi: 10.1016/j.cub.2023.07.061

20. Movalli P, Krone O, Osborn D, Pain D. Monitoring contaminants, emerging infectious diseases and environmental change with raptors, and links to human health. Bird Study 2018; 65(10): 1–10. doi: 10.1080/00063657.2018.1506735

21. European Food Safety Authority (EFSA). The European Union One health 2022 zoonoses report. EFSA J 2023; 21: e8442. doi: 10.2903/j.efsa.2023.8442

22. May FJ, Davis CT, Tesh RB, Barrett AD. Phylogeography of West Nile virus: from the cradle of evolution in Africa to Eurasia, Australia, and the Americas. J Virol 2011; 85(6): 2964–74.

23. Hernández-Triana LM, Jeffries CL, Mansfield KL, Carnell G, Fooks AR, Johnson N. Emergence of West Nile virus lineage 2 in Europe: a review on the introduction and spread of a mosquito-borne disease. Front Public Health 2014; 2: 271. doi: 10.3389/fpubh.2014.00271

24. Habarugira G, Suen WW, Hobson-Peters J, Hall RA, Bielefeldt-Ohmann, H. West Nile virus: an update on pathobiology, epidemiology, diagnostics, control and "One Health" implications. Pathogens 2020; 9(7): 589. doi: 10.3390/pathogens9070589

25. García-Carrasco JM, Muñoz AR, Olivero J, Segura M, Real R. Mapping the risk for West Nile virus transmission, Africa. Emerg Infect Dis 2022; 28(4): 777–85. doi: 10.3201/eid2804.211103

26. Watts MJ, Monteys VSI, Mortyn PG, Kotsila P. The rise of West Nile virus in Southern and Southeastern Europe: a spatial-temporal analysis investigating the combined effects of climate, land use and economic changes. One Health 2021; 13: 100315. doi: 10.1016/j.onehlt.2021.100315

27. Young JJ, Haussig JM, Aberle SW, et al. Epidemiology of human West Nile virus infections in the European Union and European Union enlargement countries, 2010 to 2018. Euro Surveill 2021; 26(19): 2001095. doi: 10.2807/1560-7917.ES.2021.26.19.2001095

28. Lanciotti RS, Ebel GD, Deubel V, et al. Complete genome sequences and phylogenetic analysis of West Nile virus strains isolated from the United States, Europe, and the Middle East. Virology. 2002; 298(1): 96–105. doi: 10.1006/viro.2002.1449

29. Pachler K, Lebl K, Berer D, Rudolf I, Hubalek Z, Nowotny N. Putative new West Nile virus lineage in Uranotaenia unguiculata mosquitoes, Austria, 2013. Emerg Infect Dis 2014; 20(12): 2119–22. doi: 10.3201/eid2012.140921

30. Valiakos G, Touloudi A, Iacovakis C, et al. Molecular detection and phylogenetic analysis of West Nile virus lineage 2 in sedentary wild birds (Eurasian magpie), Greece, 2010. Euro Surveill 2011; 16(18): 19862.

31. Savini G, Capelli G, Monaco F, et al. Evidence of West Nile virus lineage 2 circulation in Northern Italy. Vet Microbiol 2012; 158(3/4): 267–73. doi: 10.1016/j.vetmic.2012.02.018

32. Gamino V, Höfle, U. Pathology and tissue tropism of natural West Nile virus infection in birds: a review. Vet Res 2013; 44(1): 39. doi: 10.1186/1297-9716-44-39

33. Campbell GL, Marfin AA, Lanciotti RS, Gubler DJ. West Nile virus. Lancet Infect Dis 2002; 2(9): 519–29. doi: 10.1016/s1473-3099(02)00368-7

34. Samuel MA, Diamond MS. Pathogenesis of West Nile Virus infection: a balance between virulence, innate and adaptive immunity, and viral evasion. J Virol 2006; 80(19): 9349–60. doi: 10.1128/JVI.01122-06

35. Sejvar JJ. Clinical manifestations and outcomes of West Nile virus infection. Viruses 2014; 6(2): 606–23. doi: 10.3390/v6020606.

36. Van der Meulen KM, Pensaert MB, Nauwynck HJ. West Nile virus in the vertebrate world. Arch Virol 2005; 150(4): 637–57. doi: 10.1007/s00705-004-0463-z

37. Nemeth NM, Kratz GE, Bates R, Scherpelz JA, Bowen RA, Komar N. Clinical evaluation and outcomes of naturally acquired West Nile virus infection in raptors. J Zoo Wildl Med 2009; 40(1): 51–63. doi: 10.1638/2007-0109.1

38. Vidaña B, Busquets N, Napp S, Pérez-Ramírez E, Jiménez-Clavero MÁ, Johnson N. The role of birds of prey in West Nile virus epidemiology. Vaccines (Basel) 2020; 8(3): 550. doi: 10.3390/vaccines8030550

39. Kritzik KL, Kratz G, Panella NA, Burkhalter K, Clark RJ, Biggerstaff BJ, Komar N. Determining raptor species and tissue sensitivity for improved West Nile virus surveillance. J Wildl Dis 2018; 54(3): 528–33. doi: 10.7589/2017-12-292

40. Komar N, Langevin S, Hinten S, et al. Experimental infection of North American birds with the New York 1999 strain of West Nile virus. Emerg Infect Dis 2003; 9(3): 311–22. doi: 10.3201/eid0903.020628

41. Hull J, Hull A, Reisen W, Fang Y, Ernst H. Variation of West Nile virus antibody prevalence in migrating and wintering hawks in central California. Condor 2006; 108: 435–9.

42. Jiménez-Clavero MÁ. Animal viral diseases and global change: bluetongue and West Nile fever as paradigms. Front Genet 2012; 3: 105. doi: 10.3389/fgene.2012.00105

43. Nemeth NM, Gould DH, Bowen RA, Komar N. Natural and experimental West Nile virus infection in five raptor species. J Wildl Dis 2006; 42: 1–13. doi: 10.7589/0090-3558-42.1.1.

44. Ziegler U, Angenvoort J, Fischer D, et al. Pathogenesis of West Nile virus lineage 1 and 2 in experimentally infected large falcons. Vet Microbiol 2013; 161(3/4): 263–73. doi: 10.1016/j.vetmic.2012.07.041

45. Bergmann F, Fischer D, Fischer L, et al. Vaccination of zoo birds against West Nile Virus – a field study. Vaccines (Basel) 2023; 11(3): 652. doi: 10.3390/vaccines11030652

46. Steele KE, Linn MJ, Schoepp RJ, et al. Pathology of fatal West Nile virus infections in native and exotic birds during the 1999 outbreak in New York City, New York. Vet Pathol 2000; 37(3): 208–24. doi: 10.1354/vp.37-3-208

47. D'Agostino JJ, Isaza R. Clinical signs and results of specific diagnostic testing among captive birds housed at zoological institutions and infected with West Nile virus. J Am Vet Med Assoc 2004; 224(19): 1640–3. doi: 10.2460/javma.2004.224.1640

48. Jiménez de Oya N, Escribano-Romero E, Blázquez AB, Martín-Acebes MA, Saiz JC. Current progress of avian vaccines against West Nile virus. Vaccines (Basel) 2019; 7(4): 126. doi: 10.3390/vaccines7040126

49. Joyner PH, Kelly S, Shreve AA, Snead SE, Sleeman JM, Pettit DA. West Nile virus in raptors from Virginia during 2003: clinical, diagnostic, and epidemiologic findings. J Wildl Dis 2006; 42(2): 335–44. doi: 10.7589/0090-3558-42.2.335

50. Saggese MD. West Nile virus in Neotropical raptors: should we be concerned? In: Neotropical Raptors. Texas: College of Veterinary medicine and biomedical sciences, 2007: 149–73.

51. Ferraguti M, De La Puente JM, Soriguer R, Llorente F, Jiménez-Clavero, MÁ, Figuerola J. West Nile virus-neutralizing antibodies in wild birds from southern Spain. Epidemiol Infect 2016; 144(9): 1907–11. doi: 10.1017/S0950268816000133

52. Hahn DC, Nemeth NM, Edwards E, Bright PR, Komar N. Passive West Nile virus antibody transfer from maternal Eastern screech-owls (Megascops asio) to progeny. Avian Dis 2006; 50(3): 454–5. doi: 10.1637/7509-012606R1.1

53. Nemeth NM, Kratz GE, Bates R, Scherpelz JA, Bowen RA, Komar N. Naturally induced humoral immunity to West Nile virus infection in raptors. Ecohealth 2008; 5(3): 298–304. doi: 10.1007/s10393-008-0183-z

54. MarraPP,GriffingS,CaffreyC,etal.WestNilevirusandwildlife.BioScience 2004; 54(5): 393–402. doi: 10.1641/0006-3568(2004)054[0393:WNVAW]2.0.CO;2

55. Wünschmann A, Shivers J, Bender J, et al. Pathologic and immunohistochemical findings in Goshawks (Accipiter gentilis) and Great Horned Owls (Bubo virginianus) naturally infected with West Nile virus. Avian Dis 2005; 49(2): 252–9.. doi: 10.1637/7297-103104R

56. Palmieri C, Franca M, Uzal F, et al. Pathology and immunohistochemical findings of West Nile virus infection in Psittaciformes. Vet Pathol 2011; 48(5): 975–84. doi: 10.1177/0300985810391112

57. Phalen DN, Dahlhausen B. West Nile virus. Semin. Avian Exot. Pet Med. 2004; 13: 67–78.

58. Jones MP. Selected infectious diseases of birds of prey. J Exot Pet Med 2006; 15(1): 5–17. doi:10.1053/j.jepm.2005.11.008

59. Wodak E, Richter S, Bagó Z, et al. Detection and molecular analysis of West Nile virus infections in birds of prey in the eastern part of Austria in 2008 and 2009. Vet Microbiol 2011; 149(3/4): 358–66. doi: 10.1016/j.vetmic.2010.12.012

60. Bakonyi T, Ferenczi E, Erdelyi K, et al. Explosive spread of a neuroinvasive lineage 2 West Nile virus in Central Europe, 2008/2009. Vet Microbiol 2013; 165(1/): 61–70. doi: 10.1016/j.vetmic.2013.03.005

61. García-Bocanegra I, Busquets N, Napp S, et al. Serosurvey of West Nile virus and other flaviviruses of the Japanese encephalitis antigenic complex in birds from Andalusia, southern Spain. Vector Borne Zoonotic Dis 2011; 11(8): 1107–13. doi: 10.1089/vbz.2009.0237

62. Busquets N, Laranjo-González M, Soler M, et al. Detection of West Nile virus lineage 2 in North-Eastern Spain (Catalonia). Transbound Emerg Dis 2019; 66(2): 617–21. doi: 10.1111/tbed.13086

63. Bakhshi H, Beck C, Lecollinet S, et al. Serological evidence of West Nile virus infection among birds and horses in some geographical locations of Iran. Vet Med Sci 2021; 7(1): 204–9. doi: 10.1002/vms3.342

64. García-Ripollés C, López-López P, Urios V. First description of migration and wintering of adult Egyptian Vultures Neophron percnopterus tracked by GPS satellite telemetry. Bird study 2010; 57(2): 261–5. 10.1080/00063650903505762

65. Phipps WL, López-López P, Buechley ER. Spatial and temporal variability in migration of a soaring raptor across three continents. Front Ecol Evol 2019; 7: 1–14. 10.3389/fevo.2019.00323

66. Bravo-Barriga D, Aguilera-Sepúlveda P, Guerrero-Carvajal F, et al. West Nile and Usutu virus infections in wild birds admitted to rehabilitation centres in Extremadura, western Spain, 2017–2019. Vet Microbiol 2021; 255: 109020. doi: 10.1016/j.vetmic.2021.109020

67. Marinković D, Nešić V, Davitkov D, Aničić M. Causes of morbidity and mortality in European griffon vulture (Gyps fulvus) population in Serbia in the period of 2018–2022 – post-mortem findings. J Comp Pathol 2023; 203: 52. doi: 10.1016/j.jcpa.2023.03.042

68. Nash D, Mostashari F, Fine A, et al. The outbreak of West Nile virus infection in the New York City area in 1999. N Engl J Med 2001; 344(4): 1807–14. doi: 10.1056/NEJM200106143442401

69. Rideout BA, Stalis I, Papendick R, et al. Patterns of mortality in free-ranging California Condors (Gymnogyps californianus). J Wildl Dis 2012; 48(1): 95–112. doi: 10.7589/0090-3558-48.1.95

70. Straub MH, Kelly TR, Rideout BA, et al. Seroepidemiologic survey of potential pathogens in obligate and facultative scavenging avian species in California. PLoS One 2015; 10: e0143018. doi: 10.1371/journal.pone.0143018

71. Terraube J, Andevski J, Loercher F, Tavares J. Population estimates for the five European vulture species. Arnhem: The Vulture Conservation Foundation, 2022.

72. Schönenberger AC, Wagner S, Tuten HC, et al. Host preferences in host-seeking and blood-fed mosquitoes in Switzerland. Med Vet Entomol 2016; 30(1): 39–52. doi: 10.1111/mve.12155

73. Nemeth NM, Hahn DC, Gould DH, Bowen RA. Experimental West Nile virus infection in Eastern Screech Owls (Megascops asio). Avian Dis 2006; 50(2): 252–8. doi: 10.1637/7466-110105R1.1.

74. Ip HS, Van Wettere AJ, McFarlane L, et al. West Nile virus transmission in winter: the 2013 Great Salt Lake bald eagle and eared grebes mortality event. PLoS Curr. 2014; 6. doi: 10.1371/currents.outbreaks.b0f031fc8db2a827d9da0f30f0766871

75. Komar N, Lanciotti R, Bowen R, Langevin S, Bunning M. Detection of West Nile virus in oral and cloacal swabs collected from bird carcasses. Emerg Infect Dis 2002; 8(7): 741–2. doi: 10.3201/eid0807.020157

76. Heinz-Taheny KM, Andrews JJ, Kinsel MJ, et al. West Nile virus infection in free-ranging squirrels in Illinois. J Vet Diagn Invest 2004; 16(3): 186–90. doi: 10.1177/104063870401600302.

77. Bosè M, Duriez O, Sarrazin F. Intra-specific competition in foraging griffon vultures Gyps fulvus: 1. Dynamics of group feeding. Bird Study 2012; 59: 182–92. doi:10.1080/00063657.2012.658639

78. Donázar JA. Los buitres ibéricos: biología y conservación. Madrid: J. M. Reyero, 1993.

79. Donázar JA, Cortés-Avizanda A, Carrete M. Dietary shifts in two vultures after the demise of supplementary feeding stations: consequences of the EU sanitary legislation. Eur J Wildl Res. 2010; 56(4): 613–21. doi: 10.1007/s10344-009-0358-0

80. Houston DC, Meeb A, McGradyc M. Why do condors and vultures eat junk?: the implications for conservation. J Raptor Res 2007; 41: 235–8. doi: 10.3356/0892-1016(2007)41[235:WDCAVE]2.0.CO;2

81. Benmazouz I, Jokimäki J, Lengyel S, et al. Corvids in urban environments: a systematic global literature review. Animals. 2021; 11: 3226.

82. McLean RG, Ubico SR, Docherty DE, Hansen WR, Sileo L, McNamara TS. West Nile virus transmission and ecology in birds. Ann N Y Acad Sci 2001; 951: 54–7. doi: 10.1111/j.1749-6632.2001.tb02684.x

83. Ward MR, Stallknecht DE, Willis J, Conroy MJ, Davidson WR. Wild bird mortality and West Nile virus surveillance: biases associated with detection, reporting, and carcass persistence. J Wildl Dis 2006; 42(1): 92–106. doi: 10.7589/0090-3558-42.1.92

84. Jones KE, Patel NG, Levy MA, et al. Global trends in emerging infectious diseases. Nature 2008; 451(7181): 990–3. doi: 10.1038/nature06536

85. Smithburn KC, Hughes TP, Burke AW, Paul JH. A neurotropic virus isolated from the blood of a native of Uganda. Am J Trop Med Hyg 1940; s1-20: 471–92. doi: 10.4269/AJTMH.1940.S1-20.471

86. Taylor RM, Work TH, Hurlbut HS, Rizk F. A study of the ecology of West Nile virus in Egypt. Am J Trop Med Hyg 1956; 5(4): 579–20. doi: 10.4269/ajtmh.1956.5.579

87. Mencattelli G, Ndione MHD, Rosà R, et al. Epidemiology of West Nile virus in Africa: an underestimated threat. PLoS Negl Trop Dis 2022; 16(1): e0010075. doi: 10.1371/journal.pntd.0010075

88. Joubert L, Oudar J, Hannoun C, Beytout D, Corniou B, Guillon JC, Panthier R. [Epidemiology of the West Nile virus: study of a focus in Camargue. IV. Meningo-encephalomyelitis of the horse]. Ann Inst Pasteur (Paris) 1970; 118(2): 239–47.

89. Tsai TF, Popovici F, Cernescu C, Campbell GL, Nedelcu NI. West Nile encephalitis epidemic in Southeastern Romania. Lancet 1998; 352(9130): 767–71. doi: 10.1016/s0140-6736(98)03538-7

90. García-Carrasco JM, Muñoz AR, Olivero J, Figuerola J, Fa JE, Real R. Gone (and spread) with the birds: can chorotype analysis highlight the spread of West Nile virus within the Afro-Palaearctic flyway? One Health 2023; 17: 100585. doi: 10.1016/j.onehlt.2023.100585

91. Rappole JH, Derrickson SR, Hubálek Z. Migratory birds and spread of West Nile virus in the Western Hemisphere. Emerg Infect Dis 2000; 6(4): 319–28. doi: 10.3201/eid0604.000401

92. Nir Y, Goldwasser R, Lasowski Y, Avivi A. Isolation of arboviruses from wild birds in Israel. Am J Epidemiol 1967; 86(2): 372–8. doi: 10.1093/oxfordjournals.aje.a120747

93. Hubálek Z, Halouzka J. West Nile fever – a reemerging mosquito-borne viral disease in Europe. Emerg Infect Dis 1999; 5(5): 643–50. doi: 10.3201/eid0505.990505

94. Jupp PG. The ecology of West Nile virus in South Africa and the occurrence of outbreaks in humans. Ann N Y Acad Sci 2001; 951: 143–2. doi: 10.1111/j.1749-6632.2001.tb02692.x.

95. López G, Jiménez-Clavero MA, Tejedor CG, Soriguer R, Figuerola J. Prevalence of West Nile virus neutralizing antibodies in Spain is related to the behavior of migratory birds. Vector Borne Zoonotic Dis 2008; 8(5): 615–21. doi: 10.1089/vbz.2007.0200.

96. Lord RD, Calisher CH. Further evidence of southward transport of arboviruses by migratory birds. Am J Epidemiol 1970; 92(1): 73–8. doi: 10.1093/oxfordjournals.aje.a121181

97. Malkinson M, Banet C, Weisman Y, et al. Introduction of West Nile vi-rus in the Middle East by migrating white storks. Emerg Infect Dis 2002; 8(4): 392–7. doi: 10.3201/eid0804.010217

98. Smith KA, Campbell GD, Pearl DL, Jardine CM, Salgado-Bierman F, Nemeth NM. A retrospective summary of raptor mortality in Ontario, Canada (1991-2014), including the effects of West Nile virus. J Wildl Dis 2018; 54(2): 261–71. doi: 10.7589/2017-07-157

99. Giesen C, Herrador Z, Fernandez-Martinez B, et al. A systematic review of environmental factors related to WNV circulation in European and Mediterranean countries. One Health 2023; 16: 100478. doi: 10.1016/j.onehlt.2022.100478

100. Fluhr J, Benhamou S, Peyrusque D, Duriez O. Space use and time budget in two populations of griffon vultures in contrasting landscapes. J. Raptor Res 2021; 55(3): 425–37. doi: 10.3356/JRR-20-14

101. Höfle U, Blanco JM, Crespo E, et al. West Nile virus in the endangered Spanish imperial eagle. Vet Microbiol 2008; 129(1/2): 171–8. doi: 10.1016/j.vetmic.2007.11.006

102. Brugueras S, Fernández-Martínez B, Martínez-de la Puente J, et al. Environmental drivers, climate change and emergent diseases transmitted by mosquitoes and their vectors in southern Europe: a systematic review. Environ Res 2020; 191: 110038. doi: 10.1016/j.envres.2020.110038

103. Casades-Martí L, Holgado-Martín R, Aguilera-Sepúlveda P. Risk factors for exposure of wild birds to West Nile virus in a gradient of wildlife-livestock interaction. Pathogens 2023; 12(1): 83. doi: 10.3390/pathogens12010083

104. Díaz M, Campos P, Pulido FJ. The Spanish dehesas: a diversity of land use and wildlife. In: Pain D, Pienkowski M, eds. Farming and birds in Europe: The Common Agricultural Policy and its implications for bird conservation. London: Academic Press, 1997: 178–209.

105. European Environment Agency (EUNIS). https://eunis.eea.europa.eu/habitats/393 (23. 10. 2023).

106. Delgado-González A, Cortés-Avizanda A, Serrano D, et al. Apex scavengers from different European populations converge at threatened savannah landscapes. Sci Rep 2022; 12: 2500. doi: 10.1038/s41598-022-06436-9

107. Guerrero-Carvajal F, Bravo-Barriga D, Martín-Cuervo M, et al. Serological evidence of co-circulation of West Nile and Usutu viruses in equids from western Spain. Transbound Emerg Dis 2021; 68(3): 1432–44. doi: 10.1111/tbed.13810

108. Morant J, Arrondo E, Sánchez-Zapata JA, et al. Large-scale movement patterns in a social vulture are influenced by seasonality, sex, and breeding region. Ecol Evol 2023; 13(2): e9817. doi: 10.1002/ece3.9817

109. Ramírez J, de Langarica FMZG, Molina MG. Spring migration of eurasian griffon vultures across the strait of Gi-braltar: number, timing and age composition. Ardeola 2019; 66(1): 113–8. doi: 10.13157/arla.66.1.2019.sc5

110. Adelman JS, Tokarz RE, Euken AE, Field EN, Russell MC, Smith RC. Relative influence of land use, mosquito abundance, and bird communities in defining West Nile virus infection rates in Culex mosquito populations. Insects 2022; 13(9): 758. doi:10.3390/insects13090758

111. Palomar AM, Veiga J, Portillo A, et al. Novel genotypes of nidicolous argas ticks and their associated microorganisms from Spain. Front Vet Sci 2021; 8: 637837. doi: 10.3389/fvets.2021.637837

112. Blahove MR, Carter JR. Flavivirus persistence in wildlife populations. Viruses 2021; 13(10): 2099. doi: 10.3390/v13102099

113. Moraga-Fernández A, Oliva-Vidal P, Sánchez-Sánchez M, et al. Health risks associated with argasid ticks, transmitted pathogens, and blood parasites in Pyrenean griffon vulture (Gyps fulvus) nestlings. Eur J Wildl Res 2023; 69: 112. 10.1007/s10344-023-01741-8

114. Cacho IM. Exposure and carriage of West Nile virus in feathered Iberian scavengers. Master's thesis: Uppsala University, Uppsala. 2022.

115. Gangoso L, Cortés-Avizanda A, Sergiel A, et al. Avian scavengers living in anthropized landscapes have shorter telomeres and higher levels of glucocorticoid hormones. Sci Total Environ 2021; 782: 146920. doi: 10.1016/j.scitotenv.2021.146920

116. FAO & UNEP. The State of the World's Forests 2020. Forests, Biodiversity and People. Rome: FAO & UNEP, 2020: 72–9.

117. Morand S, Lajaunie C. Outbreaks of vector-borne and zoonotic diseases are associated with changes in forest cover and oil palm expansion at global scale. Front Vet Sci 2021; 8: 661063. doi: 10.3389/fvets.2021.661063

Virus Zahodnega Nila pri jastrebih iz Evrope – opaznih med drugimi ujedami

F. Loureiro, L. Cardoso, A. Matos, M. Matos, A.C. Coelho

Izvleček: Virus Zahodnega Nila (WNV) je arbovirus, ki ga prenašajo predvsem Culex spp., in je povzročitelj zoonoze, prisotne po vsem svetu. Ta patogen se endemično ohranja v življenjskem ciklu, v katerem so ptice rezervoarji, ljudje in konji pa so naključni in končni gostitelji. V Evropi so poročali o sporadičnih izbruhih WNV, potencialni vpliv okužbe z WNV na populacijo ogroženih ptic ujed pa je lahko zelo velik. Za zgodnje odkrivanje tega virusa so potrebni programi nadzora. Vse štiri vrste jastrebov, ki živijo v Evropi, so zavarovane vrste. Kot mrhovinarji so jastrebi zaradi zasedanja vrha prehranjevalne verige lahko dovzetni za patogene, kot je WNV. Z varstvenega vidika je treba obravnavati neodvisen ali z drugimi dejavniki povezan vpliv WNV na evropske jastrebe. Ta pregled dokumentiranih primerov se lahko šteje kot izhodišče za ta namen.

Ključne besede: epidemiologija; Evropa; mrhovinarji; jastrebi; virus Zahodnega Nila; zoonoza

Slov Vet Res
DOI 10.26873/SVR-1920-2024
UDC 601.4:577.21:577.27
Pages: 245–61

Original Research Article

Comparative Analysis of Reference-Based Cell Type Mapping and Manual Annotation in Single Cell RNA Sequencing Analysis

Key words

single-cell transcriptomics;
peripheral blood mononuclear cells;
reference mapping;
cell-type annotation;
immune system

Larisa Goričan[1,†], Boris Gole[1,†], Gregor Jezernik[1], Gloria Krajnc[1,3], Uroš Potočnik[1,2,3], Mario Gorenjak[1]*

[1]Centre for Human Genetics and Pharmacogenomics, Faculty of Medicine, University of Maribor, Taborska ulica 8, SI-2000 Maribor, [2]Laboratory for Biochemistry, Molecular Biology and Genomics, Faculty of Chemistry and Chemical Engineering, University of Maribor, Smetanova ulica 17, SI-2000 Maribor, [3]Department for Science and Research, University Medical Centre Maribor, Ljubljanska ulica 5, SI-2000 Maribor, Slovenia, [†]Equal contribution

***Corresponding author:** mario.gorenjak@um.si

Abstract: Single-cell RNA sequencing (scRNA-seq) offers unprecedented insight into cellular diversity in complex tissues like peripheral blood mononuclear cells (PBMC). Furthermore, differential gene expression at a single-cell level can provide a basis for understanding the specialized roles of individual cells and cell types in biological processes and disease mechanisms. Accurate annotation of cell types in scRNA-seq datasets is, however, challenging due to the high complexity of the data. Here, we compare two cell-type annotation strategies applied to PBMCs in scRNA-seq datasets: automated reference-based tool Azimuth and unsupervised Shared Nearest Neighbor (SNN) clustering, followed by manual annotation. Our results highlight the strengths and limitations of the two approaches. Azimuth easily processed large-scale scRNA-seq datasets and reliably identified even relatively rare cell populations. It, however, struggled with cell types outside its reference range. In contrast, unsupervised SNN clustering clearly delineated all the different cell populations in a sample. This makes it well suited for identifying rare or novel cell types, but the method requires time-consuming and bias-prone manual annotation. To minimize the bias, we used rigorous criteria and the collaborative expertise of multiple independent evaluators, which resulted in the manual annotation that was closely related to the automated one. Finally, pseudo-temporal analysis of the major cell types further confirmed the validity of the Azimuth and manual annotations. In conclusion, each annotation method has its merits and downsides. Our research thus highlights the need to combine different clustering and annotation approaches to manage the complexity of scRNA-seq and to improve the reliability and depth of scRNA-seq analyses.

Received: 29 December 2023
Accepted: 23 April 2024

Introduction

Over the past decade, RNA sequencing (RNA-seq) has become an indispensable tool in molecular biology, providing unprecedented insights into the transcriptomic landscape of cells. (1) By deciphering the complexity of human, animal, and plant transcriptomes, this technique has greatly enhanced our understanding of biological processes, disease mechanisms, and therapeutic interventions. (2) However, conventional RNA-seq, which analyses bulk tissue samples, inherently averages the gene expression across many cells and cell types present in the sample, resulting in a loss of resolution at the level of individual cells/cell types. (3) This obscures the understanding of cellular heterogeneity and the roles of rare cell populations in tissue function and disease. (4)

The development of single-cell RNA sequencing (scRNA-seq) has revolutionized the field by providing a lens for exploring the transcriptome at single-cell resolution. (5) The scRNA-seq provides a high-resolution view of tissue cellular diversity. It enables a more detailed understanding of complex biological processes and disease pathogenesis by revealing cell heterogeneity in a given population. Furthermore, scRNA-seq allows for the study of differential gene expression at a single-cell level, which can provide insights into the unique functional roles of individual cells and contribute to a more nuanced understanding of biological processes and disease mechanisms. (6)

Despite its transformative potential, scRNA-seq also introduces unique analytical challenges. Among these, annotation of distinct cell populations in scRNA-seq datasets is a significant hurdle due to the high dimensionality and complexity of single-cell data. (7) To address this, various computational strategies have been developed. Azimuth, a publicly available automated cell-type annotation software (8), employs machine learning algorithms to predict human and murine cell identities based on scRNA-seq data. (9) In parallel, Seurat, a popular R package for scRNA-seq data analysis, offers clustering algorithms that partition single cells into distinct groups based on their transcriptomic profiles, providing an unbiased approach to cell population identification. (10) Manual annotation methods, on the other hand, employ in-depth biological knowledge to assign cell identities based on known marker genes and expression patterns. Such methods can leverage publicly available datasets, such as those available at the Human Protein Atlas (HPA) (11) or the multi-species Single Cell Expression Atlas (12), providing a robust, albeit time-consuming, strategy.

In this study, our primary goal was to perform a comprehensive comparative analysis of different strategies for annotating peripheral blood mononuclear cell (PBMC) populations in single-cell RNA sequencing datasets: Azimuth, an automated reference-based cell type annotation approach; Shared nearest neighbor (SNN) reference annotation naive approach, recommended by the authors of the Seurat single-cell analysis package for R as best practice (10); and manual annotation using two datasets publicly available at the HPA. We evaluated the performance of these methods in terms of accuracy, efficiency, and ability to handle the high dimensionality and complexity of scRNA-seq data. By exploring the strengths and limitations of each method, we aimed to provide critical insights that will help researchers choose the most effective strategy for annotating scRNA-seq datasets.

Material and methods

A schematic representation of the steps involved in data acquisition and analysis is shown in Figure 1.

Datasets

Datasets- raw sequencing reads were obtained from the publicly available 10X Genomics database portal. (13) To validate PBMC populations, we used single-cell datasets obtained from healthy human donors, containing 10.000 (pbmc10k) and 5.000 (pbmc5k) cells. The datasets used were 5k Peripheral Blood Mononuclear Cells (PBMCs) from a Healthy Donor (v3 chemistry) (https://www.10xgenomics.com/datasets/5-k-peripheral-blood-mononuclear-cells-pbm-cs-from-a-healthy-donor-v-3-chemistry-3-1-standard-3-0-2) and 10k PBMCs from a Healthy Donor - Gene Expression with a Panel of TotalSeq™-B Antibodies (https://www.10xgenomics.com/datasets/10-k-pbm-cs-from-a-healthy-donor-gene-expression-and-cell-surface-protein-3-standard-3-0-0). Both datasets were downloaded on 10.05.2023.

scRNA-seq data analysis

Raw fastq files were first aligned to reference genome GRCh38 using CellRanger 7.1.0 software (10x Genomics). Generated matrices were further analyzed using Seurat package v5 (8) in R environment (14). Matrices were imported using Seurat and converted to Seurat objects containing at least 200 features in 3 cells.

A comprehensive quality control was performed to remove objects indicating multiplets. For the pbmc10k sample, the multiplets rate was estimated at 7.8%, and for pbmc5k, at 3.9%. These rates were also confirmed with DoubletFinder. (15) Thus, for pbmc10k and pbmc5k, all objects with features above 4000 and below 500 (empty droplets) or objects flagged as high-confidence doublets were discarded. Additionally, all objects expressing more than 10% of mitochondrial genes, which is a commonly chosen threshold. (16) Additionally, this threshold was selected based on numbers presented in 10x technical note CG000130. Objects with less than 5% of ribosomal genes were also filtered out to ensure healthy cells are retained as immune cells should have a high fraction of ribosomal proteins (Figure 2a). (16) Subsequently, X- and Y- chromosome genes were removed from the datasets to avoid sex-specific statistical bias due to the unknown genders of the samples. The genes with the highest expression were examined. *MALAT1* (metastasis-associated lung adenocarcinoma transcript 1) was identified as an extensive outlier, most probably representing a common technical issue, and was therefore also removed.

Next, both sample datasets were pooled, and cell cycle genes were flagged to calculate cell cycle scoring. The RNA assay data was first normalized using SCTransform. (17) Then cell cycle scores were calculated on the new SCT assay and used to calculate the S cycle score minus G2M cycle score difference. SCTransform normalization was again performed using the RNA assay and regressed on the difference in cell-cycle scores and the percentage of mitochondrial genes. The new SCT assay was used for

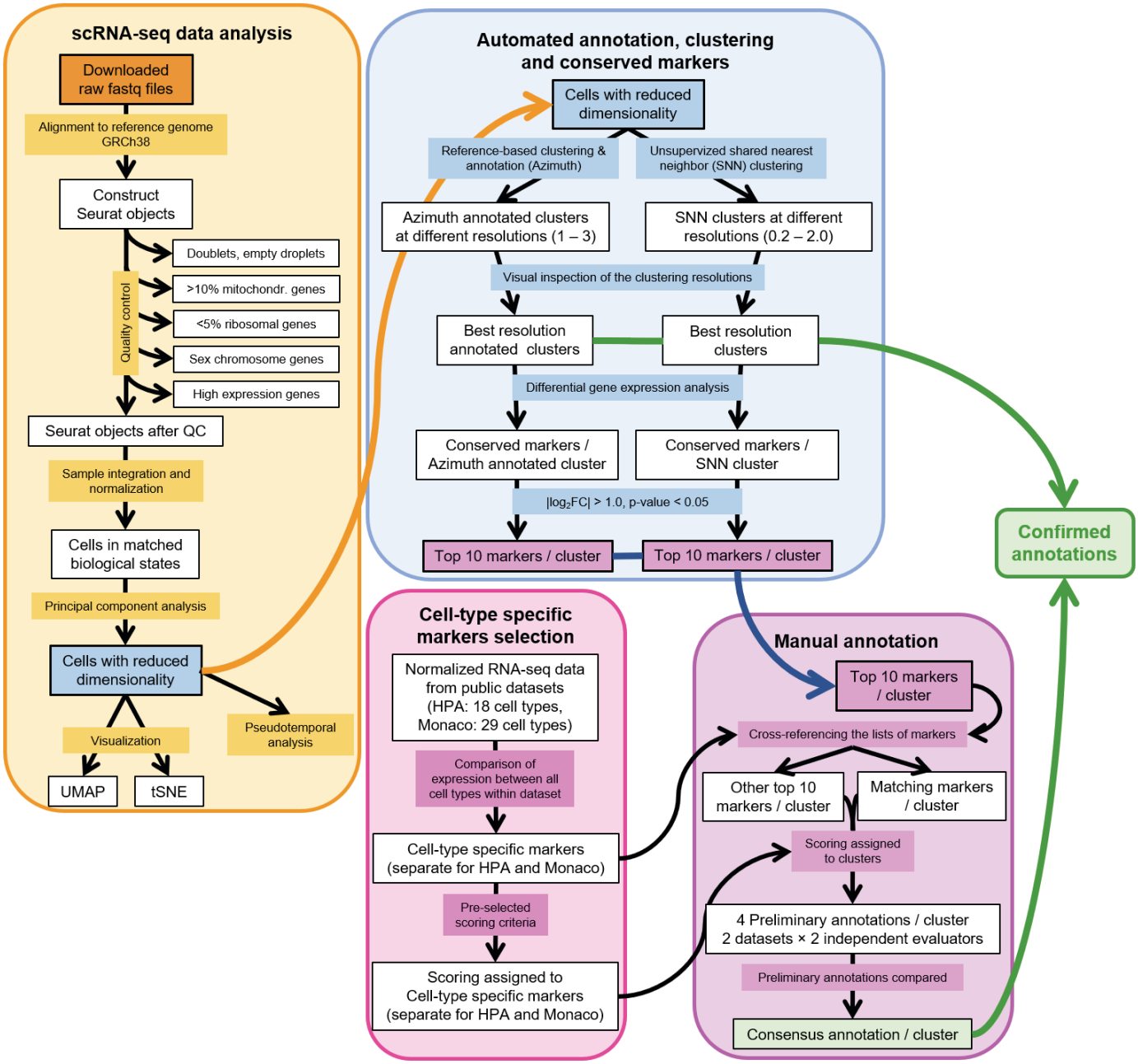

Figure 1: A schematic representation of the steps involved in data acquisition and analysis

downstream analysis and integration. We used at least 5000 features for the final anchor selection out of merged 18913 features across 10608 cells. Using integration, we identified the so-called anchors in the cross-dataset cell pairs that are in a matched biological state. These were used to correct for technical differences between datasets and align the cells between samples for comparative analyses. After integration, we performed principal component analysis for dimensionality reduction with 50 principal components (Figure 2b). Additionally, we performed uniform manifold approximation and projection (UMAP, Figure 2c) and t-distributed stochastic neighbor embedding (tSNE) analyses to visualize the high dimensional data obtained.

Automatic annotation, clustering, and conserved markers

First, automatic annotation was performed using Azimuth reference-based annotation of cells on three levels. (8) The human PBMC reference dataset was generated with 10x Genomics v3 as previously described. (8) Subsequently, the best cluster resolution was determined using the R package clustree. (18) Additionally, shared nearest-neighbor (SNN) modularity optimization clustering was deployed to cluster the cells (19).

The following resolutions were used for cluster granulation: 0.2, 0.4, 0.6, 0.8, 1.0, 1.4, 1.6, 1.8 and 2.0. After identifying

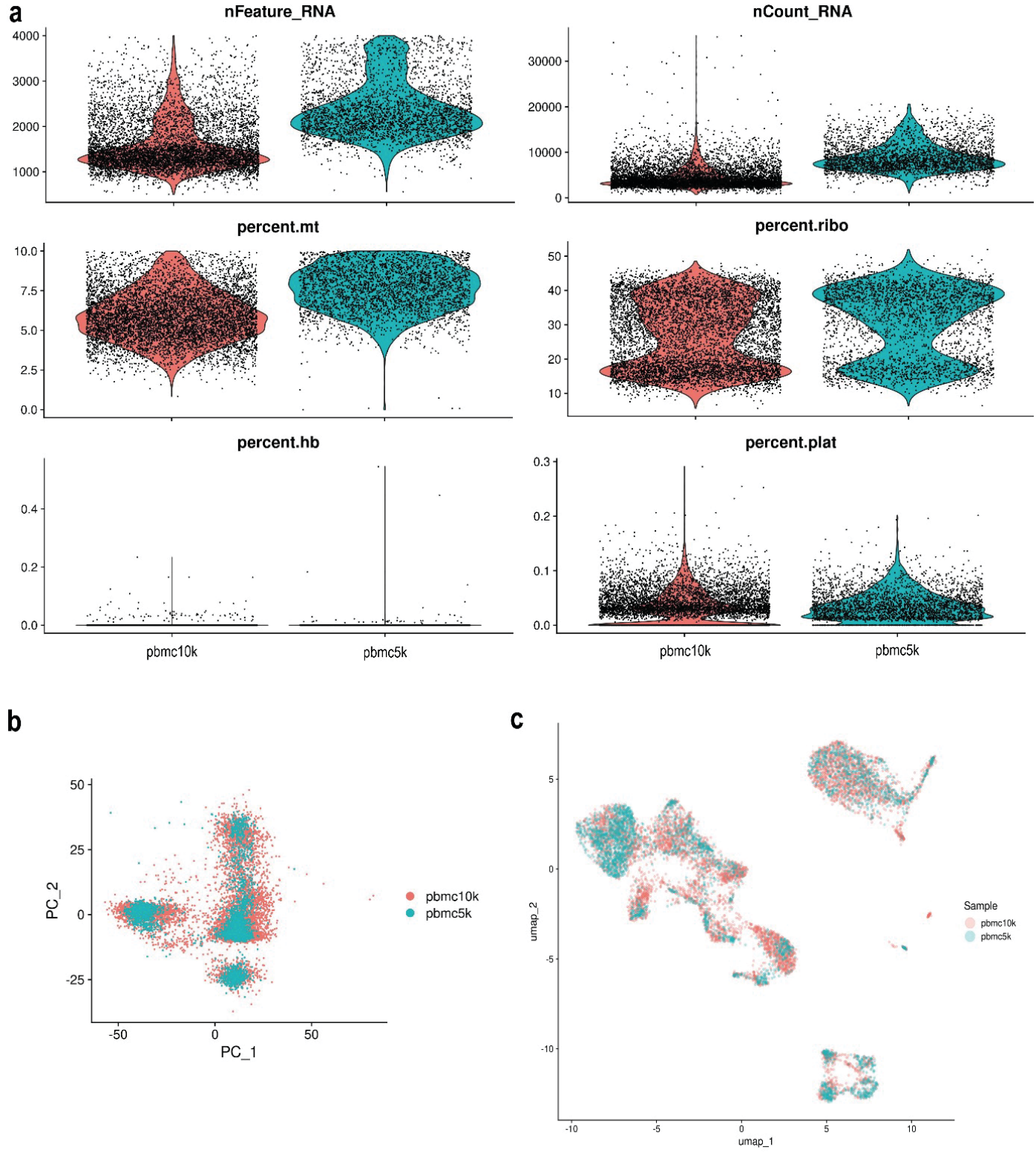

Figure 2: Quality control and dataset integration. (a) Dispersion of cells in datasets after quality control- Nfeature_RNA: number of genes per cell; nCount_RNA: number of transcripts per cell; percent.mt: percent of mitochondrial genes per cell; percent.ribo: percent of ribosomal genes per cell; percent.hb: percent of hemoglobin genes per cell; percent.plat: percent of platelet genes per cell. (b) PCA graph of the two datasets. (c) UMAP plot of aligned and integrated dataset cell landscape- pbmc10k dataset in background and pbmc5k dataset in foreground

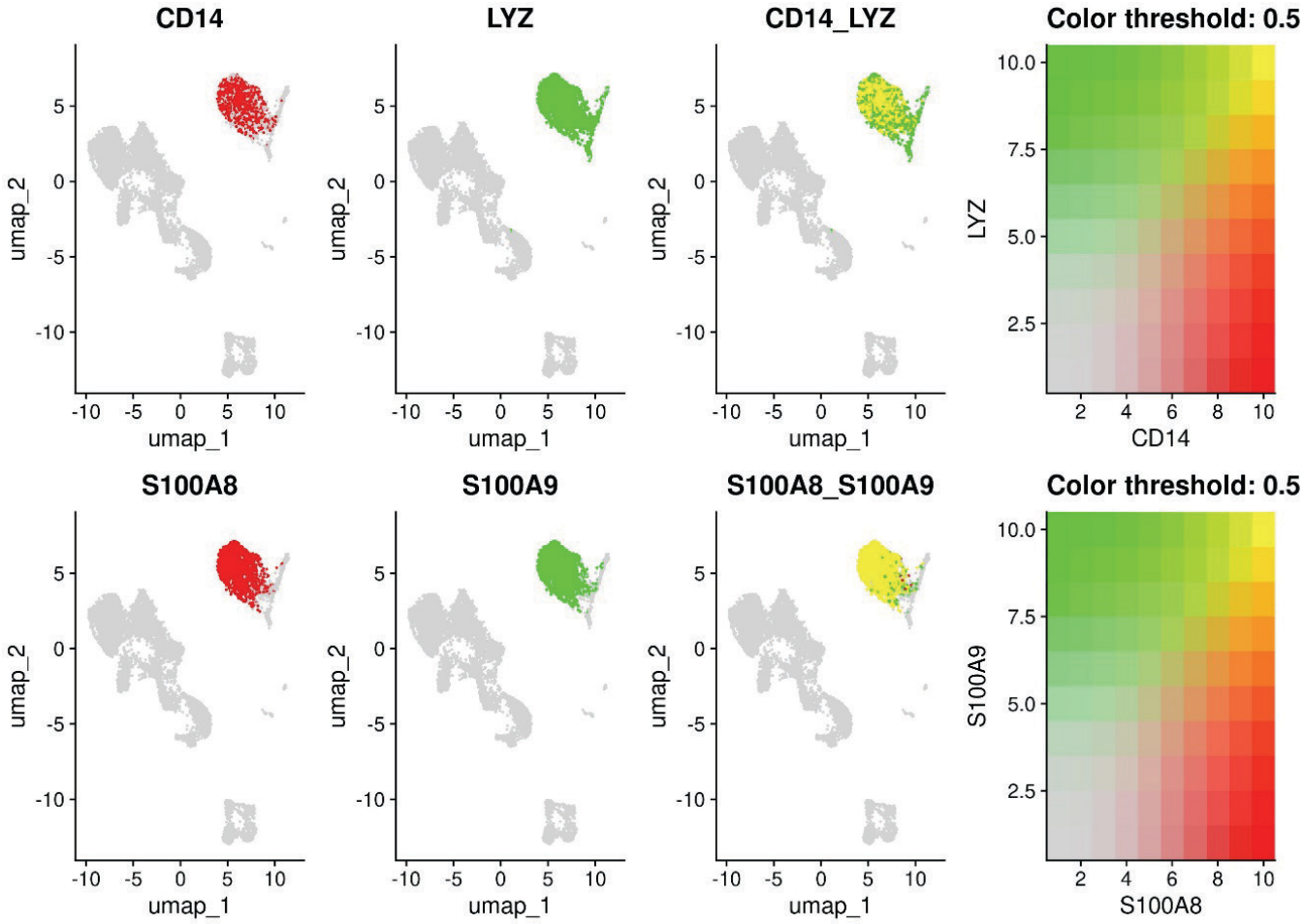

Figure 3: Visualization of selected conserved markers for classical (CD14+) monocytes. UMAP plots of *CD14* (CD14 molecule), *LYZ* (lysozyme), *S100A8* (S100 calcium-binding protein A8) and *S100A9* (S100 calcium-binding protein A9) expression, and of *CD14/LYZ* and *S100A8/S100A9* co-expression across the PBMC populations

the best annotation and cluster resolution, conserved cell-type markers with the same perturbation direction in both datasets were identified by differential gene expression testing. The MetaDE R package embedded in Seurat's FindConservedMarkers function was used for this purpose. (20) Conserved markers (see Figure 3 for an example) were only identified in cell populations where at least three cells were present in an independent sample.

Cell type-specific marker selection and manual cluster annotation

For manual annotation, we used two publicly available human datasets- the RNA HPA immune cell gene data (the HPA dataset) and the RNA Monaco immune cell gene data (the Monaco dataset), which we downloaded from the HPA website (https://www.proteinatlas.org/about/download) on 23.6.2023. The HPA dataset contains transcription data on 18 immune cell types from blood generated within the HPA project (21), while the Monaco dataset is based on the RNA-seq data generated on 29 FACS-sorted immune cell types from the PBMC of healthy donors. (22) The pipeline used to generate both datasets from the raw RNA-seq data, including quality control and normalization, is described on the HPA website. The downloaded datasets are based on The HPA version 23.0 and Ensembl version 109.

For both annotation datasets, we separately determined cell type-specific markers based on the normalized gene expression values, with a cutoff value of 4 as described on the HPA website (https://www.proteinatlas.org/about/assays+annotation#hpa_rna). Genes whose normalized expression levels in a specific immune cell type were at least 4× higher than in any other immune cell type were considered cell type-specific markers for that specific immune cell type. Similarly, genes whose normalized expression in a group of two or three immune cell types was at least 4× higher than in any other immune cell type were considered twin or group markers, respectively. In addition to the markers for the immune cell types defined in the two datasets, we also determined specific markers for several broader groups of immune cell types, for example, total CD8+ T-cells (comprised of Naïve CD8+ T-cell, Central memory CD8+ T-cells, Effector memory CD8+ T-cells and Terminal effector memory CD8+ T-cells in the Monaco dataset). For these marker genes, it was defined that the lowest

Table 1: Immune cell type-specific markers

Marker		Scoring			Nr. of markers	
Type	**Definition**	**Cell type 1**	**Cell type 2**	**Cell type 3**	**HPA dataset**	**Monaco dataset**
Single	nEL in CT1 > 4× nEL in any other CT	8	/	/	1821	1581
Twin 2	nEL in CT1, CT2 > 4× nEL in any other CT nEL in CT1 ≈ nEL in CT2	4	4	/	594	458
Twin 1+1	nEL in CT1, CT2 > 4× nEL in any other CT nEL in CT1 > 4× nEL in CT2	8	4	/	224	149
Group 3	nEL in CT1, CT2, CT3 > 4× nEL in any other CT nEL in CT1 ≈ nEL in CT2 ≈ nEL in CT3	2	2	2	436	273
Group 2+1	nEL in CT1, CT2, CT3 > 4× nEL in any other CT nEL in CT1 ≈ nEL in CT2 nEL in CT1, CT2 >4× nEL in CT3	4	4	2	36	25
Group 1+2	nEL in CT1, CT2, CT3 > 4× nEL in any other CT nEL in CT1 > 4× nEL in CT2, CT3 nEL in CT2 ≈ nEL in CT3	8	2	2	125	71
Group 1+1+1	nEL in CT1, CT2, CT3 > 4× nEL in any other CT nEL in CT1 > 4× nEL in CT2, CT3 nEL in CT2 > 4× nEL in CT3	8	4	2	15	11

(nEL- normalized expression level, CT – cell type)

normalized expression level within the broader group of immune cell types had to be at least 4× higher than in any other immune cell type not included in the specific group. Finally, scores were assigned to all the markers based on marker type. For the twin and group markers, relative differences in normalized gene expression within the pair/group were also considered (Table 1).

Next, the top 10 best-conserved markers for each cluster were determined. To this end, we first selected markers (genes) with a log2FC (fold change) >1.0 and an adjusted p-value <0.05 to ensure that only genes with both high and significant differences in expression levels between clusters were considered. The markers meeting the criteria were then ranked based on the highest $\log_2$FC values.

Then, each cluster's top 10 conserved markers were cross-referenced with the cell type-specific markers from each annotation dataset separately. In this way, clusters were assigned to possible cell types, and each possible cell type was assigned a score based on the scores of the markers identified by the cross-reference. For additional clarification, those of the top 10 conserved markers not identified as cell type specific markers were also considered. If their expression in a particular immune cell type was at least 4× or 2× higher than the average expression of all immune cell types in the annotation dataset, they were assigned a score of 2 or 1, respectively. These scores were added to the above scores of the possible cell types. The final scores obtained for each cluster from the two annotation datasets were then used by two independent evaluators to determine preliminary annotations for each cluster. Finally, the preliminary annotations were compared by the two evaluators and an additional referee to reach a consensus annotation. In ambiguous cases, a broader annotation took precedence over a narrower one (*I.e.*, B-cells vs naïve B-cells) unless multiple clusters shared the same annotation: in such situations, we aimed for consensus with the narrower annotations.

Trajectory and pseudo-time analysis

The trajectory of the cell transitions and the pseudo-temporal arrangement of cells during differentiation was analyzed using the R package monocle3 and the Python implementation. (23–25) The previously constructed Seurat object was pre-processed and partitioned into the main cell types (monocytes, B-cells, T-cells). An explicit principal graph was learned using advanced machine learning called Reverse Graph Embedding to accurately resolve biological processes in individual cells' Pseudo-time. This abstract measure of an individual cell's progress in cell differentiation was calculated as the distance between a cell and the beginning of the trajectory measured along its shortest path. The total length of a trajectory was defined as the total amount of transcriptional changes a cell undergoes on its way from start to end state. The cells with the highest expression of the *CD14* gene for monocytes and the calculated start nodes for T-cells and B-cells were chosen as the roots or so-called beginnings of a biological process. To calculate the start node, the resident cells (double negative T-cells and intermediate B-cells) were first grouped

according to the nearest node of the trajectory graph, and then the proportion of the cells at each node originating from the earliest time point was calculated. The node most heavily occupied by early cells was then selected as the root. Finally, the UMAP visualization was used to identify the pseudo-temporal cell state transition compared to the Azimuth annotation.

Results

Automatic annotation with Azimuth

After quality control and data integration, we used Azimuth's reference-based annotation of cells to automatically determine clusters and immune cell types. First, we evaluated three levels of cluster granulation to determine the best resolution of clusters using a clustering tree diagram. The first and second levels of annotation provide a clear separation between all annotated clusters, while the third level exhibits some over-clustering (Figure 4a). Similarly, UMAP plots of the first two Azimuth annotated clustering levels show clear separations between clusters. At the same time, some over-clustering is evident in level three, for example, populations NK_2, NK_3, and NK_4 (Figure 4b). Overall, the resolution at level one provides information on eight, level two on 28 and level three on 51 distinct PBMC subpopulations. Based on the cluster-tree analysis (*I.e.*, presence of over-clustering and number of distinct subpopulations), level 2 was chosen as the best solution, providing sufficient resolution and the most information.

Unsupervised clustering according to SNN

Additionally, we performed SNN modularity optimization clustering. Again, the best resolution was chosen based on the clustering-tree diagram. Here, the best resolution of granulation was achieved at a resolution of 0.8, with higher and lower resolutions showing at least some over-clustering (Figure 5a). UMAP plots of the smallest (0.2), largest (2.0), and best (0.8) resolution of clustering were also inspected. Clustering at a resolution of 0.2 provided information on 12 unannotated PBMC subpopulations, although more distinct clusters can be observed (for examples, see clusters 2, 3, and 4, Figure 5b). On the other hand, a resolution of 2.0 resulted in 28 distinctive unannotated PBMC subpopulations, with clear signs of poor cluster separation in several instances (for examples, see clusters 4, 5, and 6 or 2, 3, 7, and 19, Figure 5b). Only the best resolution (0.8) shows 18 well-separated PBMC subpopulations (Figure 5b) and was thus chosen as the best resolution for further inspection.

Manual annotation of the Azimuth and SNN clusters

As described above, manual annotation was based on two publicly available datasets and two independent evaluators. Both evaluators cross-referenced the cell-type specific markers defined from the datasets with the top 10 conserved markers from each cluster, thus creating four independent preliminary annotations for all the clusters. The four preliminary annotations were then used to define each cluster's final, consensus annotation. Of note, we could not annotate all the clusters in this way- for 10 Azimuth annotated clusters (for example, classical dendritic cells type 1, plasmablasts or hematopoietic stem/progenitor cells) and 2 of the SNN clusters (clusters 16 and 17) no conserved markers could be defined (see Tables 2 and 3, respectively).

The consensus manual annotation was identical to the Azimuth annotation for 11/19 clusters for which conserved markers could be defined (Table 2). In 5 cases (myeloid dendritic cells instead of type 2 classical dendritic cells; Memory CD4+ T-cells vs Central memory CD4+ T-cells; T cells vs Effector memory and Cytotoxic CD4+ T-cells; natural killer cells vs CD56 bright natural killer cells), the manual annotation identified a super-set and in one case (Exhausted memory B-cells instead of Memory B-cells) a sub-set of the immune cell subtype identified by the Azimuth annotation. In the last cluster, manual annotation identified a different sub-set (Non-switched memory B-cells) of the same super-set (B-cells) than the Azimuth annotation (Intermediate B-cells). Manual annotation of the 16 SNN clusters, for which conserved markers could be defined, identified 15 relatively specific immune cell subtypes, while in one cluster, only a very broad annotation (T-cells) could be determined (Table 3).

Comparison of the Azimuth and SNN clusters with manual annotation

Comparison of the 28 Azimuth annotated clusters, the 18 unsupervised SNN clusters, and the manual annotation of the latter showed good matching for all the Monocytes, Dendritic cells, and B-cells populations/clusters as well as 2/3 natural killer cells populations (Figure 6a-b, Table 4). Also matching are the Naïve CD4+ and CD8+ T-cells, Memory CD8+ T-cells, Mucosal-associated invariant T-cells, and γδ T-cells clusters. The rest of the T-cell populations do not match directly; however, in general, it is evident whether the clusters fall within CD4+ or CD8+ T-cell populations. The hematopoietic stem/progenitor cells, Innate lymphoid cells and platelet populations were not manually annotated due to the lack of appropriate conserved markers (Table 2). In the unsupervised SNN clustering, these populations do not represent separate clusters but are instead distributed among (CD4+) T-cells associated clusters (Figure 6a-b, Table 4).

Pseudo-temporal trajectory analysis

Pseudo-temporal trajectory analysis was used as a final validation method. With this analysis we followed the cell state progress through the differentiation of three distinct Azimuth superclusters. In the partition of the Monocytes supercluster, it's visible that cells start to differentiate in

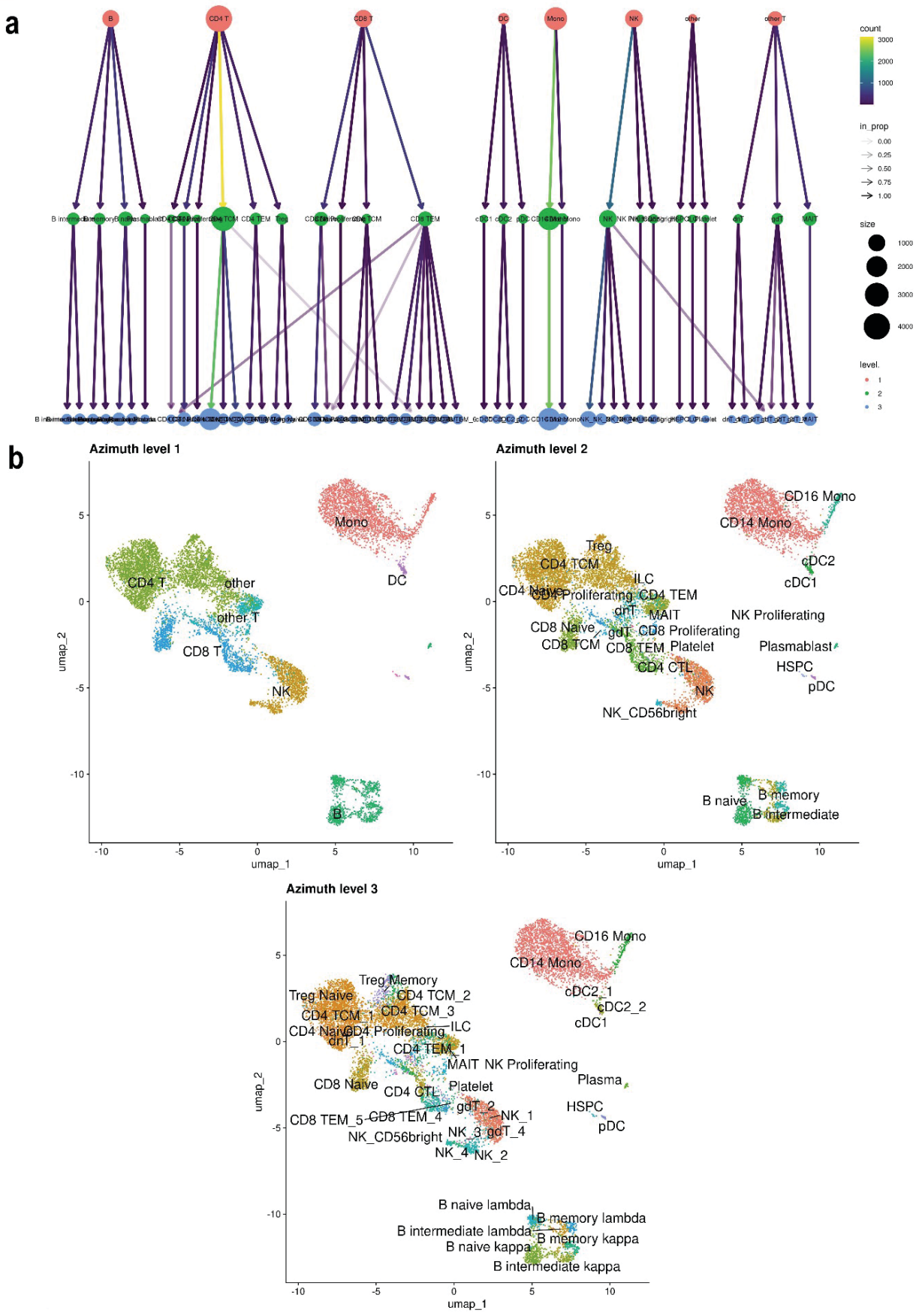

Figure 4: Automated annotation with Azimuth. (a) Evaluation of Azimuth annotation levels using clustering tree. The best resolution is encircled in red. (b) UMAP plots of annotation using all three levels from the Azimuth database. Upper left: level one annotation clusters; Upper right: level two annotation clusters; Lower: level three annotation clusters

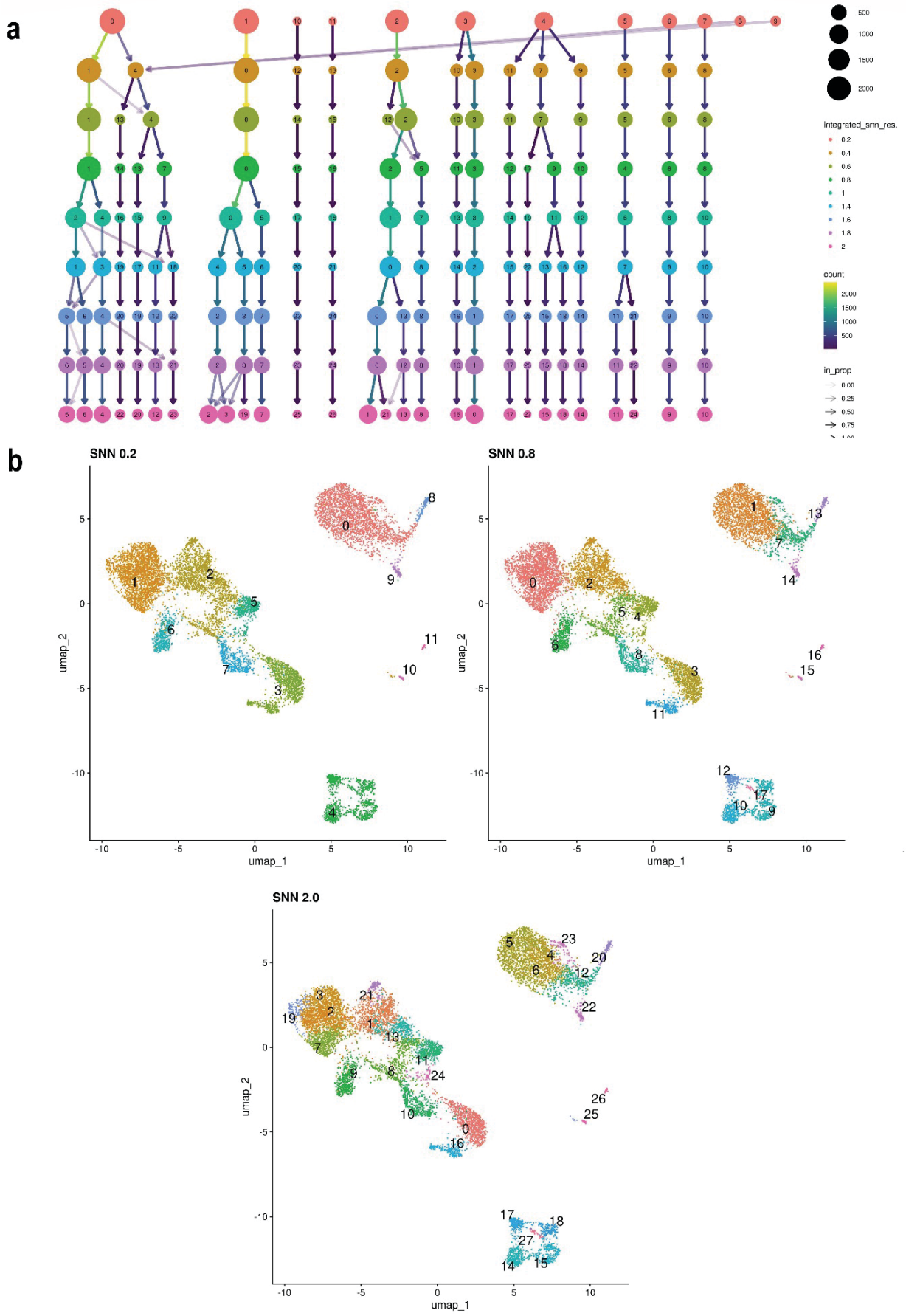

Figure 5: Shared nearest neighbor clustering optimization. (a) Evaluation of clustering levels using clustering tree. The best resolution is encircled in red. (b) UMAP plots of the smallest (0.2; upper left), the largest (2.0; upper right), and the best (0.8; lower) resolution of clustering

Table 2: Comparison between the Azimuth and manual annotation of the best resolution clusters

Azimuth annotation	1st Evaluator's provisional annotation		2nd Evaluator's provisional annotation		Consensus annotation
	HPA dataset	Monaco dataset	HPA dataset	Monaco dataset	
CD14+ Monocytes	Classical Monocytes	Classical Monocytes	Classical Monocytes	Classical Monocytes	Classical Monocytes
CD16+ Monocytes	Non-classical Monocytes	Non-classical / Intermediate Monocytes	Non-classical Monocytes	Non-classical / Intermediate Monocytes	Non-classical Monocytes
cDC, type 1	/	/	/	/	/
cDC, type 2	mDC	mDC	mDC	mDC	mDC
pDC	pDC	pDC	pDC	pDC	pDC
Naïve B-cells	Naïve / Memory B-cells	Naïve B-cells	Naïve B-cells	Naïve B-cells	Naïve B-cells
Intermediate B-cells	Memory / Naïve B-cells	Non-switched memory B-cells	Memory B-cells	Non-switched memory B-cells	Non-switched memory B-cells
Memory B-cells	Memory / Naïve B-cells	Exhausted / Switched memory B-cells	Memory B-cells	Exhausted memory B-cells	Exhausted memory B-cells
Plasmablasts	/	/	/	/	/
Double-negative T-cells	/	/	/	/	/
Naïve CD4+ T-cells	Naïve CD4+ T-cells	Naïve CD4+ T-cells	Naïve CD4+ T-cells	Naïve CD4+ T-cells	Naïve CD4+ T-cells
Proliferating CD4+ T-cells	/	/	/	/	/
TCM CD4+	Naïve / Memory CD4+ T-cells	Naïve / TFH Memory CD4+ T-cells	Naïve / Memory CD4+ T-cells	Naïve CD4+ T-cells	Memory CD+ T-cells
TEM CD4+	MAIT / γδ T-cells	MAIT / Vδ2+ γδ T-cells	MAIT	MAIT	T-cells
CTL CD4+	/	/	/	/	/
Treg	Treg	Treg	Treg	Treg	Treg
Naïve CD8+ T-cells	Naïve CD8+ T-cells	Naïve CD8+ T-cells	Naïve CD8+ T-cells	Naïve CD8+ T-cells	Naïve CD8+ T-cells
Proliferating CD8+ T-cells	/	/	/	/	/
TCM CD8+	Memory CD8+ T-cells	TCM / TEM CD8+	Memory CD8+ T-cells	TCM CD8+	TCM CD8+
TEM CD8+	Memory CD8+ T-cells	TEM CD8+	Memory CD8+ T-cells	TEM CD8+	TEM CD8+
MAIT	MAIT	MAIT	MAIT	MAIT	MAIT
γδ T-cells	γδ T-cells	Vδ2+ γδ T-cells	γδ T-cells	Vδ2+ γδ T-cells	γδ T-cells
NK	NK / γδ T-cells	NK	NK / γδ T-cells	NK	NK
CD56 bright NK	NK	NK / Vδ2+ γδ T-cells	NK	NK	NK
Proliferating NK	/	/	/	/	/
HSPC	/	/	/	/	/
ILC	/	/	/	/	/
Platelets	/	/	/	/	/

cDC (classical Dendritic Cells); CTL (Cytotoxic T-cells); HSPC (Hematopoietic stem/progenitor cells); ILC (Innate lymphoid cells); MAIT (Mucosal-associated invariant T-cells); mDC (myeloid Dendritic Cells); NK (Natural Killer Cells); pDC (plasmacytoid Dendritic Cells); TCM (Central Memory T-cells); TEM (Effector Memory T-cells); Treg (Regulatory T-cells)

Table 3: Manual annotation of the best clusters according to SNN

SNN clusters	1st Evaluator's provisional annotation		2nd Evaluator's provisional annotation		Consensus annotation
	HPA dataset	Monaco dataset	HPA dataset	Monaco dataset	
0	Naïve CD4+T-cells	Naïve CD4+T-cells	Naïve CD4+T-cells	Naïve CD4+T-cells	Naïve CD4+T-cells
1	Classical Monocytes / Neutrophils	Classical Monocytes / Neutrophils	Classical Monocytes	Classical Monocytes	Classical Monocytes
2	Memory CD4+ T-cells / Treg	Th17 Memory CD4+ T-cells	Memory CD4+ T-cells / Treg	Th17 Memory CD4+ T-cells	Memory CD4+ T-cells
3	NK / γδ T-cells	Non-Vδ2+ γδ T-cells / TEM CD8+	NK / γδ T-cells	Non-Vδ2+ γδ T-cells	T-cells
4	γδ T-cells / MAIT	MAIT	γδ T-cells	MAIT	MAIT
5	γδ T-cells / Treg	Vδ2+ γδ T-cells / Non-Vδ2+ γδ T-cells / MAIT	γδ T-cells / Treg	Vδ2+ γδ T-cells	γδ T-cells
6	Naïve CD8+ T-cells	Naïve CD8+ T-cells	Naïve CD8+ T-cells	Naïve CD8+ T-cells	Naïve CD8+ T-cells
7	Intermediate Monocytes	Intermediate Monocytes	Intermediate Monocytes	Intermediate Monocytes	Intermediate Monocytes
8	Memory CD8+ T-cells	TEM CD8+	Memory CD8+ T-cells	TEM CD8+	Memory CD8+ T-cells
9	Memory B-cells	Exhausted memory B-cells	Memory B-cells	Exhausted memory B-cells	Exhausted memory B-cells
10	Naïve B-cells	Naïve B-cells	Naïve B-cells	Naïve B-cells	Naïve B-cells
11	NK	NK	NK	NK	NK
12	Naïve / Memory B-cells	Naïve / Non-switched memory B-cells	Naïve B-cells	Naïve B-cells	Non-switched memory B-cells
13	Non-classical Monocytes	Non-classical / Intermediate Monocytes	Non-classical Monocytes	Non-classical / Intermediate Monocytes	Non-classical Monocytes
14	mDC	mDC	mDC	mDC	mDC
15	pDC	pDC	pDC	pDC	pDC
16	/	/	/	/	/
17	/	/	/	/	/

MAIT (Mucosal-associated invariant T-cells); mDC (myeloid Dendritic Cells); NK (Natural Killer Cells); pDC (plasmacytoid Dendritic Cells); TEM (Effector Memory T-cells); Treg (Regulatory T-cells)

the middle of the CD14+ Monocytes cluster, progressing outwards (Figure 7a). The trajectory distinctively shows progression into Non-classical CD16+ monocytes, whereas type 2 cDC cells are not connected with any trajectory. Within the B-cells supercluster, the starting node resides in the Intermediate B-cells with trajectory soon forking into two arms, both pointing towards Memory and Naïve B-cells (Figure 7b). The starting node within the T-cells supercluster resides in the middle of the cluster (Figure 7c), a position corresponding to the double negative T cells according to the Azimuth annotation (Figure 4b). One trajectory clearly shows differentiation into CD4+ sub-populations and other-T cells, while the other branches early into CD8+ sub-populations and the natural killer cells.

Discussion

ScRNA-seq enables the simultaneous analysis of expression profiles and their interdependencies in multiple cell types present in a tissue of interest. This represents a qualitative leap forward in studying complex biological processes and the role of individual cell subtypes in these processes. Previously, several separate studies were required to achieve the same result. However, reliable and accurate identification of the cell subtypes present in a selected biological sample cannot be taken for granted. (26) In the work presented here, we compared the cell-type annotation techniques/tools used in scRNA-seq to highlight their strengths and potential pitfalls. Specifically, we used an automated reference-based tool, Azimuth, and an SNN clustered reference-naïve approach followed by manual annotation to

Table 4: Comparison of the best Azimuth annotation, the best SNN clustering resolution, and manual annotation.

Azimuth annotation	SNN cluster with cells present in the Azimuth annotation	Manual annotation consensus	
		The best-resolution Azimuth clusters	The best clusters, according to SNN
CD14+ Monocytes	0, **1*** , 2, 3, **7***, 9, 14, 16	Classical Monocytes	Classical Monocytes; Intermediate Monocytes
CD16+ Monocytes	1, 2, 7, **13***	Non-classical Monocytes	Non-classical Monocytes
cDC, type 1	**14**	/	mDC
cDC, type 2	7, 9, **14***	mDC	mDC
pDC	**15**	pDC	pDC
Naïve B-cells	1, **10***, **12***, 17	Naïve B-cells	Naïve B-cells; Non-switched memory B-cells
Intermediate B-cells	**9***, 10, 12, 17	Non-switched memory B-cells	Exhausted memory B-cells
Memory B-cells	**9***, 17	Exhausted memory B-cells	Exhausted memory B-cells
Plasmablasts	**16**	/	/
Double-negative T-cells	**0**, **5**	/	Naïve CD4+T-cells; γδ T-cells
Naïve CD4+ T-cells	**0***, 1, 6	Naïve CD4+ T-cells	Naïve CD4+T-cells
Proliferating CD4+ T-cells	**1**, **2**, **4**	/	Classical Monocytes; Memory CD4+ T-cells; MAIT
TCM CD4+	**0***, 1, **2***, 3, 4, 5, 6, 8, 10	Memory CD+ T-cells	Naïve CD4+T-cells; Memory CD4+ T-cells
TEM CD4+	0, 2, 4, **5***, 8	T-cells	γδ T-cells
CTL CD4+	**3**, **8**	/	T-cells; Memory CD8+ T-cells
Treg	0, **2***, 6	Treg	Memory CD4+ T-cells
Naïve CD8+ T-cells	0, 2, 4, **6***, 8	Naïve CD8+ T-cells	Naïve CD8+ T-cells
Proliferating CD8+ T-cells	**1**, **4**, **8**	/	Classical Monocytes; MAIT; Memory CD8+ T-cells
TCM CD8+	0, 2, **5***, **6***, 8	TCM CD8+	γδ T-cells; Naïve CD8+ T-cells
TEM CD8+	0, 1, 2, 3, 4, 5, 6, **8***	TEM CD8+	Memory CD8+ T-cells
MAIT	2, 3, **4***, 5	MAIT	MAIT
γδ T-cells	0, 2, 3, **4***, **5***, 6, 8, 11	γδ T-cells	MAIT; γδ T-cells
NK	**3***, 4, 8, **11***, 17	NK	T-cells; NK
NK CD56 bright	**11**	NK	NK
NK proliferating	**1**, **3**	/	Classical Monocytes; T-cells
HSPC	**0**, **1**, **2**	/	Naïve CD4+T-cells; Classical Monocytes; Memory CD4+ T-cells
ILC	**2***, 5	/	Memory CD4+ T-cells
Platelets	**3**	/	T-cells

* The most abundant SNN cluster; cDC (classical Dendritic Cells); CTL (Cytotoxic T-cells); HSPC (Hematopoietic stem/progenitor cells); ILC (Innate lymphoid cells); MAIT (Mucosal-associated invariant T-cells); mDC (myeloid Dendritic Cells); NK (Natural Killer Cells); pDC (plasmacytoid Dendritic Cells); TCM (Central Memory T-cells); TEM (Effector Memory T-cells); Treg (Regulatory T-cells)

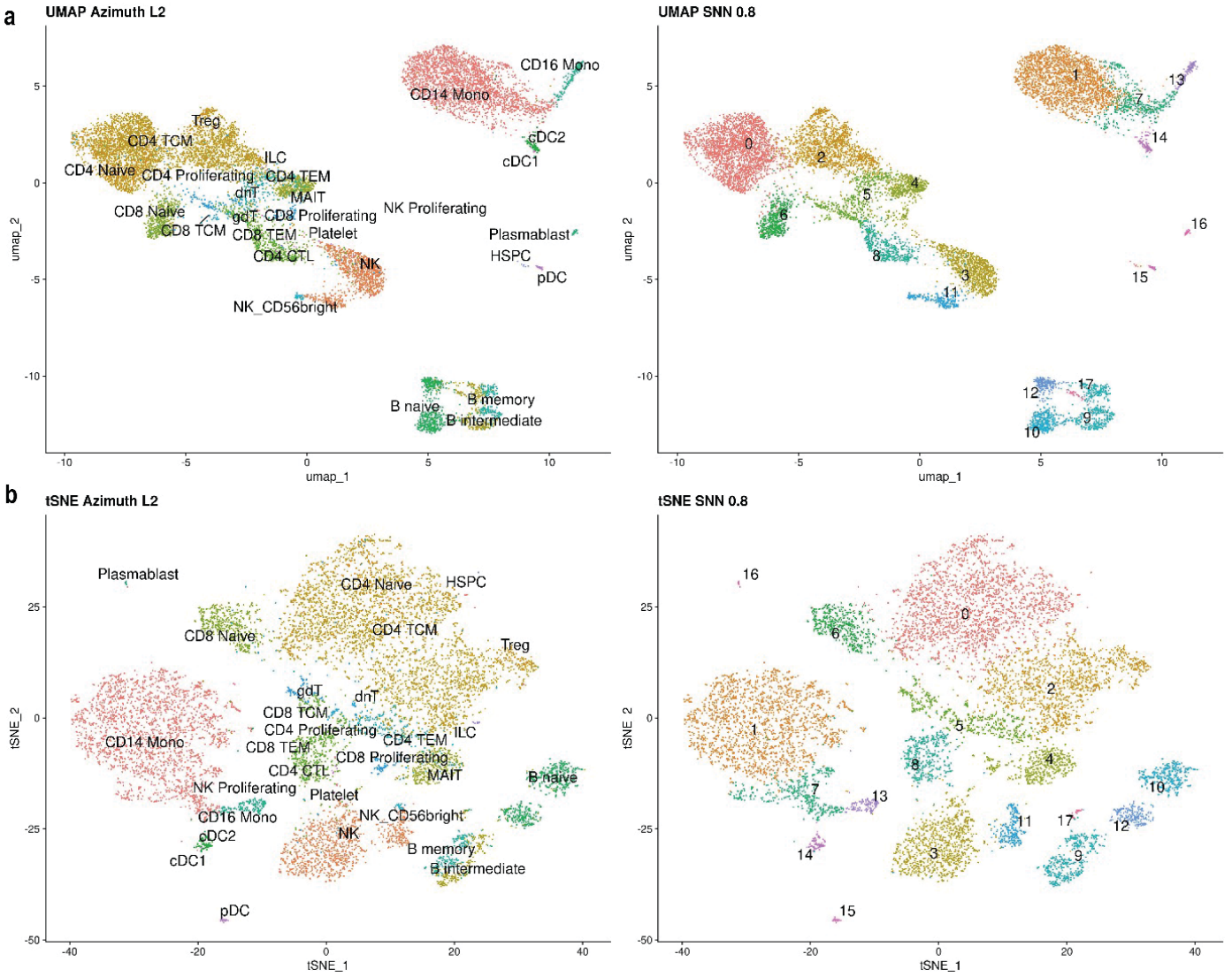

Figure 6: Comparison of Azimuth and SNN clustered cell landscapes (a) UMAP plots of the best resolution Azimuth clusters (left) and the best resolution SNN clusters (right). (b) tSNE plots of the best-resolution Azimuth clusters (left) and the best-resolution SNN clusters (right)

gain insights into their utility and effectiveness in deciphering complex cellular compositions in scRNA-seq datasets.

As a starting point for the analyses, we chose PBMC, a relatively complex but easily accessible biological sample commonly used in medical and veterinary research. We first used the automatic annotation tool Azimuth. Its annotations are based on a reference PBMC dataset generated from 24 samples processed with a CITE-seq (Cellular Indexing of Transcriptomes and Epitopes by Sequencing) panel, which performs RNA sequencing along with obtaining quantitative and qualitative information about proteins (i.e., cell type-specific antigens) on the cell surface. (8) Azimuth automatic annotation has demonstrated the ability to process large scRNA-seq datasets quickly and accurately. The performance of this machine learning-based tool reflects ongoing advances in computational biology, particularly in the automated processing of biological data. (27–29) Performance of the automated annotation tools may decline when confronted with rare cell types, as the classifier may be unable to learn their information during the training phase (30).

In that regard, Azimuth also proved relatively well, as it defined several PBMC populations with low abundance (i.e., classical dendritic cells, plasmacytoid dendritic cells, hematopoietic stem/progenitor cells, Innate lymphoid cells) (31–33) of which the first two we could independently confirm with the manual annotation. Like any other reference-based tool, however, it cannot recognize / annotate populations that lie outside its frame of reference. (34) For example, $CD14^{+}$ and $CD16^{+}$ monocyte populations were annotated that roughly correspond to the classical ($CD14^{+}CD16^{neg}$) and non-classical ($CD14^{dim}CD16^{+}$) monocytes in the HPA and Monaco datasets, respectively, but the intermediate ($CD14^{+}CD16^{+}$) monocytes could not be distinguished.

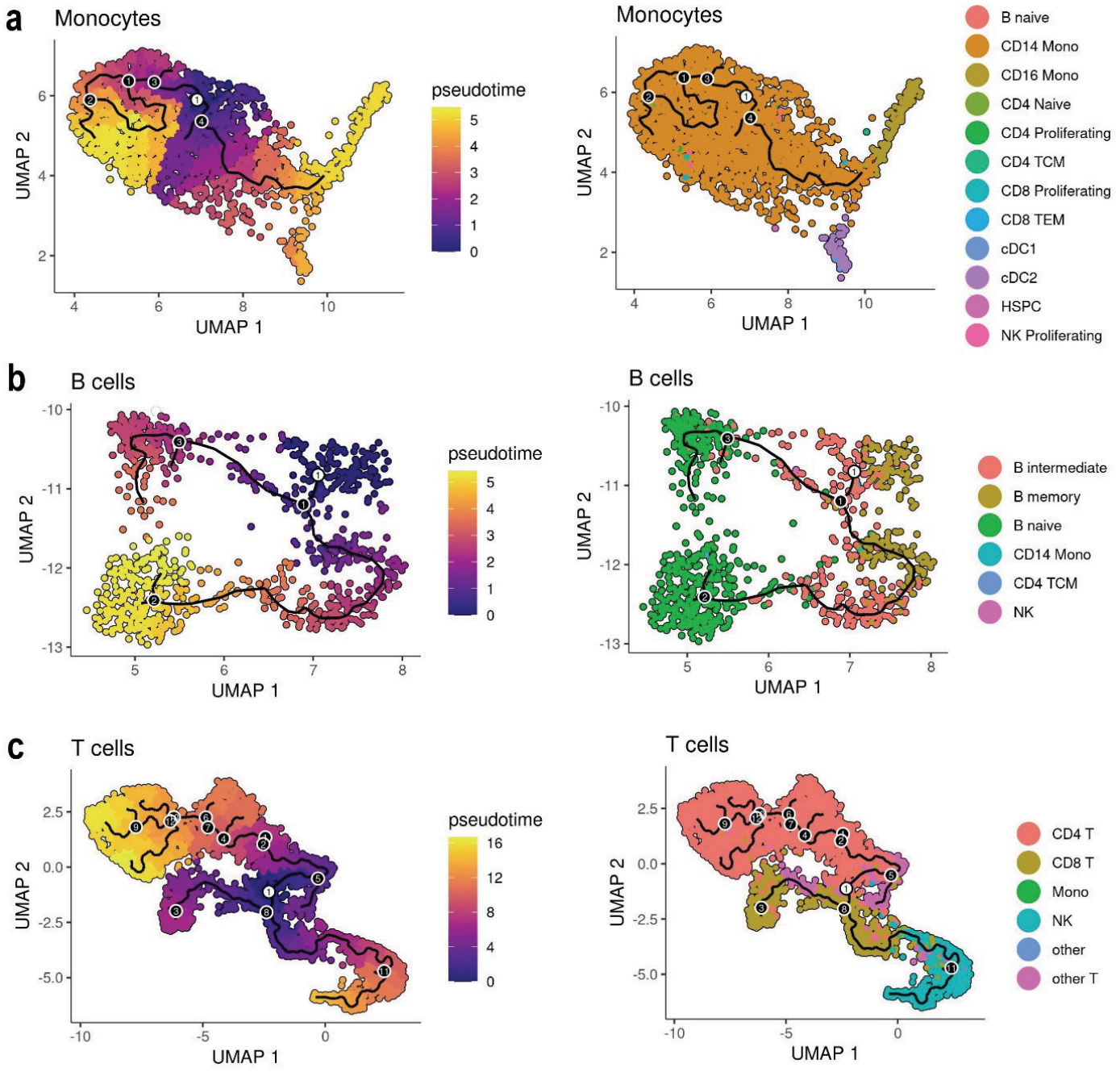

Figure 7: Pseudo-temporal analysis of selected immune cell types. (a) UMAP visualization of pseudo-temporal trajectories (left) and Azimuth annotations (right) of the monocytes partition on levels one and two. (b) UMAP visualization of pseudo-temporal trajectories (left) and Azimuth annotations (right) of the B-cells partition on levels one and two. (c) UMAP visualization of pseudo-temporal trajectories (left) and Azimuth annotations (right) of the T-cells partition on levels one and two

Unsupervised SNN clustering, on the other hand, easily defined three distinct populations at the position corresponding to the monocytes in the Azimuth analysis. Subsequent manual annotation identified them as the three monocyte types mentioned above. The ability of this method to effectively delineate cell populations is well documented (27), and our results confirm its robustness in unsupervised clustering. The main advantage of unsupervised clustering over the reference-based one is that it does not attempt to fit cells into the pre-existing reference frame. Instead, the cells are clustered merely according to their similarity. Unsupervised clustering thus provides more opportunities to recognize rare or even new populations. (34) Conversely, the same fact is also a major disadvantage of the unsupervised method, as one cannot avoid the time-consuming manual annotation of the individual clusters. (34)

In our manual annotation we prioritized biological relevance and statistical rigor. We followed strict criteria, similar to the HPA protocols, for cell type-specific markers selection.

Similarly, we used rigorous criteria to define the top 10 best-conserved markers per cluster, which were then used for comparison with the cell type-specific markers and, thus, cell type annotation of the clusters. We also tried annotation with all the conserved markers (15 – 855 conserved markers per cluster, not shown). A similar approach was used for the scSorter tool, where they combined the expression of marker and non-marker genes for clustering. (35) We found no significant differences in annotation with all versus only the top 10 markers, so we chose the latter, a somewhat less time-consuming approach, for further analysis. Of note is that the stringency of the above criteria for conserved markers resulted in no conserved markers being defined for some clusters. This further meant that these clusters could not be manually annotated; we however decided against loosening the criteria. Besides objective data, manual interpretation also benefits from the evaluator's understanding of the biological processes, but at the same time, it inherently creates bias. (34) To minimize bias, we used two independent annotation datasets, both based on the FACS sorted cell populations (21, 22), and employed two independent evaluators, plus an additional arbiter, to reach consensus annotation for each cluster. This careful approach ensured high accuracy in identifying different cell types, as asserted by the high similarity of the manual and the automated (Azimuth) annotations.

Many discrepancies between the two annotations can be explained by the differences in how specific cell subtypes are defined in the respective reference datasets. Particularly challenging are the phenotypically and functionally highly heterogeneous subsets of the T-cells (36), where the HPA dataset recognizes 7 and the Monaco dataset 15 separate entities (21, 22), which were in turn used to validate the 13 T-cell clusters identified by the Azimuth manually. At the exact coordinates, the unsupervised SNN clustering identified only 6 distinct populations, all manually annotated as various T-cell subsets. Directly comparing the SNN clusters with the Azimuth annotations further emphasizes the invaluability of using multiple approaches when tackling complex populations/clusters. Namely, it clearly shows that a population, coherent at a given level, may consist of several distinct subpopulations. These are not necessarily closely related, and vice-versa, the well-defined cell types may be dispersed over several distinct clusters. In clinical samples related to a specific pathology, such instances can provide opportunities for the identification of important rare and potentially even novel subpopulations. They should thus be more thoroughly investigated at a higher resolution.

The selected resolution of the clustering directly influences the granularity of the identified cell types and, thus, the depth of the biological insights that can be gained. (18) A high resolution can reveal subtle differences between cell populations and possibly visualize rare or transitional states of cells, but at a risk of decreased reliability of clustering- for example, see CD4+ T-cells sub-clusters at resolution level 3 (Figure 4a). Conversely, lower resolution may be highly reliable, but risks conflating cell types with different functions (for example looking at combined CD4+ T-cells instead of the subsets with very distinct roles- regulatory, helper, effector, etc.) and can thus miss important biological differences. (36) Hence, the optimal resolutions we chose for both reference-based and unsupervised clustering are compromises, balancing between distinguishing meaningful cellular subtypes and avoiding fragmentation of homogeneous populations into overly granular clusters. Alas, as with any compromise, the optimal resolution does not satisfy completely, which is most evident when clustering the B-cells. Here, at optimal resolutions, Azimuth and SNN clustering identify 3 and 4 distinct subpopulations, respectively. Visually, though, one can easily distinguish 5-6 entities, suggesting that a higher resolution would be needed here.

The meaningfulness of a granularity higher than the one defined by the optimal resolution for the B-cell subsets was also confirmed by the pseudo-temporal analysis. The pseudo-temporal dimension introduces a framework for mapping progression states and inferring transitional states and lineage relationships. It highlights not only the end states cells reach but also the paths they take to get there. (24) Using this method, we further validated the T-cell and monocyte subsets annotations. The pseudo-temporal trajectories also clearly show that the automatic Azimuth annotations cohere with known cell differentiation stages. The method has previously been instrumental in charting developmental trajectories, and our application further underscores its value in modeling cellular dynamics, as has been explored in other studies focusing on differentiation and immune cells. (37, 38)

Regardless of the sample type, its origin, underlying pathology, and the scientific question, single-cell RNA sequencing has little value if one cannot properly identify the single cells. Novel and ever more powerful tools for accurate and reliable annotation of the cells/clusters are therefore being developed. (39–41) However, as demonstrated here, each method has its merits and downsides. The methods and results of our study have significant implications for the further development of scRNA-seq applications, not only in the field of human medicine but even more in the field of veterinary medicine. Unlike in human medicine, namely, in veterinary medicine, there is often a lack of comprehensive databases for reference-based annotation. (12, 42) This makes using automated annotation tools such as Azimuth difficult and emphasizes the importance of integrating different annotation approaches. In the future, integrated tools may be developed that will combine the efficiency of the automated annotation and expert insight of the manual one, the accuracy of the reference-based annotation with the flexibility of the unsupervised clustering. Until then, a skillful combination of automated and manual annotation techniques is needed to manage the complexity of scRNA-seq data when reference databases are limited or non-existent. This approach is particularly crucial in veterinary science,

where the study of different species requires a customized approach to cell type annotation, given the variability in genetic and cellular profiles of different species. With it, scRNA-seq research can open new avenues for discovery in cell biology and its applications in health and disease.

Acknowledgments

This work was not supported by any specific funding.

References

1. Wang Z, Gerstein M, Snyder M. RNA-Seq: a revolutionary tool for transcriptomics. Nat Rev Genet 2009; 10(1): 57–63. doi: 10.1038/nrg2484
2. Stark R, Grzelak M, Hadfield J. RNA sequencing: the teenage years. Nat Rev Genet 2019; 20(11): 631–56. doi: 10.1038/s41576-019-0150-2
3. Haque A, Engel J, Teichmann SA, Lönnberg T. A practical guide to single-cell RNA-sequencing for biomedical research and clinical applications. Genome Med 2017; 9(1): 75. doi: 10.1186/s13073-017-0467-4
4. Wagner A, Regev A, Yosef NC. Revealing the vectors of cellular identity with single-cell genomics. Nat Biotechnol 2016; 34(11): 1145–60. doi: 10.1038/nbt.3711
5. Tang F, Barbacioru C, Wang Y, Nordman E, Lee C, Xu N, et al. mRNA-Seq whole-transcriptome analysis of a single cell. Nat Methods 2009; 6(5):3 77–82. doi: 10.1038/nmeth.1315
6. Wang T, Li B, Nelson CE, Nabavi S. Comparative analysis of differential gene expression analysis tools for single-cell RNA sequencing data. BMC Bioinformatics 2019; 20(1): 40. doi: 10.1186/s12859-019-2599-6
7. Poirion OB, Zhu X, Ching T, Garmire L. Single-cell transcriptomics bioinformatics and computational challenges. Front Genet 2016; 7: 163. doi: 10.3389/fgene.2016.00163
8. Hao Y, Hao S, Andersen-Nissen E, et al. Integrated analysis of multimodal single-cell data. Cell 2021; 184(13): 3573–7, e29. doi: 10.1016/j.cell.2021.04.048
9. Stuart T, Butler A, Hoffman P, et al. Comprehensive integration of single-cell data. Cell 2019; 177(7): 1888–902, e21. doi: 10.1016/j.cell.2019.05.031
10. Butler A, Hoffman P, Smibert P, Papalexi E, Satija R. Integrating single-cell transcriptomic data across different conditions, technologies, and species. Nat Biotechnol 2018; 36(5): 411–20. doi: 10.1038/nbt.4096
11. The Human Protein Atlas. Stockholm: Affinity proteomics, 2023. https://www.proteinatlas.org/ (18. 11. 2023)
12. EMBL-EBI. Single cell expression atlas. Hinxton: European Molecular Biology Laboratory, 2023. https://www.ebi.ac.uk/gxa/sc/home (5. 12. 2023)
13. 10x Genomics Datasets. Pleasanton: 10x Genomics, 2023. https://www.10xgenomics.com/datasets?query=&page=1&configure%5BhitsPerPage%5D=50&configure%5BmaxValuesPerFacet%5D=1000 (3. 7. 2023)
14. R Foundation. The R project for statistical computing. Wien: The R Foundation, 2023. https://www.r-project.org/ (3. 7. 2023)
15. McGinnis CS, Murrow LM, Gartner ZJ. Doubletfinder: doublet detection in single-cell RNA sequencing data using artificial nearest neighbors. Cell Syst 2019; 8(4): 329–37, e4. doi: 10.1016/j.cels.2019.03.003
16. Subramanian A, Alperovich M, Yang Y, Li B. Biology-inspired data-driven quality control for scientific discovery in single-cell transcriptomics. Genome Biol 2022; 23(1): 267. doi: 10.1186/s13059-022-02820-w
17. Hafemeister C, Satija R. Normalization and variance stabilization of single-cell RNA-seq data using regularized negative binomial regression. Genome Biol 2019; 20(1): 296. doi: 10.1186/s13059-019-1874-1
18. Zappia L, Oshlack A. Clustering trees: a visualization for evaluating clusterings at multiple resolutions. Gigascience 2018; 7(7): giy083. doi: 10.1093/gigascience/giy083
19. Waltman L, van Eck NJ. A smart local moving algorithm for large-scale modularity-based community detection. Eur Phys J B. 2013; 86(11): 471. doi: 10.1140/epjb/e2013-40829-0
20. Lu S, Li J, Song C, Shen K, Tseng GC. Biomarker detection in the integration of multiple multi-class genomic studies. Bioinformatics 2010; 26(3): 333–40. doi: 10.1093/bioinformatics/btp669
21. Uhlen M, Karlsson MJ, Zhong W, et al. A genome-wide transcriptomic analysis of protein-coding genes in human blood cells. Science 2019 ; 20; 366(6472): eaax9198. doi: 10.1126/science.aax9198
22. Monaco G, Lee B, Xu W, et al. RNA-seq signatures normalized by mrna abundance allow absolute deconvolution of human immune cell types. Cell Rep 2019; 26(6): 1627–40, e7. doi: 10.1016/j.celrep.2019.01.041
23. Qiu X, Mao Q, Tang Y, et al. Reversed graph embedding resolves complex single-cell trajectories. Nat Methods 2017; 14(10): 979–82. doi: 10.1038/nmeth.4402
24. Trapnell C, Cacchiarelli D, Grimsby J, et al. The dynamics and regulators of cell fate decisions are revealed by pseudotemporal ordering of single cells. Nat Biotechnol 2014; 32(4): 381–6. doi: 10.1038/nbt.2859
25. Cao J, Spielmann M, Qiu X, et al. The single-cell transcriptional landscape of mammalian organogenesis. Nature 2019; 566(7745): 496–502. doi: 10.1038/s41586-019-0969-x
26. Li X, Wang CY. From bulk, single-cell to spatial RNA sequencing. Int J Oral Sci 2021; 13(1): 36. doi: 10.1038/s41368-021-00146-0
27. Lähnemann D, Köster J, Szczurek E, et al. Eleven grand challenges in single-cell data science. Genome Biol 2020; 21(1): 31. doi: 10.1186/s13059-020-1926-6
28. Pasquini G, Rojo Arias JE, Schäfer P, Busskamp V. Automated methods for cell type annotation on scRNA-seq data. Comput Struct Biotechnol J 2021; 19: 961–9. doi: 10.1016/j.csbj.2021.01.015
29. Abdelaal T, Michielsen L, Cats D, et al. A comparison of automatic cell identification methods for single-cell RNA sequencing data. Genome Biol 2019; 20: 194. doi: 10.1186/s13059-019-1795-z
30. Cheng Y, Fan X, Zhang J, Li Y. A scalable sparse neural network framework for rare cell type annotation of single-cell transcriptome data. Commun Biol 2023; 6: 545. doi: 10.1038/s42003-023-04928-6
31. Flórez-Grau G, Escalona JC, Lacasta-Mambo H, et al. Human dendritic cell subset isolation by magnetic bead sorting: a protocol to efficiently obtain pure populations. Bio Protoc 2023; 13(20): e4851. doi: 10.21769/BioProtoc.4851
32. Nishide M, Nishimura K, Matsushita H, et al. Single-cell multi-omics analysis identifies two distinct phenotypes of newly-onset microscopic polyangiitis. Nat Commun 2023; 14(1): 5789. doi: 10.1038/s41467-023-41328-0
33. Bonne-Année S, Bush MC, Nutman TB. Differential Modulation of Human Innate Lymphoid Cell (ILC) Subsets by IL-10 and TGF-β. Sci Rep. 20191004th ed. 2019 Oct;9(1):14305.

34. Bej S, Galow AM, David R, Wolfien M, Wolkenhauer O. Automated annotation of rare-cell types from single-cell RNA-sequencing data through synthetic oversampling. BMC Bioinformatics 2021; 22(1): 557. doi: 10.1186/s12859-021-04469-x

35. Guo H, Li J. scSorter: assigning cells to known cell types according to marker genes. Genome Biol 2021; 22(1): 69. doi: 10.1186/s13059-021-02281-7

36. Andreatta M, Corria-Osorio J, Müller S, Cubas R, Coukos G, Carmona SJ. Interpretation of T cell states from single-cell transcriptomics data using reference atlases. Nat Commun 2021; 12(1): 2965. doi: 10.1038/s41467-021-23324-4

37. Bendall SC, Davis KL, Amir el-AD, et al. Single-cell trajectory detection uncovers progression and regulatory coordination in human B cell development. Cell. 2014; 157(3): 714–25. doi: 10.1016/j.cell.2014.04.005

38. Yao C, Sun HW, Lacey NE, et al. Single-cell RNA-seq reveals TOX as a key regulator of CD8+ T cell persistence in chronic infection. Nat Immunol 2019; 20(7): 890–901. doi: 10.1038/s41590-019-0403-4

39. Wan H, Chen L, Deng M. scEMAIL: universal and source-free annotation method for scRNA-seq data with novel cell-type perception. Genomics Proteomics Bioinformatics 2022; 20(5): 939–58. doi: 10.1016/j.gpb.2022.12.008

40. Ji X, Tsao D, Bai K, Tsao M, Xing L, Zhang X. scAnnotate: an automated cell-type annotation tool for single-cell RNA-sequencing data. Bioinform Adv 2023; 3(1): vbad030. doi: 10.1093/bioadv/vbad030

41. Nguyen V, Griss J. scAnnotatR: framework to accurately classify cell types in single-cell RNA-sequencing data. BMC Bioinformatics 2022; 23(1): 44. doi: 10.1186/s12859-022-04574-5

42. Yao Z, Liu H, Xie F, et al. A transcriptomic and epigenomic cell atlas of the mouse primary motor cortex. Nature 2021; 598(7879): 103–10. doi: 10.1038/s41586-021-03500-8

Primerjalna analiza referenčno osnovanega mapiranja celičnih tipov in ročne anotacije pri analizi sekvenciranja RNA posamezne celice

L. Goričan, B. Gole, G. Jezernik, G. Krajnc, U. Potočnik, M. Gorenjak

Izvleček: Sekvenciranje RNA v posamezni celici (scRNA-seq) omogoča edinstven vpogled v celično raznolikost kompleksnih tkiv, kot so mononuklearne celice periferne krvi (PBMC). Dodatno je diferencialno izražanje genov na ravni posameznih celic lahko osnova za razumevanje specializiranih vlog posameznih celic in celičnih tipov v bioloških procesih in bolezenskih mehanizmih. Zaradi velike kompleksnosti pa je točna določitev celičnih tipov v zbirkah podatkov scRNA-seq zahtevna. V članku primerjamo dve strategiji določanja celičnih tipov, ki se uporabljata za PBMC v zbirkah podatkov scRNA-seq: avtomatizirano, na referenčnih bazah podatkov temelječe orodje »Azimuth« in nenadzorovano razvrščanje v grozde »Shared Nearest Neighbour« (SNN), ki mu sledi ročno določanje celičnih tipov. Naši rezultati poudarijo prednosti in omejitve obeh pristopov. »Azimuth« je zlahka obdelal obsežne podatkovne nize scRNAseq in zanesljivo prepoznal tudi razmeroma redke populacije celic. Imel pa je težave s celičnimi tipi izven svojega referenčnega območja. Nasprotno je nenadzorovano razvrščanje SNN jasno razmejilo vse različne celične populacije v vzorcu. Metoda SNN je zato zelo primerna za prepoznavanje redkih ali novih tipov celic, vendar zahteva dolgotrajno ročno določanje celičnih tipov, ki je nagnjeno k pristranskosti. S strogimi merili in skupnim strokovnim znanjem več neodvisnih ocenjevalcev smo to pristranskost minimalizirali. Naše ročno določanje celičnih tipov je tako le malo odstopalo od avtomatiziranega. Nazadnje je veljavnost določitve celičnih tipov z orodjem »Azimuth« in ročno metodo potrdila še psevdočasovna analiza glavnih celičnih tipov. Naša raziskava tako poudarja nujo po kombiniranju različnih pristopov razvrščanja in določanja celičnih populacij za izboljšanje zanesljivosti in globine analiz scRNA-seq.

Ključne besede: transkriptomika posamezne celice; mononuklearne celice periferne krvi; referenčno mapiranje; anotacija celičnih tipov; imunski sistem

Slov Vet Res
DOI 10.26873/SVR-1708-2024
UDC 601.4:575.116.4: 599.731.111
Pages: 263–9

Original Research Article

PCV2 and PCV3 Genotyping in Wild Boars From Serbia

Key words

PCV2;
PCV3;
genotyping;
PCR;
wild boar

Jakov Nišavić[1], Andrea Radalj[1]*, Nenad Milić[1], Isidora Prošić[1], Aleksandar Živulj[2], Damir Benković[3], Branislav Vejnović[4]

[1]Department for Microbiology, Faculty of Veterinary Medicine, University of Belgrade, 11000 Belgrade, [2]Veterinary Specialized Institute „Pančevo", 26000 Pančevo, [3]Veterinary Specialized Institute „Sombor", 25000 Sombor, [4]Department for Economics and Statistics, Faculty of Veterinary Medicine, University of Belgrade, 11000 Belgrade, Serbia

***Corresponding author:** andrea.zoric@vet.bg.ac.rs

Abstract: Porcine circoviruses 2 and 3 (PCV2 and PCV3) are known agents of diseases in domestic pigs and wild boars. PCV2 is an economically important pathogen causing porcine circovirus-associated diseases (PCVAD), while the recently discovered PCV3 is associated with similar disorders. Wild boars can serve as a PCV reservoir for domestic pigs, which is a particular risk for pig farms with low biosecurity. Reports of these infections in Serbia are sporadic, and this study was intended as a follow-up to an earlier study. Our aim was to assess the prevalence and genetic characteristics of PCVs circulating in wild boars in a region in north-eastern Serbia with extensive hunting areas. In our study of 103 samples, 17.48% tested positive for PCV2 and 15.53% for PCV3. The low co-infection rates in 2.94% of the PCR-positive samples, suggests these viruses circulate independently. PCV2 prevalence was lower than in our previous study (40.32% out of 124 samples), but the genetic stability of circulating strains was detected with a clear genotype shift towards PCV2d-2. Moreover, this is the first report of PCV3 occurrence in wild boar in Serbia, and the detected strains were grouped into two genotypes: PCV3-1 and PCV3-3c. The PCV3-1 sequences were clustered with German strains, indicating the prevalence of this genotype in Europe. However, no further geographical correlation could be established, as the PCV3-3c representative was separated within the cluster containing Chinese and Indian strains. Furthermore, there was no correlation between PCV positivity and pathological findings in the sampled animals indicating subclinical infection.

Received: 20 February 2023
Accepted: 22 April 2024

Introduction

Over Porcine circoviruses (PCV) are one of the smallest DNA viruses with a circular genome and belong to the family *Circoviridae* (1). These known pathogens are associated with disease in both domestic pigs and wild boars. In recent years, new PCVs and genotypes of already known viruses have been gradually discovered (2, 3). Porcine circovirus 2 (PCV2) is the best-studied porcine circovirus and causes several diseases collectively known as porcine circovirus-associated disease (PCVAD), including postweaning multisystemic wasting syndrome (PMWS), porcine dermatitis and nephropathy syndrome (PDNS), pneumonia, reproductive problems, and so on (3, 4). PCV2 can spread easily in a susceptible population, mainly through direct contact and can be shed over a long period of time, exposing susceptible pigs to contaminated respiratory secretions, feces and urine (3). PCV3 was initially identified in 2016 through metagenomic sequencing within the domestic pig population and this discovery was linked to instances of reproductive failure and PDNS (2, 4, 5). It is widely recognized that factors beyond PCV2 infection are required to cause severe disease, however, PCV2 impacts the immune response in wild boars, which can exacerbate other existing diseases in these animals (3). Similarly, PCV3 has also been found in apparently healthy animals and it is believed that

this virus serves as a contributing factor in intensifying the severity of diseases during concurrent infections (6, 7, 8). These viruses are genetically heterogeneous and PCV2 is currently divided into eight genotypes (PCV2a-PCV2h), while PCV3 is divided into three genotypes and several subtypes (9, 10, 11). Evidence of a global genotype shift of PCV2 is accumulating, as the PCV2d genotype is gradually becoming dominant worldwide (12-15). Frequently, the primary origin of virus spread is rooted in the structure of the domestic pig farming sector. These small units, mostly owned by families, do not implement any biosecurity measures and the pigs are typically raised in a free-range manner, occasionally coming into close contact with wild boars (15, 16). Moreover, high prevalence of PCVs in wild boars and the genetic similarity between PCV3 strains found in domestic and wild populations could imply that wild boars serve as virus reservoirs (17-20). Generally, the occurrence of PCVs in the wild is typically greater in regions with extensive pig farming (15, 21). The estimated density of the wild boar population in Serbia is 0.2 - 1.38 animals per km^2, and the country has the highest density of pigs in the Western Balkans, with around 2.7 million domestic pigs (3). The prevalence of PCVs in the wild boar population varies from country to country. In our recent study, conducted in hunting areas in a region with traditional pig breeding, we confirmed the dominant presence of genotype PCV2d in the wild boar population, but no PCV3-positive animals were detected at that time (15). Aside from our study, the only available literature information dates back to 2012, and demonstrates the presence of PCV2b in the domestic pig population in Serbia (30). Published European studies indicate the presence of PCV3 in over 70% of the tested samples from wild boars (19). Savić et al. (8) reported the prevalence of PCV3 in domestic pig farms and link this virus to the occurrence of PCVAD, which serves as the only data available from Serbia concerning this topic. The aim of this study was to follow up on our previous work and analyse the presence and genetic characteristics of porcine circoviruses in wild boars from the same hunting areas three years later.

Materials and methods

Samples

Samples of lymph nodes and spleen were collected from 103 adult wild boars during the 2021/2022 hunting season in the South Banat district of Vojvodina in north-eastern Serbia. The collection of wild boar samples was carried out as part of regular monitoring for African and classical swine fever organized by the Veterinary Directorate of the Ministry of Agriculture, Forestry and Water Management. Sampling was performed in the field without a complete pathoanatomical section, and general condition of the sampled animals was noted. The hunting areas covered by this survey included: Opovo (45°3'N, 20°25'E), Plandište (45°22'N, 21°12'E), Bela Crkva (44°87'N, 21°43'E), Alibunar (45°4'N, 20°58'E), Vršac (45°13'N, 21°36'E), Pančevo (44°82'N, 20°63'E), and Kovin (44°44' N, 20°58' E). The samples were transported on ice to the Faculty of Veterinary Medicine, University of Belgrade for further examination. Samples from each animal were pooled and homogenised in phosphate buffered saline (PBS 7.2). Tissue suspensions were centrifuged at 1.677 × g for 10 minutes, and DNA was extracted using the GeneJET Genomic DNA Purification Kit (Thermo Scientific, USA).

PCR, sequencing and phylogeny

PCR detection of PCV2 and PCV3 was performed using primers and protocols described by Castro et al. (22) and Franzo et al. (23). Internal reference strains of PCV2 (GenBank acc. no. MW550043) and PCV3 from the Department of Microbiology, Faculty of Veterinary Medicine, University of Belgrade were used as positive controls. The PCR products that were positive for PCV2 and PCV3 were selected for sequencing. All PCV2-positive samples were sequenced with the PCR primers described previously, and PCV3-positive samples from different hunting areas were sequenced with primers specific for the viral capsid gene (24). The PCV2 and PCV3 nucleotide sequences obtained were compared with analogous sequences from GenBank using the tool BLAST (http://www.ncbi.nlm.nih.gov/BLAST/). Generation of consensus sequences, analysis and quality control of the raw sequences were performed using the STADEN package (25).

For phylogenetic analysis, MEGA 11 software (26) was used, and trees were generated by the neighbour-joining algorithm after Kimura-2 parameter correction with 1,000 bootstrap repeats, using appropriate sequences as outgroups. Bootstrap values of more than 70 % were reported. Genotype and cluster representative strains were selected (9-11).

The representative PCV2 and PCV3 sequences obtained in this study were submitted to GenBank and are available under the following accession numbers: OP784785 - OP784793.

Results

The PCR results were as follows: PCV2 DNA was detected in 18/103 animals (17.48%), and 16/103 samples were PCV3 positive (15.53%), with rare mixed infections in 0.97% of the tissues examined (i.e. 2.94% of the PCR-positive samples). The distribution of positive animals among the different hunting areas in this study is shown in Figure 1. PCV3-positive animals were sampled in Plandište (7/16; 43.75 %), Vršac (7/16; 43.75 %) and Pančevo (2/16; 12.5 %), while PCV2-positive samples were from Plandište (5/18; 27.8 %), Kovin (7/18; 38.9 %) and Bela Crkva (6/18; 33.3 %).

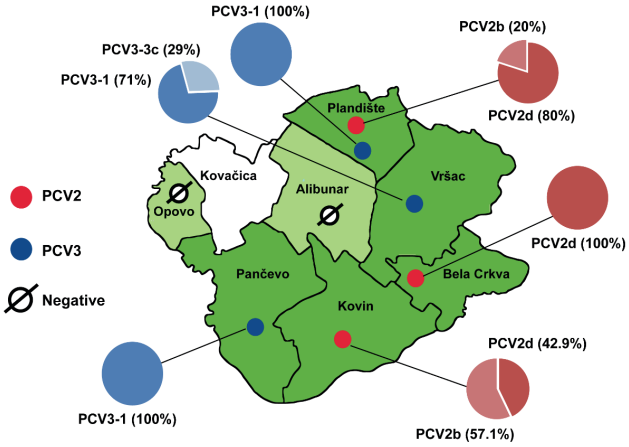

Figure 1: PCV2- and PCV3-positive wild boar samples in different hunting areas and distribution of genotypes.

The overall similarity of the detected PCV2 strains with other strains from GenBank, including previously reported strains from the same hunting grounds (MW550042-MW550059), was 90-100%, while they were 93-100% similar to each other.

Phylogeny revealed that the detected strains belonged to PCV2b (5/18; 27.8%) and PCV2d (13/18; 72.2%) genotypes. The detected PCV2d strains were clustered with PCV2d-2 sequences detected in 2018/2019 in wild boar from the same hunting areas, as well as with analogous strains from Hungary, China and the USA. In addition, the PCV2b sequences from this study also clustered with PCV2b sequences detected in wild boar from the same hunting areas (Figure 2). The PCV3 sequences from this study had an overall similarity of 98-100 % with other sequences examined from GenBank and had a similarity of 98-99 % with a previously reported Serbian PCV3 strain detected in domestic pigs. In addition, the detected PCV3 strains were 99-100 % similar to each other. The results of the phylogenetic analysis showed that the sequences examined belonged to the PCV3-1 (14/16; 87.5%) and PCV3-3c (2/16; 12.5%) genotypes. The PCV3-1 sequences formed a cluster with analogous sequences from Germany, while the PCV3-3c genotype representative in this study did not form a cluster with sequences from India and China belonging to the same genotype (Figure 3). The distribution of the PCV2 and PCV3 genotypes in positive samples from different hunting areas is shown in Figure 1.

Discussion

This study is a continuation of our previous work on wild boar samples from the same hunting area taken in 2018/2019 (15). These results showed a high frequency of PCV2 infection, while PCV3 was not detected. Similarly, the reported detection frequency of PCV3 in South Korean wild boar was also relatively low (27). Our current results are more in line with European studies showing high PCV3 infection

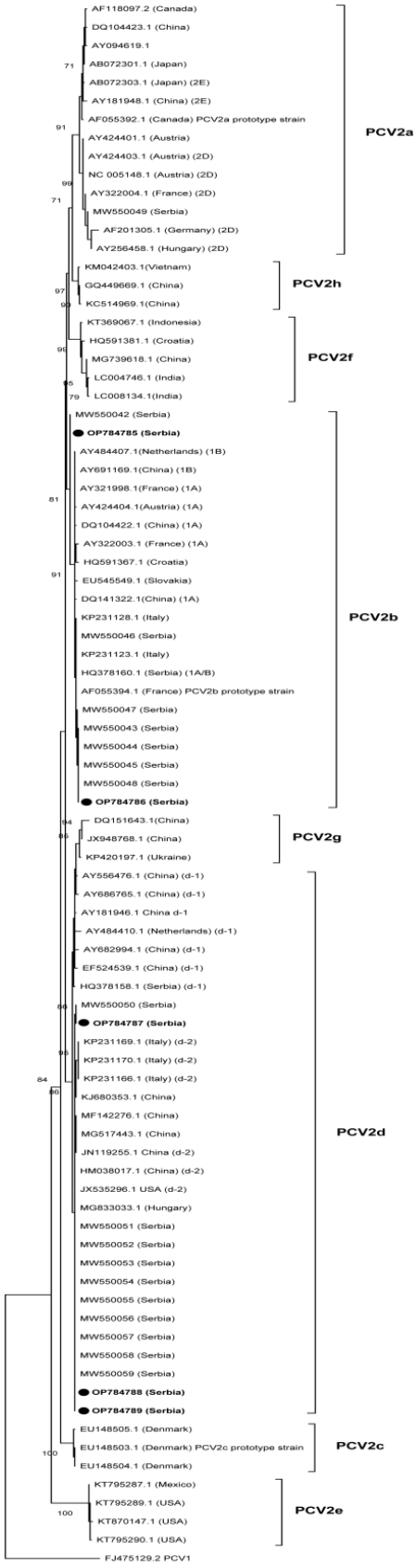

Figure 2: Neighbour-joining tree constructed from wild boar PCV2 sequences (OP784785 - OP784789) and sequence representatives of different genotypes. Previously detected PCV2 strains from the same area are marked MW550042–MW550059. The sequences from this study are marked by a black circle.

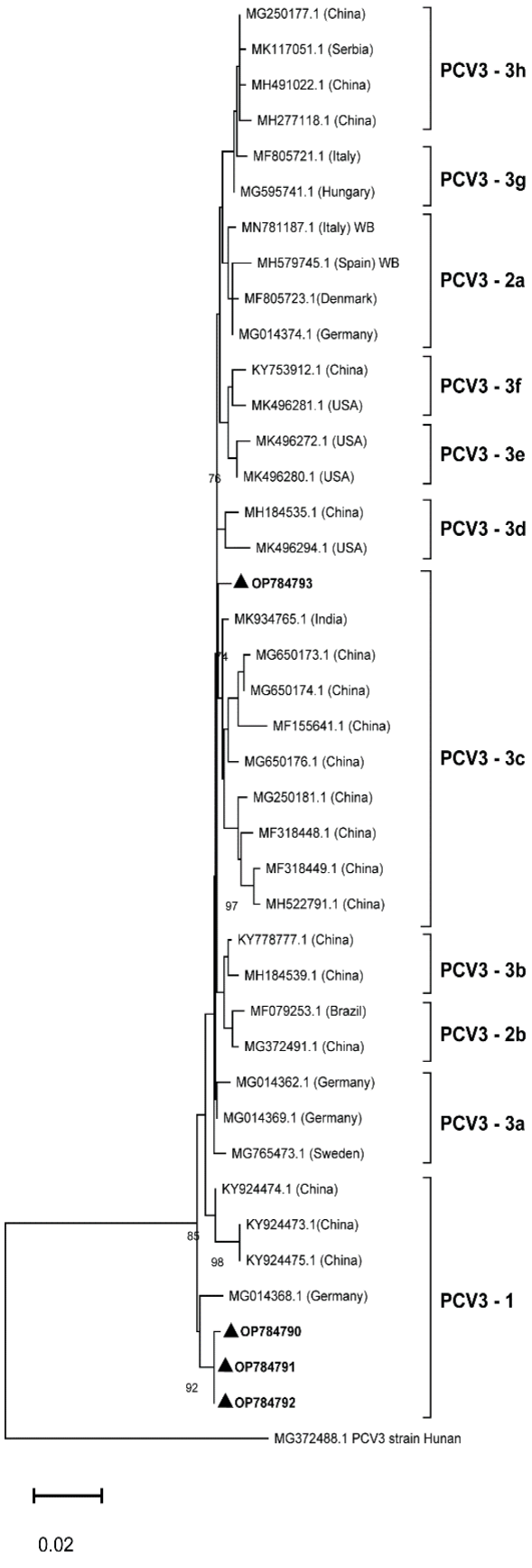

Figure 3: Neighbour-joining tree constructed from wild boar PCV3 sequences (OP784790 - OP784793) and sequence representatives of different genotypes. The sequences from this study are marked by a black triangle.

rates in wild boar ranging from 23% to 71% (6, 7, 19, 28). These results agree with studies confirming the ubiquity of PCV3 in pig farms across Europe (13). Furthermore, Savić et al. (8) suggested that PCV3 is widespread in the pig population in Serbia.

In a study similar to ours, conducted by Dal Santo et al. (29), PCV2 and PCV3 were detected in 57.7% and 15.4%, respectively, of the Brazilian wild boar samples tested. The proportions of European wild boar that are PCV2-positive are variable, ranging from 10 % to 47.3 % in different hunting districts (17, 19, 28). In contrast to our current results, PCV2 was previously detected in 40.32 % of wild boar from this area (15). In general, the higher PCV2 prevalence in wild boar in certain countries and areas is associated with extensive domestic pig farming (15, 21).

Many reports show different co-infection rates of PCV3 and other relevant swine viruses, including PCV2 (2). Prevalence rates of PCV2/PCV3 co-infections detected in wild boar populations in Germany and Italy ranged from 7.5 % to 24.4 %, while these rates are higher in domestic pigs, especially in relation to animals with observed clinical signs (4, 17, 19, 28). Accordingly, the prevalence of PCV3 infections has been reported to be higher in domestic pig farms with PRDC (5). Savić et al. (8) also noted a possible association between PCV3 infection of domestic pigs in Serbia and clinical disease. In contrast, the wild animals in our study were in good condition, and similar to the results reported by Franzo et al. (6), there was no correlation between PCV3 positivity and pathological findings. Our results show that mixed PCV2/PCV3 infections are rare, accounting for 2.94% of all positive samples, comparable to the findings of Saporiti et al. (13) and Dal Santo et al. (29).

The genetic heterogeneity of PCV2 can be demonstrated by phylogenetic analysis of the corresponding gene segments (10). The strains detected in this study were assigned to PCV2d genotype in 72.2% and to PCV2b genotype in 27.8% of PCV2-positive samples. The latest available data on genetic variability of PCV2 in domestic and wild pigs in Serbia showed that PCV2b was the dominant genotype in the field, which is consistent with results from other countries from that time (20, 30, 31). However, the results of our previous study represented an update showing a visible dominance of PCV2d, consistent with the global PCV2 genotype shift (15). Data from PCV2 strains detected in domestic pigs from different regions of China also show the gradual replacement of PCV2b by the PCV2d genotype (4, 12, 14). A comprehensive analysis of the prevalence of the PCV2 genotype in European domestic pigs by Saporiti et al. (13) also revealed that PCV2d is the most frequently found genotype, followed by PCV2b and 2a. Accordingly, we confirmed the decreasing prevalence of PCV2a in Serbia, as there were no representatives of this genotype in contrast to the 2018/2019 sampling period, when 5.5% were positive, which remains in line with the situation in domestic pigs worldwide (13-15). Further evidence for our

findings is that the PCV2 strains detected in wild boars in Italy in 2021 belong predominantly to PCV2d, followed by PCV2b (19). The representatives of genotypes 2d and 2b in this study were clustered with PCV2d-2 and PCV2b sequences detected in 2018/2019 in wild boar from the same hunting areas, indicating the genetic stability of circulating virus strains in this wild boar population. Overall, the current PCV2d strains are most often representatives of the PCV2d-2 cluster, and our current results confirm the assumption of their dominance in the studied area (9, 15). This is also supported by studies conducted in Italy in both domestic pigs and wild boars (19, 32). Interestingly, Rudova et al. (21) detected genotype f in wild boars, demonstrating the possible PCV2 diversity in the wild. Furthermore, the authors found an accumulation of representatives of the PCV2 genotype in domestic and wild animals, suggesting an ecological interaction. Unfortunately, there are no recent data on PCV2 genotype diversity in Serbian domestic pigs, and the latest available data suggest that domestic pigs are predominantly infected with PCV2b (30, 31).

The PCV3 sequences obtained in this study had a high overall similarity rate of 98-100% to each other and to analogous sequences from GenBank. These data on PCV3 molecular diversity are consistent with other studies showing a relatively high degree of genetic homology between PCV3 strains (2, 4, 5, 7, 13, 14). The phylogenetic analysis of German PCV3 strains performed by Fux et al. (33) describes two main groups of PCV3 strains (PCV3a and b) with corresponding subclusters. This strain classification has also been reported elsewhere (8, 23, 34). Li et al. (34) reported that diversification of PCV3 into PCV3a and b occurred between 2013 and 2014, and also reported the existence of branches PCV3a-1 and PCV3a-2. However, there is no correlation between the distribution of PCV3 strains and their respective geographical origins (2). Mutations within the PCV3 genome are mostly found in the region encoding the cap protein, which can be useful for genotyping strains (4, 35). Accordingly, several authors have proposed the subdivision of PCV3 into three genotypes (PCV3a, PCV3b and PCV3c) (12, 35, 36). According to the PCV3 genotype classification recently proposed by Chung et al. (11), most of the wild boar strains detected in our study are classified as PCV3-1, followed by PCV3-3c (12.5%). A similar study from Italy gave different results and all PCV3 strains from wild boars were classified as subtype 2a, mostly together with other European, Chinese and Brazilian strains (19). PCV3-1 strains from wild boars in Serbia were clustered with German strains, which might be due to the increase of wild boar populations in Europe and their migratory characteristics. Interestingly, the PCV3-3c genotype representative in this study was distantly related within the genotype to strains from India and China, confirming that there is no geographical correlation with the PCV3 genotyping method. Similar results were obtained by Savić et al. (8), who showed clustering of Serbian PCV3 strains in domestic pigs with Chinese strains. When compared with the available analogue sequence of a PCV3 domestic pig strain from Serbia, the overall differences from the wild boar sequences obtained were about 2 %, and the strains did not show clustering, suggesting independent circulation.

Conclusions

In this paper we have described the occurrence of PCV2 and PCV3 in wild boar, focusing on their genetic characteristics. These viruses are widespread, but there are rare cases of co-infection, suggesting that they mostly occur as single pathogens. There was no correlation between PCV positivity and general condition of the sampled animals, indicative of subclinical infection. Although PCV2 has been detected in wild boar populations in our previous study, this is the first report of PCV3 in these animals in Serbia. The most common genotype of PCV2 found in this study was PCV2d (PCV2d-2 cluster), confirming the previously reported global trend of genotype shift. In addition, we confirmed the circulation of the same PCV2 strains in the sampled hunting areas as in the 2018/2019 season. Most of the PCV3 sequences found were closely related, especially to strains from Germany, suggesting the existence of a single genotype circulating in Europe. Nevertheless, our data are in agreement with the results of other authors showing no geographical correlation with genotype association. Details on the molecular epizootiology of PCV3 are still scarce, and data presented here add to the lack of information on the genetic characteristics of wild boar strains for this part of Europe. The occurrence of PCV2 and PCV3 in wild boar may pose a challenge for commercial pig production and the potential risk of transmission between wild and domestic pigs needs to be considered. In addition, wild boar and domestic pig PCV strains demonstrate phylogenetic clustering, confirming the possibility of pathogen exchange between these species. Therefore, biosecurity measures must be taken in pig farms to ensure distancing from wild populations. As there are large numbers of wild boars in Serbia and extensive domestic pig farming is common, it is important to monitor the occurrence of pathogens in these populations. Since we did not study the local pig population, we do not have information on the genetic diversity of PCV2 and PCV3 in pig farms, so no exact correlation could be established. There are no recent data on PCV2 genotype diversity in Serbian domestic pigs, and none of the detected PCV3 strains from wild boars were clustered with the available domestic pig strain, which could indicate an independent spread of PCV3. However, studies comparing the genetic characteristics of strains from the wild population and from surrounding pig farms could provide more conclusive information. In view of the results presented, we emphasize the importance of screening wild boar samples to contribute to the understanding of the role of porcine circoviruses and epizootiology in different animal populations.

Acknowledgments

This work was supported by the Ministry of Science, Technological Development and Innovation of the Republic of Serbia [Contract number 451-03-66/2024-03/200143].

Conflict of interest. The authors declare no conflict of interest.

References

1. ICTV. Current ICTV taxonomy release: taxonomy browser. Utrecht: International Committee on Taxonomy of Viruses, 2024. https://talk.ictvonline.org/taxonomy/ (12.02.2023)
2. Ouyang T, Niu G, Liu X, Zhang X, Zhang Y, Ren L. Recent progress on porcine circovirus type 3. Infect Genet Evol 2019; 73: 227–33. doi: 10.1016/j.meegid.2019.05.009.
3. Nišavić J, Radalj A, Milić N, et al. A review of some important viral diseases of wild boars. Biotechnol Anim Husb 2021; 37(4): 235–54. doi: 10.2298/BAH2104235N
4. Guo Z, Ruan H, Qiao S, Deng R, Zhang G. Co-infection status of porcine circoviruses (PCV2 and PCV3) and porcine epidemic diarrhea virus (PEDV) in pigs with watery diarrhea in Henan province, central China . Microb Pathog 2020; 142: 104047. doi: 10.1016/j.micpath.2020.104047
5. Kedkovid R, Woonwong Y, Arunorat J, et al. Porcine circovirus type 3 (PCV3) infection in grower pigs from a Thai farm suffering from porcine respiratory disease complex (PRDC). Vet Microbiol 2018; 215: 71–6. doi: 10.1016/j.vetmic.2018.01.004
6. Franzo G, Tucciarone CM, Drigo M, et al. First report of wild boar susceptibility to porcine circovirus type 3: high prevalence in the Colli euganei regional park (Italy) in the absence of clinical signs. Transbound Emerg Dis 2018; 65(4): 957–62. doi: 10.1111/tbed.12905
7. Klaumann F, Dias-Alves A, Cabezón O, et al. Porcine circovirus 3 is highly prevalent in serum and tissues and may persistently infect wild boar (Sus Scrofa Scrofa). Transbound Emerg Dis 2019; 66(1): 91–101. doi: 10.1111/tbed.12988
8. Savić B, Milicevic V, Radanovic O, et al. Identification and genetic characterization of porcine circovirus 3 on pig farms in Serbia. Arch Virol 2020; 165(1): 193–9. doi: 10.1007/s00705-019-04455-y
9. Xiao C-T, Halbur PG, Opriessnig T. Global molecular genetic analysis of porcine circovirus type 2 (PCV2) sequences confirms the presence of four main pcv2 genotypes and reveals a rapid increase of PCV2d. J Gen Virol 2015; 96(7): 1830–41. doi: 10.1099/vir.0.000100
10. Franzo G, Segalés J. Porcine circovirus 2 (PCV-2) genotype update and proposal of a new genotyping methodology. PLoS One 2018; 13(12): e0208585. doi: 10.1371/journal.pone.0208585
11. Chung H-C, Nguyen VG, Park Y, Park B-K. Genotyping of PCV3 based on reassembled viral gene sequences. Vet Med Sci 2021; 7(2): 474–82. doi: 10.1002/vms3.374
12. Chen N, Huang Y, Ye M, et al. Co-infection status of classical swine fever virus (CSFV), porcine reproductive and respiratory syndrome virus (PPRSV) and porcine circoviruses (PCV2 and PCV3) in eight regions of china from 2016 to 2018. Infect Genet Evol 2019; 68: 127–35. doi: 10.1016/j.meegid.2018.12.011
13. Saporiti V, Huerta E, Correa-Fiz F, et al. Detection and genotyping of porcine circovirus 2 (PCV-2) and detection of Porcine circovirus 3 (PCV-3) in sera from fattening pigs of different european countries. Transbound Emerg Dis 2020; 67(6): 2521–31. doi: 10.1111/tbed.13596
14. Xu T, Zhang Y-H, Tian R-B, et al. Prevalence and genetic analysis of porcine circovirus type 2 (PCV2) and type 3 (PCV3) between 2018 and 2020 in central China. Infect Genet Evol 2021; 94: 105016. doi: 10.1016/j.meegid.2021.105016
15. Nišavić J, Milic N, Radalj A, et al. Detection and characterisation of porcine circoviruses in wild boars in northeastern Serbia. Vet Med (Praha) 2022; 67(3): 131–7. doi: 10.17221/32/2021-VETMED
16. Ladoşi I, Păpuc TA, Ladoşi D. The impact of african swine fever (ASF) on romanian pig meat production: a review. Acta Vet 2023; 73(1): 1–12. doi: 10.2478/acve-2023-0001
17. Amoroso MG, Serra F, Esposito C, et al. Prevalence of infection with porcine circovirus types 2 and 3 in the wild boar population in the campania region (southern Italy). Animals (Basel) 2021; 11(11): 3215. doi: 10.3390/ani11113215
18. Nišavić J, Milic N, Radalj A, et al. Genetic analysis and distribution of porcine parvoviruses detected in the organs of wild boars in Serbia. Acta Vet 2021; 71(1): 32–46. doi: 10.2478/acve-2021-0003
19. Fanelli A, Pellegrini F, Camero M, et al. Genetic diversity of porcine circovirus types 2 and 3 in wild boar in Italy. Animals (Basel) 2022; 12(8): 953. doi: 10.3390/ani12080953
20. Franzo G, Grassi L, Tucciarone CM, et al. A wild circulation: high presence of porcine circovirus 3 in different mammalian wild hosts and ticks. Transbound and Emerg Dis 2019; 66(4): 1548–57. doi: 10.1111/tbed.13180
21. Rudova N, Buttler J, Kovalenko G, et al. Genetic diversity of porcine circovirus 2 in wild boar and domestic pigs in Ukraine. Viruses 2022; 14(5): 924. doi: 10.3390/v14050924
22. Castro AMMG, Castro Jr. FG, Budiño FEL, et al. Detection of genetic characterization of porcine circovirus 2 (PCV2) in Brazilian wildlife boars. Braz J Microbiol 2012; 43(3): 1022–5. doi: 10.1590/S1517-838220120003000025
23. Franzo G, Legnardi M, Hjulsager CK, et al. Full-genome sequencing of porcine circovirus 3 field strains from denmark, Italy and Spain demonstrates a high within-Europe genetic heterogeneity. Transbound Emerg Dis 2018; 65(3): 602–6. doi: 10.1111/tbed.12836
24. Wen S, Sun W, Li Z, et al. The detection of porcine circovirus 3 in Guangxi, China. Transbound Emerg Dis 2018; 65(1): 27–31. doi: 10.1111/tbed.12754
25. Staden R, Beal KF, Bonfield JK. The Staden Package, 1998. Methods Mol Biol 2000; 132: 115–130. doi: 10.1385/1-59259-192-2:115
26. Tamura K, Stecher G, Kumar S. MEGA11: molecular evolutionary genetics analysis version 11. Mol Biol Evol 2021; 38(7): 3022–7. doi: 10.1093/molbev/msab120
27. Dhandapani G, Yoon S-W, Noh JY, et al. Detection of porcine circovirus 3 from captured wild boars in Korea. Vet Med Sci 2021; 7(5): 1807–14. doi: 10.1002/vms3.518
28. Prinz C, Stillfried M, Neubert LK, Denner J. Detection of PCV3 in German wild boars. Virol J 2019; 16(1): 25. doi: 10.1186/s12985-019-1133-9
29. Santo ACD, Gressler LT, Costa SZR, et al. Porcine circovirus 2 and 3 in wild boars in southern Brazil. Ciência Rural 2022; 52(2): e20210209. doi: 10.1590/0103-8478cr20210209
30. Savić B, Milićević V, Jakić-Dimic D, et al. Genetic characterization and phylogenetic analysis of porcine circovirus type 2 (PCV2) in Serbia. Arch Virol 2012; 157(1): 21–8. doi: 10.1007/s00705-011-1130-9
31. Toplak I, Lazić S, Lupulović D, et al. Study of the genetic variability of porcine circovirus type 2 detected in Serbia and Slovenia. Acta Vet Hung 2012; 60(3): 409–20. doi: 10.1556/AVet.2012.035

32. Dei Giudici S, Lo Presti A, Bonelli P, et al. Phylogenetic analysis of porcine circovirus type 2 in Sardinia, Italy, shows genotype 2d circulation among domestic pigs and wild boars. Infect Genet Evol 2019; 71: 189–96. doi: 10.1016/j.meegid.2019.03.013

33. Fux R, Söckler C, Link EK, et al. Full genome characterization of porcine circovirus type 3 isolates reveals the existence of two distinct groups of virus strains. Virol J 2018; 15(1): 25. doi: 10.1186/s12985-018-0929-3

34. Li G, He W, Zhu H, et al. Origin, genetic diversity, and evolutionary dynamics of novel porcine circovirus 3. Adv Sci (Weinh) 2018; 5(9): 1800275. doi: 10.1002/advs.201800275

35. Qi S, Su M, Guo D, et al. Molecular detection and phylogenetic analysis of porcine circovirus type 3 in 21 provinces of china during 2015–7. Transbound Emerg Dis 2019; 66(2): 1004–15. doi: 10.1111/tbed.13125

36. Fu X, Fang B, Ma J, et al. Insights into the epidemic characteristics and evolutionary history of the novel porcine circovirus type 3 in southern China. Transbound Emerg Dis 2018; 65(2): e296–e303. doi: 10.1111/tbed.12752

Genotipizacija PCV2 in PCV3 pri divjih prašičih iz Srbije

J. Nišavić, A. Radalj, N. Milić, I. Prošić, A. Živulj, D. Benković, B. Vejnović

Izvleček: Prašičja cirkovirusa 2 in 3 (PCV2 in PCV3) sta znana povzročitelja bolezni pri domačih in divjih prašičih. PCV2 je gospodarsko pomemben patogen, ki povzroča bolezni, povezane s prašičjimi cirkovirusi (PCVAD), medtem ko je nedavno odkriti PCV3 povezan s podobnimi boleznimi. Divji prašiči so lahko rezervoar PCV za domače prašiče, kar predstavlja tveganje zlasti za prašičerejske farme z nizko stopnjo biološke varnosti. Poročila o teh okužbah v Srbiji so sporadična, ta študija pa je bila zasnovana kot nadaljevanje predhodne študije. Naš cilj je bil oceniti razširjenost in genetske značilnosti PCV, ki krožijo med divjimi prašiči v regiji severovzhodne Srbije z obsežnimi lovišči. Testirali smo 103 vzorce, od katerih je bilo 17,48 % pozitivnih na PCV2 in 15,53 % na PCV3. Nizka stopnja sočasne okužbe pri 2,94 % vzorcev, pozitivnih na PCR, kaže, da ti virusi krožijo neodvisno. Prevalenca PCV2 je bila nižja kot v naši prejšnji študiji (40,32 % od 124 vzorcev), vendar je bila ugotovljena genetska stabilnost krožečih sevov z jasnim premikom genotipa v smeri PCV2d-2. To je tudi prvo poročilo o pojavu PCV3 pri divjih prašičih v Srbiji, odkriti sevi pa so bili razvrščeni v dva genotipa: PCV3-1 in PCV3-3c. Sekvence PCV3-1 so bile povezane z nemškimi sevi, kar kaže na razširjenost tega genotipa v Evropi. Vendar nadaljnje geografske povezave ni bilo mogoče ugotoviti, saj je bil predstavnik PCV3-3c ločen v skupini kitajskih in indijskih sevov. Poleg tega ni bilo povezave med pozitivnostjo PCV in patološkimi ugotovitvami pri vzorčenih živalih, kar kaže na subklinično okužbo.

Ključne besede: PCV2; PCV3; genotipizacija; PCR; divji prašiči

Slov Vet Res
DOI 10.26873/SVR-1882-2024
UDC 636.2.09:618.19-002:579.887
Pages: 271–9

Original Research Article

Molecular Characterization, Virulence, and Antimicrobial Susceptibility of *Mycoplasma bovis* Associated With Chronic Mastitis in Dairy Cows

Key words

antimicrobial susceptibility;
chronic mastitis;
Mycoplasma bovis;
sequence analysis;
virulence genes

Magdy Gioushy[1], Eid Elsaid Abdelaziz Soliman[2], Rasha M. Elkenany[3]*, El-Sayed El-Alfy[4], Ahmed Abd Elaal[6], Khaled Abd-El Hamid Abd-El Razik[7], Sabry El-Khodery[5]

[1]Department of Animal Medicine, Faculty of Veterinary Medicine, Aswan University, Aswan 37916, [2]Mycoplasma department Animal Health Research Institute, Dokki, Giza, 12618, [3]Department of Bacteriology, Mycology and Immunology, [4]Department of parasitology, [5]Department of Internal Medicine and Infectious Diseases, Faculty of Veterinary Medicine, Mansoura University, Mansoura, 35516, [6]Department of Animal Medicine, Faculty of Veterinary Medicine, Zagazig University, Zagazig 44511, [7]Department of Animal Reproduction, National Research Center, Giza, 12622, Egypt

***Corresponding author:** dr_rashavet22@mans.edu.eg

Abstract: *Mycoplasma bovis (M. bovis)* is the most common *Mycoplasma* species, which has a growing impact on the dairy industry. The purpose of this study was to investigate the molecular characterization, virulence, and antibiotic susceptibility of *M. bovis* isolates from dairy cows with chronic mastitis in Egypt. Eighty-four composite milk samples from mastitic cows were aseptically collected from dairy farms in Egypt. Based on microbiological examination and the polymerase chain reaction (PCR) technique targeting the 16S rRNA, 14 (16.7%) of all milk samples were positive for *Mycoplasma* spp. PCR targeting *M. bovis*-specific gene identified six (7.14%) of the 14 mycoplasma isolates as *M. bovis*. PCR assays for different virulence genes showed that all *M. bovis* isolates exhibited the presence of vsp_A gene, while other virulence genes (*uvr*C, *gap*, and *p40* pseudogenes) were determined in only two *M. bovis* isolates (2/6). The 16S rRNA gene phylogenetic analysis demonstrated 100% homology with reference strains of *M. bovis* isolated from different species and locations. When compared to other isolates in the GenBank, the amino acid sequence alignment of our isolate VspA-like protein indicated a distinct mutation. The *in vitro* antimicrobial susceptibility testing of the six *M. bovis* isolates in this study to seven antimicrobial drugs revealed that tilmycosin and tylosin had the lowest minimum inhibitory concentrations (MIC) values (≤1 µg/mL), while danofloxacin, streptomycin and florfenicol had the highest MIC values (<4 µg/mL). Nonetheless, this study showed the virulence of *M. bovis* in dairy cows in Egypt, and macrolides were found to be the most potent compounds *in vitro* against all tested isolates, but further studies in nationwide surveys are needed.

Received: 28 November 2023
Accepted: 9 April 2024

Introduction

Mycoplasma-caused bovine mastitis is an emergent issue in the dairy industry of various countries. The prevalence of mastitis caused by *Mycoplasma* spp. is increasing, especially in large dairy herds (1-3). This kind of infection causes significant economic losses as it is highly contagious, difficult to detect with conventional culture media, does not respond to antibiotic treatments, could be affect several quarters, produces a significant decrease in milk production with increasing purulent and abnormal secretions, and infected animals are separated or discarded (4). The most frequent *Mycoplasma* species isolated from intramammary infections in cows is *M. bovis*, causing severe clinical cases, followed by other *Mycoplasma* species involving *M. agalactiae, M. californicum, M. bovigenitalium, M. alkalescens*,

and *M. canadense* (5). The major concern associated with *M. bovis* is that causes pneumonia, arthritis, otitis, and reproductive disorders in cattle (5). This pathogen spreads quickly in affected herds and is extremely infectious, making its eradication challenging. The largest obstacle in preventing *M. bovis* infections on farms is represented by asymptomatic carrier animals that spread the disease to other individuals within the population (6).

Laboratory diagnosis is vital to detect *M. bovis* in clinical specimens since there are no specific symptoms associated with *M. bovis* infection; culture is commonly used in combination with polymerase chain reaction (PCR) based detection and identification. Bacterial culture is a gold standard method for detecting infections caused by this pathogen, but it may be laborious, time-consuming, and non-specific, especially if a mixed infection is supposed (7). Compared to bacterial culture, PCR and sequencing-based techniques are very specific but demand a massive amount of effort. For identifying *Mycoplasma* spp. strains in milk samples, PCR is well recognized as a reliable technique. The majority of *Mycoplasma* spp. can be easily distinguished using PCR assays that specifically target the 16S rRNA spacer region (8). Additionally, sequence analysis enables the recognition and differentiation of a number of *Mycoplasma* and *Acholeplasma* species when the *Mycoplasma* 16-23S rDNA and *Acholeplasma* 16-23S rDNA were targeted (9).

Although *M. bovis* is capable of adhering to and invading host cells, produces hydrogen peroxide, avoids phagocytosis, and is resistant to being killed by the alternate complement system, there was limited data on the molecular basis of *Mycoplasma* pathogenicity (10). Variable surface lipoproteins (Vsp) are a class of surface adhesion proteins that exhibit phase and size variation as a result of high frequency configurations of the DNA sequence encoding the Vsp genes, which are crucial for *Mycoplasma* cell attachment (11). Being a part of the DNA repair pathway makes the very stable gene *uvr*C, which produces deoxy-ribodipyrimidine photolyase, necessary for bacterial reproduction (12). The glyceraldehyde-3-phosphate dehydrogenase (GAPDH) protein encoded by the *gap* gene has been demonstrated to encourage an immunological response in beef cattle, which could aid in the development of an effective vaccine (13). An analog of the *Mycoplasma agalactiae* adhesion gene *p40* occurs as a pseudogene in *M. bovis*, where nucleotide sequence analysis found a substantial loss with a frameshift that results in the translation of the protein being prematurely truncated (14).

M. bovis lacks a cell wall and can't produce folic acid, so it is intrinsically resistant to antimicrobials targeting the cell wall e.g., fosfomycin, glycopeptides, or β-lactam antibiotics, sulphonamides, nalidixic acid, trimethoprim, polymixins, and rifampicin, limiting the number of antimicrobial drugs available during treatment may develop chronic mastitis (15). Antimicrobial drugs that affect protein synthesis, such as macrolides and tetracyclines, are frequently utilized for treatment of mycoplasmal infections in animals. There are numerous records on the antibiotic sensitivity of *M. bovis* strains associated with bovine pneumonia, whereas data on strains associated with cattle mastitis is much more limited (16,17). Therefore, identifying changes in this pathogen's susceptibility to antibiotics requires assessing the antimicrobial resistance in *M. bovis* linked to mastitis.

Despite global advances in the study of *M. bovis* virulence factors and pathogenesis mechanisms, a limited number of studies is available from Egypt (1-3). Thus, the objectives of this study were to (i) estimate *M. bovis* prevalence in milk samples from chronic mastitis cases (CM); (ii) determine virulence genes including vsp_A, *uvr*C, *gap*, and *p40* pseudogenes of isolates; (3) perform the phylogenetic analysis of the 16S rRNA and vsp_A sequences in the selected *M. bovis* isolate; and (4) determine the antibiotic susceptibility of isolates using microbroth dilution method.

Materials and methods

Study areas and Ethics

The present study was carried out at 10 dairy cattle farms and 16 small holder farms in three governorates of middle and eastern Delta region of River Nile named Menofia, Dakahlia, and Sharkia.

Ethical approval for collection of samples and clinical data from dairy farms was gained from the Animal Research Ethical Committee at the Faculty of Veterinary Medicine, Mansoura University, Egypt (Code VM.R. 22.11.30). Verbal owner consent for participation in the study was obtained before enrollment.

Clinical examination and sample collection

A total of 84 mastitic cows at 10 dairy farms and 16 small holder farms were investigated. Cows were clinically examined, and a complete clinical report for each animal was constructed. Physical examination of udder, teats, and milk characteristics was conducted. Moreover, duration of the disease and evidence of systemic signs were recorded. In details, 68 samples were obtained from three large loose-housing dairy Holstein cattle herds suffering from chronic mastitis without response to drug treatment in Menofia Governorate and 16 sporadic samples from cattle of mixed breeds in Dakahlia and Sharkia Governorates. The cases had a history of repeated failure of mastitis treatment with a high somatic cell count (SCC) using California Mastitis Test. Following cleaning of teat ends with 70% ethanol, 84 composite milk samples were obtained under aseptic conditions from affected quarters of each animal. Milk samples were uniformly mixed in a 100 mL sterile tube after the first few streams of milk were discarded. During the whole collection and transfer process to the laboratory for

bacteriological examination, samples were preserved on dry ice, and samples were afterwards held at -80 °C until DNA extraction.

Bacteriological analysis

The *Mycoplasma* species isolation from milk samples was carried out as previously described (18). In brief, 100 µl of each milk sample was inoculated into 2.9 mL of pleuropneumonia-like organism (PPLO) broth (Difco, MI, USA) and incubated at 37°C for 72 h. Then, the broth was spread onto PPLO agar plates and incubated under a 10% CO_2 atmosphere at 37°C and inspected for typical *Mycoplasma* colonies every 2 days up to 28 days. The digitonin sensitivity test was performed for differentiation between *Mycoplasma* and *Acholeplasma* genera by filter paper discs saturated with 200 µl of 1.5% (W/V) ethanol solution of digitonin and dehydrated overnight (19). Biochemical characterization using glucose fermentation, arginine deamination, and urea hydrolysis tests, and film and spot formation was carried out for further testing of *Mycoplasma* species (20,21).

Molecular identification of M. bovis and their virulence genes

The genus identification of all strains was established with the 16S rRNA gene by polymerase chain reaction (PCR) test. When the suspicious strains were confirmed as *Mycoplasma* spp., a species-specific PCR was performed for identifying *M. bovis*. Subsequently, the determination of four potential *M. bovis* virulence genes (vsp_A, *uvr*C, *gap*, and *p40* pseudogenes) was also performed by PCR. Briefly, DNA samples were prepared by boiling method from overnight broth cultures as previously described (22). The extracted DNA samples were subjected to PCR amplification by specific oligonucleotide primers and specific cycling conditions (Table 1). PCR amplification was performed in a total reaction volume of 50 µl containing 25 µl Master Mix (Thermoscientific™, K1081), 3 µl target DNA, 1 µl of each forward and reverse primers (10 pmol) and completed to 50 µl by nuclease free molecular biology grade water. Positive control (*M. bovis* reference strain that was previously identified in our laboratory), and negative control were included in the reaction.

Sequencing of 16S rRNA and vsp_A genes

The positive PCR products of one representative strain were sequenced in both directions by Macrogen (South Korea). Using the BLAST and Protein-BLAST search programmes (National Center for Biotechnology Information NCBI" http://www.ncbi.nlm.nih.gov/), the selected *M. bovis* strain (MYEG1) nucleotide and amino acid sequences were compared with those of other strains published in GenBank. The nucleotide sequences obtained during this examination were examined by the BioEdit 7.0.4.1 and Muscle (EMBL's European Bioinformatics Institute, 2020) programs. The subsequent sequences were aligned with those of reference sequences of *M. bovis* utilizing a neighbour-joining analysis of the aligned sequences executed in the program CLC Genomics Workbench 3.

The nucleotide sequences of the *M. bovis* strain (MYEG1), comprising the 16S rRNA and vsp_A genes were deposited in GenBank under accession number OK336362 and OK349676, respectively.

Antimicrobial susceptibility testing

Antimicrobial susceptibility testing of confirmed *M. bovis* strains for seven antibiotics was performed using PPLO broth supplemented with 0.5% (w/v) sodium pyruvate, 0.5% (w/v) glucose, and 0.005% (w/v) phenol red following the minimum inhibitory concentrations (MIC) guidelines (23) from two different methods, the micro-broth method and Sensititre® plate method. The tested antimicrobial agents were frequently utilized in the treatment of *Mycoplasma* infections. The subsequent antimicrobial substances were investigated: danofloxacin (25%), tulathromycin (10%), doxycycline (50%), florofenicol (10%), oxytetracyclin (20%),

Table 1: Target genes and primer sequences used for PCR amplifications

Target	Specificity	Sequence	Reference
16S rRNA gene	*Mycoplasma* genus	16SmunivF (5'- AGA CTC CTA CGG GAG GCA GCA-3') 16SmunivR (5'- ACT AGC GAT TCC GAC TTC ATG -3')	(8)
Species specific gene	*M. bovis*	MboF (5′CCT TTT AGA TTG GGA TAG CGG ATG-3′) MboR (5′CCG TGA AGG TAG CAT CAT TTC CTA T 3′)	(37)
vsp_A gene		MYBF (5'- CTT GGA TCA GTG GCT TCA TTA GC -3') MYBREV (5'-GTC ATC ATG CGG AAT TCT TGG GT -3')	(8)
uvrC gene		TTACGCAAG bouvrc2-L (5'- TTACGCAAGAGAATGCTTCA-3') M bouvrc2-R (5'-TAGGAAAGCACCCTATTGAT-3')	(40)
gap gene		M.b.gap7(5'-ATAGGAGGATCCAAAAGAGTCGCTATCAATGGTTT TGGACG-3') M.b.gap8 (5'-GGAAATGGTACCTTACTTAGTTAGTTTAGCAAAG TATGTTAATG-3')	(13)
p40 pseudogene		MBO-P40-L (5'-ATGAAAACAAATAGAAAAATAAGTC-3') MBO-P40-R (5'-GTAGCTTTTTCCAATAATTTTCC-3')	(14)

Table 2: Prevalence of Mycoplamsa and *Acholeplasma* in chronic mastitis milk samples (n=84)

Source	Milk Samples No.	*Mycoplasma*			*Acholeplasma*	Total
		M. bovis	Other *Mycoplasma* spp.	Total		
Dairy cattle farms	68	6 (8.8%)	4 (5.9%)	10 (14.7%)	4 (5.9%)	14(20.6%)
Sporadic cases	16	0	4 (25%)	4 (25%)	0	4(25%)
Total	84	6 (7.14%)	8 (9.52%)	14 (16.7%)	4 (4.8%)	18(21.4%)

Table 3: Minimum inhibitory concentrations (µg/mL) of antimicrobials for *Mycoplasma bovis* isolates (n=6) obtained from chronic mastitis

Antimicrobial class	Antimicrobial agents	S* 17	S 26	S 28	S 29	S 30	S 31	MIC ranges
Fluoroquinolones	Danofloxacin	4	4	8	4	8	4	4-8
Tetracycline	Doxycyclin	4	0.312	1.248	4	2	4	0.312-4
Aminoglycosides	Streptomycin	8	0.078	4	0.312	8	8	0.078-8
Phenicols	Florfenicol	8	4	4	8	4	8	4-8
Macrolides	Tulathromycin	4	0.312	1.248	4	4	4	0.312-4
	Tilmycosin	0.039	0.009	0.39	0.009	0.009	0.39	0.009-0.39
	Tylosin	0.009	0.009	1	0.009	1	1	0.009-1

tilmicosin (30%), and tylosin (100%). For each *M. bovis* strain, a sufficient volume of frozen stock culture was thawed and diluted to a concentration of 10^4 color changing units (CCU)/ml as previously described (24) in order to allow for a serial two-fold dilution in fresh broth. In the microbroth assay, the antimicrobials were examined in serial twofold dilutions at concentrations in the range 0.008-16 µg/ml. In Sensititre® plate assay, the antimicrobials were again examined in serial twofold dilutions with concentrations in the range 4-32 µg/ml. Both assays were conducted concurrently so that the outcomes could be readily compared and so that the CCU titration would be useful for both experiments. The endpoint reading of the MIC was the lowest drug concentration that showed no color change in the medium. The final reading was taken between 2-14 days and expressed in µg/ml of active compound. The Clinical and Laboratory Standards Institute's guidelines were used to interpret the results (25). For MIC determination, the susceptibility of *M. bovis* to each drug was tested in triplicate.

Statistical analysis

Statistical analysis of the results by calculation of the ratio was conducted using the SPSS Statistics 17.0 software program.

Results

Clinical signs

The clinically affected cows had a sandy nature, hard quarter (s) (84/84), decreased size (70/84), and reduced milk yield (80/84) without any indication of systemic symptoms.

Bacterial analysis and molecular identification

Out of 84 milk samples, 14 (16.7%) isolates were identified as belonging to the *Mycoplasma* genus based on the culture on PPLO media, the digitonin and PCR tests, while four (4.8%) samples were *Acholeplasma* genus positive (Table 2).

All mycoplasma isolates (n=14) formed typical 'fried-egg' colonies on PPLO medium, were digitonin sensitive, showed film and spot formation and PCR-positive for 16S rRNA gene. Based on the presence of the species-specific gene, only six (7.14%, 6/84) isolates were identified as *M. bovis* from dairy cattle farms. The determination of the virulence genes in *M. bovis* strains showed the presence of vsp_A gene in all strains (6/6), while other virulence genes (*uvrC*, *gap*, and *p40* pseudogenes) were detected in only two *M. bovis* strains (33.3%).

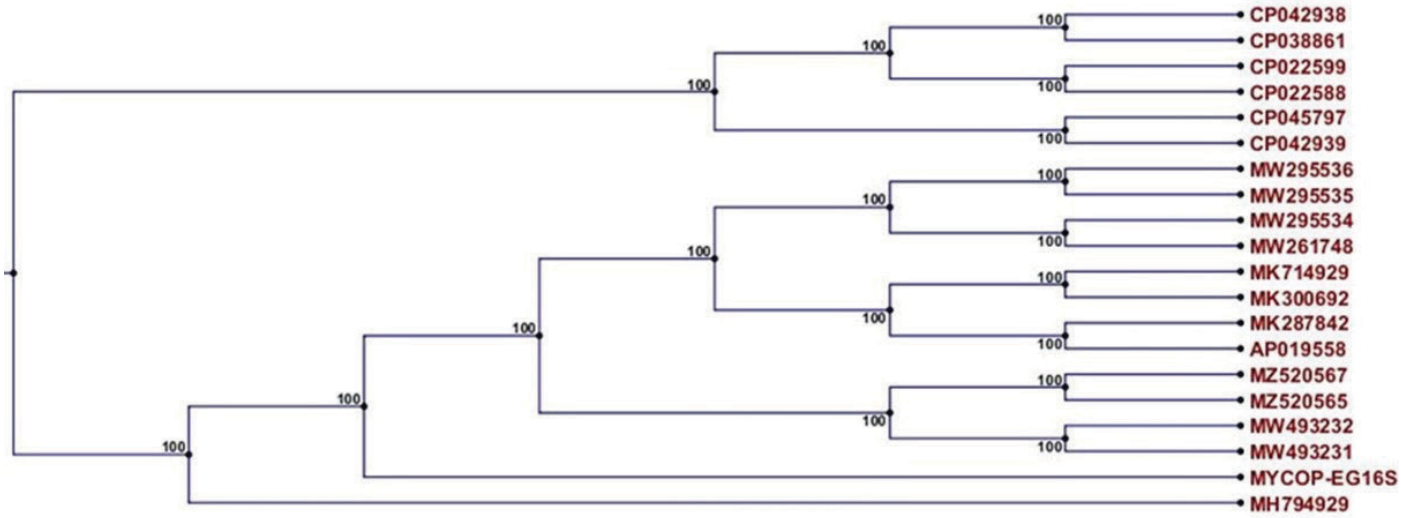

Figure 1: Phylogenetic analysis based on 16S ribosomal RNA gene. This study isolate is designated as MYCOP-EG 16S (OK336362)

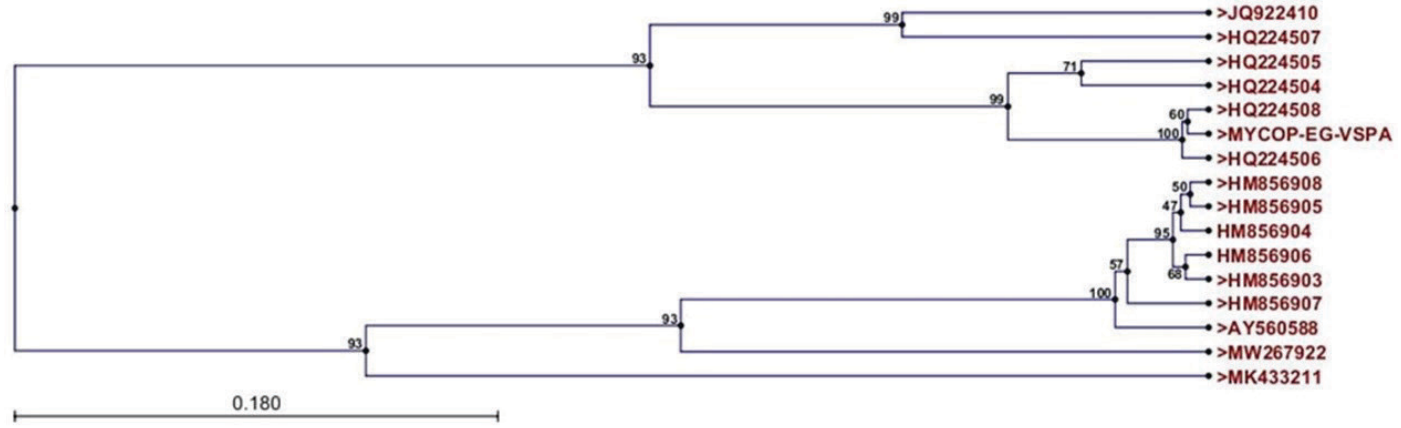

Figure 2: Phylogenetic analysis based on Vsp*A*-like protein gene. This study isolate is designated as MYCOP-EG-VSPA (OK349676)

Molecular and phylogenetic characterization of M. bovis strain

Phylogenetic analysis (Figure 1) showed identical homology with that of *M. bovis* isolated from milk, lung, nasal swab and reproductive organs of bovines, cattle, camel, and poultry from different countries (Egypt, Pakistan, China, and Belgium). Phylogenetic analysis based on VspA-like protein gene (Figure 2) showed high homology of our isolate with that of *M. bovis* isolated from cattle and buffalo milk in Egypt. Sequence alignment of the amino acid sequence of our isolates VspA-like protein responsible for virulence in comparison with other isolates in the GenBank (Figure 3) clearly shows a mutation in amino acid sequence of our isolate's virulence protein even in comparison with other *M. bovis* isolates that were previously isolated from cattle and buffalo milk in Egypt. Phylogenetic analysis based on VspA-like protein sequence (Figure 4) showed a high homology of our isolate with that of *M. bovis* isolated from cattle lung in France (UUA23324) and from cattle and buffalo milk in Egypt (ADT82653 and ADT82657).

Evaluation of the MIC among M. bovis strains

Macrolides were found to be the most active compounds *in vitro* against all examined *M. bovis* isolates from dairy cattle farms. The antibiotic susceptibility results of the Egyptian strains revealed that tilmycosin and tylosin had the lowest MIC values (≤1 µg/mL), while the danofloxacin, streptomycin, and florfenicol had the highest MIC values (<4 µg/mL) for all examined isolates. The isolates were found to be susceptible to tulathromycin and doxycycline with MIC of ≤4 µg/ml (Table 3). The *M. bovis* isolate (S26) was shown to be inhibited by tetracycline, aminoglycosides, and macrolides with low minimum inhibitory concentrations (MIC values). Conversely, strains S17, S30, and S31 were reported to have higher MIC values when most antimicrobials were examined.

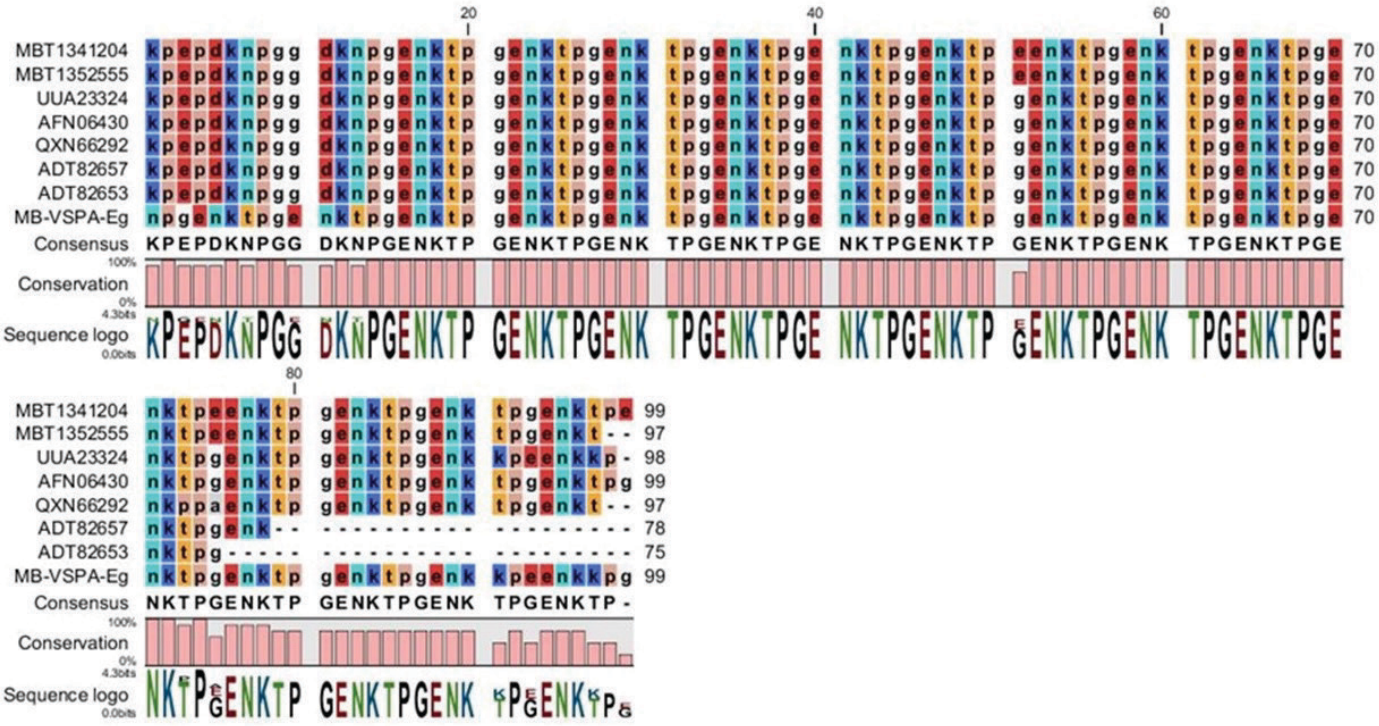

Figure 3: Sequence alignment of the present study *M.bovis* VspA-like protein (UTD45284.1) with the closely related isolates from different sources. Only variable sites are shown with different color

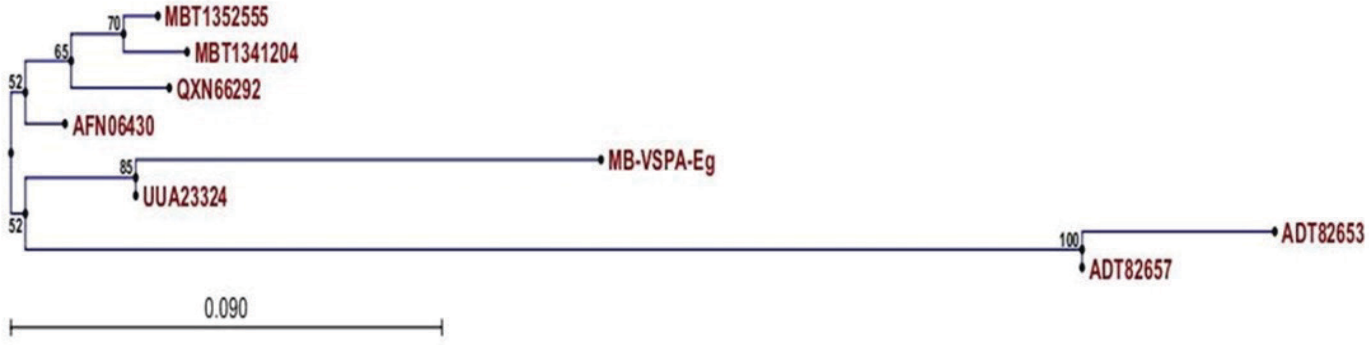

Figure 4: Phylogenetic analysis of the present study M.bovis VspA-like protein (UTD45284.1) with the closely related isolates

Discussion

Mycoplasma, particularly *M. bovis*, is a highly contagious pathogen associated with intramammary infection in the dairy industry, with economic and welfare concerns throughout the world (2). *Mycoplasma* mastitis is thought to be mostly caused by *M. bovis* (26). The ability of *Mycoplasma* species to produce numerous micro-abscesses inside the infected mammary gland causes chronic mastitis, which is extremely costly (27). The current research was assumed to investigate the prevalence of *M. bovis* infections in dairy animals in northern Egypt by both conventional and PCR techniques. The current results showed that 16.7% of the milk samples collected from the dairy farms and sporadic cases were positive for *Mycoplasma* either by conventional culture or PCR technique, while 4.8% of the samples were identified as *Acholeplasma*. Among these, *M. bovis* isolates isolated from dairy farms were identified in percentage of 7.14%. Similarly, Abd El Tawab et al. (1) found relatively low prevalence (8.96%) of *Mycoplasma* including 7.53% of *M. bovis* in Egypt, perhaps as a consequence of variances in farm size (small or large size of the herds), management practices (facility design, pen bedding material, bedding change frequency, and feeding frequency), and hygiene ranking (staff, teat, and equipment hygiene). Also, the low occurrence of *M. bovis* in clinical mastitis samples (8.7%) and bulk tank milk samples (42.3%) was reported in China (3). *Mycoplasma* was previously isolated with a low prevalence (5.3%) from bulk tank and individual cow milk samples with one strain of *M. bovis* in Chile (2). Conversely, the prevalence of *M. bovis* (34.5%) was relatively high in bovine mastitis in Japan (28). The animal cases had a history of

unsuccessful mastitis treatments and high SCC. This issue has persisted for a long time, which may be related to the various ways it might spread, including direct touch, and milking machines (29). Another significant factor for the incidence of *Mycoplasma* mastitis in the examined animals may be intermittent shedding of the pathogen from cows suffering from chronic mastitis.

With the work existing in this investigation, some virulent factors were concerned in the pathogenicity of *M. bovis*. The vsp_A gene was exhibited in all examined *M. bovis* strains (100%), while other virulence genes (*uvr*C, *gap*, and *p40* pseudogenes) were detected in only 33.3% of strains in our study. Diverse repertoires of *vsp* genes have been detected in *M. bovis* (8). These variable surface lipoproteins vsp may be related to *M. bovis* virulence. To distinguish effectively between *M. bovis* and *M. agalactiae*, a PCR based on the DNA repair *uvr*C gene was developed (30). A previous study on *uvr*C gene showed that 19 from 20 of tested *M. bovis* strains isolated from various origins possess 100% identity with the *uvr*C gene sequence (12). Perez-Casal and Prysliak (13) had isolated the *gap* gene of *M. bovis* encoding for glyceraldehyde-3-phosphate dehydrogenase (GAPDH). Nucleotide sequence analysis of the *p40* * gene in *M. bovis* indicates that *p40* * exists as a pseudogene in *M. bovis* (14).

In the current study the superior PCR technique and partial sequencing of 16S rRNA and vsp_A genes permits for precise diagnosis of infections caused by *Mycoplasma* in cattle and molecular typing of the diverse strains. The sequencing of one representative strain of *M. bovis* MYEG1 strain isolated from a case of chronic mastitis was designated as one of *M. bovis* cluster and showed high homology to other *M. bovis* strains isolated from different countries as published on the gene bank. The sequenced gene of *M. bovis* in the current study was shown to be highly connected genetically to numerous clones from local and global linages, according to our results. The Belgian isolates of *M. bovis* clustered with Israeli, European, and American strains in a different phylogenetic research based on gene sequences of 100 *M. bovis* isolates from dairy, beef, and veal farms over a five-year period (31). In Egypt, El-Tawab et al. (32) demonstrated a close relationship between four sequenced *M. bovis* isolates from respiratory system of cattle. The vsp_A gene sequencing of *M. bovis* isolates from pneumonic lung of camel in Egypt indicated the conserved nature of the vsp_A gene (33) mutation in amino acid sequence in vsp_A protein gene of our strain could lead to variations in antigenicity indices and accordingly these variations might disturb the antigenicity and explain the high virulence of such isolates somewhere *M. bovis* strains could modify the expression of surface antigens and thus to modify the ''antigenic profile'' existing to the host's immune system (20). This is consistent with Eissa et al. (34), who point out the prevalence of circulating *M. bovis* with high diversity power in Egyptian bovine herds that experience mastitis. To better expose its content and dynamics important to disease control methods, the *M. bovis* genome's comprehensive sequencing and assembly could be pursued.

The current research screened the antimicrobial susceptibility profiles of six *M. bovis* strains against the most frequently used antimicrobial agents in the field to control *Mycoplasma* infection in Egyptian dairy farms. The present investigation showed that all isolates had the lowest MICs for tilmicosin and tylosin and highest MICs for danofloxacin, streptomycin, and florfenicol. Tetracyclines and macrolides have always been in the forefront of antibiotic practice for treatment of mycoplasma infection (32). Tilmicosin and tylosin tend to have a bimodal distribution. However, members of the fluoroquinolone (as danofloxacin) and phenicol (as florfenicol) classes of antimicrobials had the lowest MIC_{50} levels across all three decades and were considered effective agents against bovine mycoplasmal disease (3,6,35). The efficiency of tulathromycin in the treatment of *M. bovis* infection was previously detected (35). The MIC_{50} levels for tetracyclines, tilmicosin, and tylosin tartrate were high. It has been reported that tetracycline, spectinomycin, and macrolides have been used to treat diseases associated with *M. bovis*, but resistance and decreased effectiveness have been reported worldwide (35). Tylosin, tilmicosin, tulathromycin, and spectinomycin showed a significant rise in the MIC_{50} while enrofloxacin, danofloxacin, marbofloxacin, and oxytetracycline exhibited a modest increase in France (36). Although mycoplasmas are often susceptible to antibiotics that prevent protein or nucleic acid synthesis, some strains have evolved resistance to these antibiotics by gene mutation or the acquisition of a resistance gene (35). Thus, the prudent use of antimicrobial agents in agriculture and persistence of monitoring of antimicrobial susceptibility of *M. bovis* strains in Egypt should be considered.

In summary, the prevalence of *M. bovis* isolates in the Egyptian dairy farms is potentially a matter of concern. The present study also investigated potential virulence genes and antimicrobial susceptibility profiles of *M. bovis* strains isolated from cattle with chronic mastitis in Egypt. According to the *in vitro* tests that were conducted, macrolides may be the most effective treatment for *M. bovis* infections in Egypt. Furthermore, to prevent and control the introduction and spread of the disease on the farm, priority should be given to farm biosecurity, preventative, and management techniques.

Acknowledgments

Author Contributions: conceptualization, MG, SE, ES, RE; methodology, MG, RE, EA.; formal analysis, KA, AA; writing—original draft preparation, MG.; writing—review and editing, RE, and SE. Data Availability Statement. All data in manuscript. The authors declare no conflict of interest.

References

1. Abd El Tawab AA, El-hofy FI, Hassan NI et al. Prevalence of Mycoplasma bovis in bovine clinical mastitis milk in Egypt. Benha Vet Med J 2019; 36(2): 57-65. doi: 10.21608/BVMJ.2019.13850.1025
2. Ulloa F, Soto JP, Kruze, J, et al. Mycoplasma isolation in milk samples from dairy herds in Chile. Austral J Vet Sci 2021; 53(2): 109–13. doi: 10.4067/S0719-81322021000200109
3. Liu Y, Xu S, Li M, et al. Molecular characteristics and antibiotic susceptibility profiles of Mycoplasma bovis associated with mastitis on dairy farms in China. Prev Vet Med 2020; 182: 105106. doi: 10.1016/j.prevetmed.2020.105106
4. Nicholas RA, Fox LK, Lysnyansky I. Mycoplasma mastitis in cattle: to cull or not to cull. Vet J 2016; 216: 142–7. doi: : 10.1016/j.tvjl.2016.08.001
5. Fox LK. Mycoplasma mastitis: causes, transmission, and control. Vet Clin North Am Food Anim Pract 2012; 28(2): 225–37. doi: 10.1016/j.cvfa.2012.03.007
6. Maunsell F, Woolums A, Francoz D, et al. Mycoplasma bovis infections in cattle. J Vet Intern Med 2011; 25(4): 772–83. doi: 10.1111/j.1939-1676.2011.0750.x
7. Salina A, Timenetsky J, Barbosa MS, et al. Microbiological and molecular detection of Mycoplasma bovis in milk samples from bovine clinical mastitis. Pesq Vet Bras 2020; 40(2): 82–7. doi: 10.1590/1678-5150-PVB-6259
8. Alberti A, Addis MF, Chessa B, et al. Molecular and antigenic characterization of a Mycoplasma bovis strain causing an outbreak of infectious keratoconjunctivitis. J Vet Diagn Invest 2006; 18(1): 41–51. doi: 10.1177/104063870601800106
9. Abdelazeem WM, Zolnikov TR, Mohammed ZR, et al. Virulence, antimicrobial resistance and phylogenetic analysis of zoonotic walking pneumonia Mycoplasma arginini in the one-humped camel (Camelus dromedarius). Acta trop 2020; 207: 105500. doi: 10.1016/j.actatropica.2020.105500
10. Gelgie AE, Korsa MG, Dego OK. Mycoplasma bovis Mastitis. Curr Res Microb Sci 2022; 3: 100123. doi: 10.1016/j.crmicr.2022.100123
11. Thomas A, Sachse K, Farnir F, et al. Adherence of Mycoplasma bovis to bovine bronchial epithelial cells. Microb Pathog 2003; 34(3): 141–8. doi: 10.1016/s0882-4010(03)00003-2
12. Thomas A, Dizier I, Linden A, et al. Conservation of the uvrC gene sequence in Mycoplasma bovis and its use in routine PCR diagnosis. Vet J 2004; 168(1): 100–2. doi: 10.1016/j.tvjl.2003.10.006
13. Perez-Casal J, Prysliak T. Detection of antibodies against the Mycoplasma bovis glyceraldehyde-3-phosphate dehydrogenase protein in beef cattle. Microb Pathog 2007; 43(5/6): 189–97. doi: 10.1016/j.micpath.2007.05.009
14. Thomas A, Linden A, Mainil J, et al. The p40* adhesin pseudogene of Mycoplasma bovis. Vet Microbiol 2004; 104(3/4): 213–7. doi: 10.1016/j.vetmic.2004.09.009
15. Lysnyansky, I, Ayling RD. Mycoplasma bovis: mechanisms of resistance and trends in antimicrobial susceptibility. Front Microbiol 2016; 7: 595. doi: 10.3389/fmicb.2016.00595
16. Barberio A, Flaminio B, De Vliegher S, et al. Short communication: *in vitro* antimicrobial susceptibility of Mycoplasma bovis isolates identified in milk from dairy cattle in Belgium, Germany, and Italy. J Dairy Sci 2016; 99(8): 6578–84. doi: 10.3168/jds.2015-10572
17. Klein U, de Jong A, Youala M, et al. New antimicrobial susceptibility data from monitoring of Mycoplasma bovis isolated in Europe. Vet Microbiol 2019; 238: 108432. doi: 10.1016/j.vetmic.2019.108432
18. Blanchard A, Bébéar CM. Mycoplasmas of humans. In: Razin S., eds. Molecular biology and pathogenicity of mycoplasmas. Berlin: Springer, 2002: 45-71.
19. Freundt E, Andrews B, Ernø H, et al. The sensitivity of Mycoplasmatales to sodium-polyanethol-sulfonate and digitonin. Zentralbl Bakteriol Parasitenkd Infektionskr Hyg 1973; 225(1): 104–12.
20. Ernø H., Stipkovits L. Bovine mycoplasmas: cultural and biochemical studies. Acta Vet Scand 1973; 14(3): 436–49.
21. Howard W, eds. Textbook of mycoplasmosis in animals: laboratory diagnosis. Ames: Iowa State Univerity Press, 1994.
22. Queipo-Ortuño MI, De Dios Colmenero J, Macias M, et al. Preparation of bacterial DNA template by boiling and effect of immunoglobulin G as an inhibitor in real-time PCR for serum samples from patients with brucellosis. Clin Vaccine Immunol 2008; 15(2): 293–6. doi:10.1128/CVI.00270-07
23. Bradbury JM, Yavari CA, Giles C. *In vitro* evaluation of various antimicrobials against Mycoplasma gallisepticum and Mycoplasma synoviae by the micro-broth method, and comparison with a commercially-prepared test system. Avian Pathol 1994; 23(1): 105–15. doi: 10.1080/03079459408418978
24. Senterfit L, Taylor-Robinson D, Niitu Y, et al. Round table II: Antimycoplasmal substances. Yale J Biol Med 1983; 56(5/6): 831–4.
25. CLSI. CLSI VET01S: Performance standards for antimicrobial disk and dilution susceptibility tests for bacteria isolated from animals, 5th ed. Malveran: Clinical and Laboratory Standards Institute, 2018.
26. Nicholas R, Ayling R, McAuliffe L. Mycoplasma mastitis. Vet Rec 2007; 160(11): 382. doi: 10.1136/vr.160.11.382-b
27. Jasper D. The role of Mycoplasma in bovine mastitis. J Am Vet Med Assoc 1982; 181(2): 158–62.
28. Kawai K, Higuchi H, Iwano H, et al. Antimicrobial susceptibilities of Mycoplasma isolated from bovine mastitis in Japan. Anim Sci J 2014; 85(1): 96–9. doi: 10.1111/asj.12144
29. Justice-Allen A, Trujillo J, Corbett R, et al. Survival and replication of Mycoplasma species in recycled bedding sand and association with mastitis on dairy farms in Utah. J Dairy Sci 2010; 93(1): 192–202. doi: 10.3168/jds.2009-2474
30. Subramaniam S, Bergonier D, Poumarat F, et al. Species identification of Mycoplasma bovis and Mycoplasma agalactiae based on theuvrC genes by PCR. Mol Cell Probes 1998; 12(3): 161–9. doi: 10.1006/mcpr.1998.0160
31. Bokma J, Vereecke N, De Bleecker K, et al. Phylogenomic analysis of Mycoplasma bovis from Belgian veal, dairy and beef herds. Vet Res 2020; 51(1): 121. doi: 10.1186/s13567-020-00848-z
32. El-Tawab A, Awad A, Elhofy F, et al. Identification and genetic characterization of Mycoplasma species affecting respiratory system in Egyptian cattle. Benha Vet Med J 2021; 40(1): 21–6. doi: 10.21608/bvmj.2021.67213.1361
33. Mohammed Z, Saad A, Deif H. Hydrogen sulphide, an avant-garde potential virulence factor of Mycoplasma bovis isolated from the lungs of the Camelus dromedarius exhibiting silent pneumonia: virulence, antimicrobial resistance and phylogeny. Authorea Preprints, 2020. doi: 10.22541/au.159986250.04612374
34. Eissa S, Hassan A, Hashem Y, et al. Comparative molecular study of Mycoplasma bovis isolates from Egyptian buffaloes and cows suffered from mastitis. Eur J Biol Sci 2012; 4(4): 114–20. doi: 10.5829/idosi.ejbs.2012.4.4.6668

35. Cai HY, McDowall R, Parker L, et al. Changes in antimicrobial susceptibility profiles of Mycoplasma bovis over time. Can J Vet Res 2019; 83(1): 34–41.

36. Gautier-Bouchardon AV, Ferre S, Le Grand D, et al. Overall decrease in the susceptibility of Mycoplasma bovis to antimicrobials over the past 30 years in France. PLoS One 2014; 9(2): e87672. doi: 10.1371/journal.pone.0087672

37. Yleana R. *In vitro* amplification of the 16S rRNA genes from Mycoplasma bovis and Mycoplasma agalactiae by PCR. Vet Microbiol 1995; 47: 183–90. doi: 10.1016/0378-1135(95)00058-i

Molekularna karakterizacija, virulenca in protimikrobna občutljivost z mikoplazmo M. bovis povezanega kroničnega mastitisa pri kravah molznicah

M. Gioushy, E.E.A. Soliman, R.M. Elkenany, E. El-Alfy, A.A. Elaal, K.A.H. Abd-El Razik, S. El-khodery

Izvleček: *Mycoplasma bovis* (*M. bovis*) je najpogostejša vrsta mikoplazme, ki ima vse večji vpliv na mlečno industrijo. Namen te študije je bil molekularno karakterizirati in raziskati virulenco in občutljivost izolatov *M. bovis* za antibiotike, in sicer iz krav molznic s kroničnim mastitisom v Egiptu. Štiriinosemdeset mešanih vzorcev mleka krav z mastitisom je bilo aseptično zbranih na mlečnih farmah v Egiptu. Na podlagi mikrobiološkega pregleda in analize izražanja 16S rRNA z verižno reakcijo s polimerazo (PCR) je bilo 14 (16,7 %) od vseh vzorcev mleka pozitivnih na *Mycoplasma spp.* Z metodo PCR smo šest (7,14 %) od 14 izolatov mikoplazme identificirali kot *M. bovis*. Analize PCR za različne gene virulence so pokazale, da je bil pri vseh izolatih *M. bovis* prisoten gen vsp_A, medtem ko so bili drugi geni virulence (*uvr*C, *gap* in psevdogeni *p40*) izraženi le pri dveh izolatih *M. bovis* (2/6). Filogenetska analiza gena 16S rRNA je pokazala 100-odstotno homolognost z referenčnimi sevi *M. bovis*, izoliranimi iz različnih vrst in lokacij. V primerjavi z drugimi izolati podatkovne zbirke GenBank je poravnava aminokislinskega zaporedja proteina, podobnega VspA, pokazala na značilno mutacijo. In vitro testiranje protimikrobne občutljivosti šestih izolatov *M. bovis* za sedem protimikrobnih zdravil je pokazalo, da sta imela tilmikozin in tilozin najnižje vrednosti minimalnih inhibitornih koncentracij (MIC) (≤1 µg/ml), medtem ko so imeli danofloksacin, streptomicin in florfenikol najvišje vrednosti MIC (<4 µg/ml). Kljub temu da je ta študija pokazala virulenco *M. bovis* pri kravah molznicah v Egiptu, makrolidi pa so se izkazali za najmočnejše spojine proti vsem *in vitro* testiranim izolatom, so potrebne nadaljnje študije v nacionalnih raziskavah.

Ključne besede: antimikrobna občutljivost; kronični mastitis; *Mycoplasma bovis*; analiza zaporedja; geni virulence

Slov Vet Res

DOI 10.26873/SVR-2069-2024
UDC 599.323.55:612.014.43:615.2:616.24-002:631.816.1
Pages: 281–90

Original Research Article

High Doses Of Ivermectin Cause Toxic Effects After Shortterm Oral Administration in Rats

Key words

ivermectin;
toxicity;
SARS-CoV-2;
cytochrome P-450;
P-gp;
histopathological changes;
rats

Vladimir Marjanović[1], Dragana Medić[2], Djordje S. Marjanović[2], Nenad Andrić[3], Miloš Petrović[1], Jelena Francuski Andrić[4], Milena Radaković[4], Darko Marinković[5], Vanja Krstić[3], Saša M. Trailović[2]*

[1]Veterinary Specialist Institute Niš, [2]Department of Pharmacology and Toxicology, [3]Department of Equine, Small animal, Poultry and Wild animal Diseases, [4]Department of Pathophysiology, [5]Department of Pathology, Faculty of Veterinary Medicine, University of Belgrade, Serbia

***Corresponding author:** sasa@vet.bg.ac.rs

Abstract: The anthelmintic macrocyclic lactones (MLs) are the most important endectocides in modern pharmacotherapy of parasitic infections. However, during the COVID 19 pandemic, ivermectin was used in humans against infection with the SARS-CoV-2 virus in doses significantly higher than the approved antiparasitic doses. This kind of application was created solely on the basis of *in vitro* tests, and is not officially approved in any country in the world. Therefore, we conducted a study on rats treated orally with 0.6, 1.2, 2.4 and 4.8 mg/kg of ivermectin for 5 days. Based on our investigation, ivermectin at the doses used in humans against the SARS-Co-2 virus (3, 6, 12 and 24 times higher than the antiparasitic dose 0.2mg/kg), causes changes in red blood cell counts and increases the levels of liver enzymes without visible clinical symptoms. Histopathological changes were recorded in the liver, kidneys and testicles of rats, and the highest dose tested led to bleeding in the brain tissue. Obviously, ivermectin somewhat increases concentration of the enzyme P-450 isoform 3A4, whose substrate it is, but the highest tested dose reduces its concentration in plasma to the control level. Notably, the concentrations of ivermectin recorded in plasma of treated rats, indicate that even high doses do not reach the *in vitro* IC50 value of ivermectin for SARS-CoV-2 reported in the literature. On the other hand, the concentrations of ivermectin in the brain approach the values that can manifest extremely toxic effects described in humans.

Received: 18 June 2024
Accepted: 23 July 2024

Introduction

The anthelmintic macrocyclic lactones (MLs) are the most important endectocides in modern pharmacotherapy of parasitic infections. This large group of hydrophobic, structurally related compounds are widely used in animals and humans (1). Therapeutic doses of ivermectin in veterinary medicine range from 0.2-0.3mg/kg, with a second administration after one to two weeks. In human medicine, antiparasitic doses of ivermectin approved by the FDA and EMA range from 0.15 to 0.4 mg/kg of body weight, depending on the type of parasite and repeated twice. The avermectins are often referred to as endectocides because of their activity against both endo- and ectoparasites, have received considerable interest from the agricultural chemical industry. Thay have extremely high activity against arachnoid and nematode pests, low toxicity in mammals, generally benign environmental characteristics, and a unique mode of action. The median lethal oral dose (LD_{50}) of ivermectin for rats (male and female) ranges from 42.8 to 52.8 mg/kg (2).

The mechanism of antiparasitic action of ivermectin is the activation or positive allosteric modulation of invertebrate specific glutamate-gated chloride channels, with a secondary inhibitory action on $GABA_A$ receptors. In mammals, ivermectin can also inhibit GABA-ergic neurotransmission by promoting GABA release and acting as a GABA receptor agonist when exhibits neurotoxic activity. Most likely, ivermectin causes neurotoxic disorders by acting on GABA-dependent as well as GABA-independent chloride channels (3), showing the ability to exert its effect on both central

and peripheral GABA-ergic structures (4, 5). At ten times therapeutic doses, ivermectin does not show any obvious visible clinical symptoms of neurotoxicity, but it disrupts integration of the CNS and motor coordination in the Rota-rod test (4).

The potential neurotoxic activity of ivermectin depends, in part, on the absorptionextrusion activity of the drug in the gastrointestinal tract/blood-brain barrier, which is regulated by multiple transport systems (P-gp, MRP, ABCB1 and other ABC transporters). With ivermectin, severe adverse effects in the central nervous system have been observed in various vertebrates due to the absence or functional deficiency of P-gp (6). Due to the wide spectrum of clinical use and common simultaneous use with other drugs used for the treatment of various diseases, there is a strong possibility of toxic and/or clinically significant drug-drug interactions. The consequences of a toxic drug-drug interaction that can occur during simultaneous treatment with ivermectin with other drugs depends on the metabolic and pharmacokinetic properties of both ivermectin and the simultaneously administered drugs.

Furthermore, it depends on their interaction with enzymes that metabolize the drug (cytochrome P450) and drug transporters involved in the metabolic pathways of ivermectin. Interactions could therefore result in changes in the activity of enzymes involved in drug metabolism and/or transporters, potentially leading to altered responses to drug therapy or significant side effects/toxic effects (7).

Several *in vitro* tests and several human clinical studies were conducted during the COVID-19 pandemic to test the effectiveness of ivermectin against the SARS-CoV-2 virus. The expectation that ivermectin will exert an antiviral effect possibly arose from the previous use of antimalarials (chloroquine and hydroxychloroquine) in some treatment protocols against COVID-19 infection, together with the fact that ivermectin acts *in vitro* on the causative agent of malaria, the protozoan *Plasmodium falciparum*. Unfortunately, none of the many studies demonstrated therapeutic efficacy; the doses used in clinical trials often showed toxicity. The doses of ivermectin used ranged from 0.6 to 2 mg/kg, given orally (usually for 5 days), and the studies were frequently interrupted due to the severe condition of the patients, which was attributed to the effects of ivermectin (8).

Based on data from the Oregon State Poison Center (USA) published in the New England Journal of Medicine, the doFses of ivermectin taken by people hospitalized at the center during the pandemic were up to 1.8 mg/kg, orally, while the therapy usually lasted 5-7 days. Confusion, ataxia, convulsions and hypotension were reported in hospitalized patients (9).

The toxicity of ivermectin administered orally over a 5-day period has not published to date. All ivermectin toxicity studies refer to classic acute, subacute and chronic toxicity protocols. We decided to examine potential toxic effects of the high doses of ivermectin that were applied against the SARS-CoV-2 virus and to determine the plasma and brain concentrations of ivermectin in treated rats. Also, it is important to compare these *in vivo* concentrations of ivermectin with the concentrations tested *in vitro* against the SARS-CoV-2 virus.

Material and methods

Housing of rats and study design

A total of 30 adult Wistar male rats (140-150 g), 7 months old used in the present study were obtained from the Military Medical Academy breeding farm, Belgrade, Serbia. The study was performed on male rats due to data from the literature on the potential toxic effect of ivermectin on testicular function. On the other hand, according to Oregon Poison Center data, the toxic effects of ivermectin were more often recorded in male patients during the COVID-19 pandemic (9, 10).

After arriving at the facility, the animals were acclimated 10 days before the start of the study. Rats were housed in the groups of 6 in home cages on autoclaved wood shavings bedding under standard conditions: temperature of 21±1 ºC, relative humidity of 55-60 % and 12/12 h light/dark cycle. Food and water were provided *ad libitum*. Bedding (wood shavings) and water bottles were changed daily under strict, aseptic conditions. All cages and implements were washed in a mechanical washer and autoclaved prior to entry into the room.

Rats were randomly divided into 5 groups, each group consisting of 6 rats per dose of ivermectin (0.6, 1.2, 2.4, and 4.8 mg/kg), in addition to a control group. Each day at 10:00 am animals were treated with the assigned dose of ivermectin, while control animals were treated with the same volume of solvent. Ivermectin treatment lasted for 5 days. Ivermectin was dissolved in propylene glycol and applied orally through a rigid gastric tube in a volume of 0.1 ml/100 g of body weight.

At the end of five-day treatment (24 hours after last administration of ivermectin) rats were anesthetized with thiopentone sodium 35mg/kg applied intravenously in the tail vein and the blood sampling procedure was undertaken.

All experimental procedures in the study were approved by the Ministry of Agriculture, Forestry and Water Management of the Republic of Serbia - Veterinary Directorate (permit N°323-07-11564/2022-05/4), according to the Serbian Animal Welfare Protection Law, and Directive 2010/63/ EU.

Assessment of the coordination and balance

The Rota-rod test was used to investigate the potential CNS effects of ivermectin. This test measures the ability of rats to maintain balance on a rotating rod. The testing was performed on the Rota-rod apparatus under software control (ElUnit, Serbia). Prior to the investigation, animals were trained for 5 days to remain 5 min on the rod rotating at constant speed of 15 rpm. Thirty (n=30) rats able to balance on a rotating rod for 5 minutes without falling were selected for the study. The effect of increasing doses of ivermectin on the integrity of motor coordination was assessed based on the ability of rats to stay on rotated rod for 5 min without falling. Testing was carried out every day 30 minutes after administration of ivermectin or solvent (control group).

Hematological and biochemical analyses

Blood sampling was performed 24 hours after the last ivermectin administration. A blood samples were taken by cardiac puncture, and then the rats were euthanized by decapitation. Blood was collected in tubes with anticoagulant (Ethylenediaminetetraacetic acid) and serum tubes. From the blood samples with anticoagulant, the parameters of the blood count were determined in the 5-part veterinary hematology analyzer Mindray BC-500 Vet immediately after sampling. After separating the serum, the concentration of total proteins (TP), urea, creatinine, and triglycerides (TG) were measured. We also measured the enzymatic activity of alanine aminotransferase (ALT), aspartate aminotransferase (AST), alkaline phosphatase (ALP), creatine kinase (CT) and gamma glutamyl transferase (gamma-GT) in an automatic biochemical analyzer (Mindray BC-240). These analyzes were performed immediately after sampling.

Cytochrome P450 concentration was determined in the rat serum, because ivermectin is metabolized *in vivo* and *in vitro* by cytochrome P450 enzymes through C-hydroxylation and O-demethylation reactions. Given that most of the metabolism of ivermectin is carried out via the cytochrome P450 3A4, its concentration was determined by Enzyme-Linked Immunosorbent Assay (ELISA) using the double sandwich ELISA method according to the manufacturer's instructions (MyBioSource, San Diego, CA, USA). Serum samples for determination of cytochrome P450 concentration were frozen at -20°C immediately after sampling.

Liquid chromatography-tandem mass spectrometry assay of ivermectin in rat serum and brain tissue

Ivermectin concentrations were determined after Whelan and al. (11), with the following modifications. For chromatographic separation Kinetex® (Phenomenex, Torrance, CA, USA) column (100×2.1 mm, 2 µm) was used coupled with Shimadzu 8040 (Shimadzu Corporation, Kyoto, Japan) LC-MS/MS system explained by Simunovic et al. (12). Extraction was performed using 20 ml of acetonitrile/acetone (5:1) mixture, centrifugation, filtration and subsequent evaporation under nitrogen at 50°C. Reconstitution was performed using 1 ml of acetonitrile after which extract was transferred to HPLC vial. Validation of the method was performed according to European Regulation 2002/657/EC. Calculated limits of quantification for samples of brain and plasma were 1 µg/kg and 0.5 µg/l, respectively. For quantification, calibration standards were prepared by spiking blank samples with ivermectin working solution.

Gross and histopathological examination of rat tissues

After decapitation, a gross and histopathological examination of the organs and tissues of the rats was performed. Concurrently, tissue samples of the brain, liver, kidneys and testicles were taken for histopathological analysis. Tissue samples were fixed in 10% buffered formalin. After standard processing in an automated tissue processor, tissue samples were embedded in paraffin blocks and 5µm sections were stained with hematoxylin and eosin (HE). The results of histochemical staining were analyzed by light microscopy (BX51, Olympus Optical, Japan).

Images were taken with Olympus Color View III® digital camera.

Substances and drugs

Substances and drugs used in this study were: Ivermectin (Sigma-Aldrich, St. Louis, USA), Thiopental Panpharma (Panpharma, France).

Statistical analysis

All values are expressed as mean ± standard error of the mean (mean ± SE). Unless stated otherwise, results were tested using the one-way ANOVA or t-test, and differences were considered significant at $p<0.05$. Furthermore, linear regression was used to examine doseresponse relationship. All data was analyzed using GraphPad Prism version 6.00 for Windows (GraphPad Software, La Jolla California USA).

Results

General Observation

During the five-day treatment, rats were continuously observed for clinical manifestations of health disorders. No symptoms were observed in any of the treated rats or in the control group. The rats in each group consumed food and water normally, their behavior was normal and with no observable difference between control and treated rats.

Table 1: Mean values (± SE) of monitored hematological parameters in rats after treatment

Parameters	Unit	Mean ± SE				
		Control (n=6)	Ivermectin 0.6 mg/kg (n=6)	Ivermectin 1.2 mg/kg (n=6)	Ivermectin 2.4 mg/kg (n=6)	Ivermectin 4.8 mg/kg (n=6)
WBC	10^9/l	6.08±1.10	5.92±0.61	6.57±1.24	7.90±1.25	5.55±0.92
RBC	10^{12}/l	6.57±0.11	7.71±0.12**+ (p=0.004) (p=0.041)	7.02±0.65	6.98±0.21	6.83±0.27
HGB	g/l	127.50±2.43	142.83±1.47**++ (p=0.0072) (p=0.0086)	126.66±11.92	127.83±4.46	125.83±3.97
HCT	%	38.55±0.83	41.63±0.46	37.23±3.29	37.83±1.23	38.71±1.16
MCV	fl	58.66±0.33	53.73±0.36*** (p=0.0004)	53.23±0.37** (p=0.0028)	54.15±0.37** (p=0.0065)	56.76±1.50
MCH	pg	19.45±0.07	18.36±0.13** (p=0.0015)	18.06±0.11*** (p=0.0002)	18.31±0.15** (p=0.0072)	18.40±0.44
MCHC	g/l	331.00±1.43	342.50±1.20**++ (p=0.0030 (p=0.0038)	339.16±3.11	338.16±2.02++ (p=0.0458)	327.33±2.87

*-Statistically significant difference compared to control; +- Statistically significant difference compared to ivermectin 4.8 mg/kg

Table 2: Mean values (± SE) of monitored biochemical parameters in rats after treatment

Parameters	Unit	Mean ± SE				
		Control (n=6)	Ivermectin 0.6 mg/kg (n=6)	Ivermectin 1.2 mg/kg (n=6)	Ivermectin 2.4 mg/kg (n=6)	Ivermectin 4.8 mg/kg (n=6)
ALT	U/l	57.63±3.25	94.26±3.55**** (p=0.0001)	90.86±3.75**** (p=0.0002)	97.90±5.81**** (p=0.0001)	93.45±5.84**** (p=0.0001)
AST	U/l	143.36±20.32+ (p=0.0284)	126.08±12.87++ (p=0.0084)	120.06±7.06+ (p=0.0116)	115.93±8.29++ (p=0.0065)	165.11±24.28
ALP	U/l	83.93±9.47	11.05±3.18****+++ (p<0.0001) (p=0.0005)	19.31±7.22****++ (p<0.0001) (p=0.0034)	19.60±3.19****++ (p<0.0001) (p=0.0036)	64.33±11.95
gamma - GT	U/l	1.38±0.13	1.68±0.20++++ (p<0.0001)	1.36±0.30++++ (p<0.0001)	2.06±0.17++ (p=0.0015)	5.20±1.68**** (p<0.0001)
TP	g/l	58.03±1.28	64.10±1.75	63.31±1.51	60.90±2.04	61.90±2.11
TG	mmol/l	0.40±0.04	0.59±0.06	0.56±0.09	0.55±0.05	0.89±0.17* (p=0.0128)
CREA	µmol/l	23.36±1.49	17.85±4.15+ (p=0.0232)	23.10±0.67	22.35±1.32	27.60±0.64
UREA	mmol/l	7.00±0.34	7.38±1.81	8.29±0.53	8.24±0.34	7.29±0.68

*-Statistically significant difference compared to control; +- Statistically significant difference compared to ivermectin 4.8 mg/kg

Table 3: Mean values (± SE) of ivermectin concentration in rat plasma and brain tissue

Parameters	Mean ± SE			
	Ivermectin 0.6 mg/kg	Ivermectin 1.2 mg/kg	Ivermectin 2.4 mg/kg	Ivermectin 4.8 mg/kg
Ivermectin concentration in the plasma (µg/L)	18.217±2.317** (P=0.0018)	32.717±4.671** (P=0.0046)	61.167±11.745* (P=0.0290)	165.317±46.450
Ivermectin concentration in the brain (µg/kg)	1.467±0.312*++ (P=0.0148) (P=0.0076)	3.783±0.930* (P=0.0149)	6.667±0.932* (P=0.0193)	33.033±6.313

*-Statistically significant difference compared to ivermectin 4.8 mg/kg; +- Statistically significant difference compared to ivermectin 2.4 mg/kg

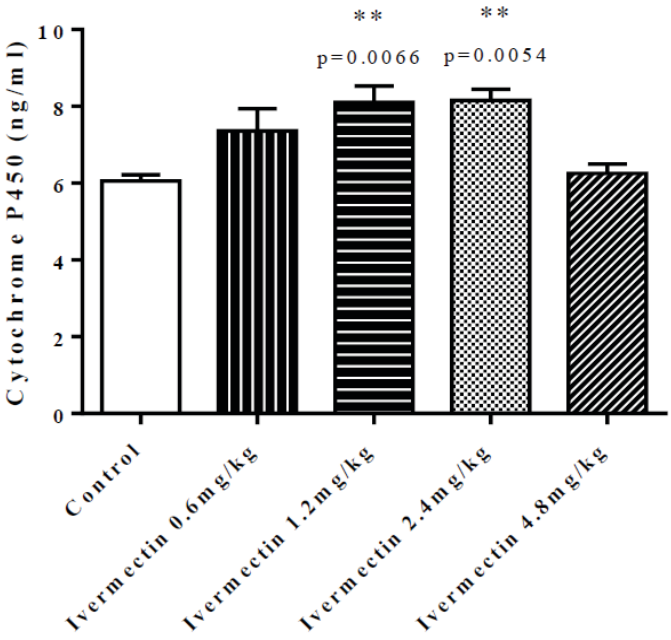

Figure 1: Cytochrome P450 concentration in rat plasma after 5 days treatment with increasing doses of ivermectin

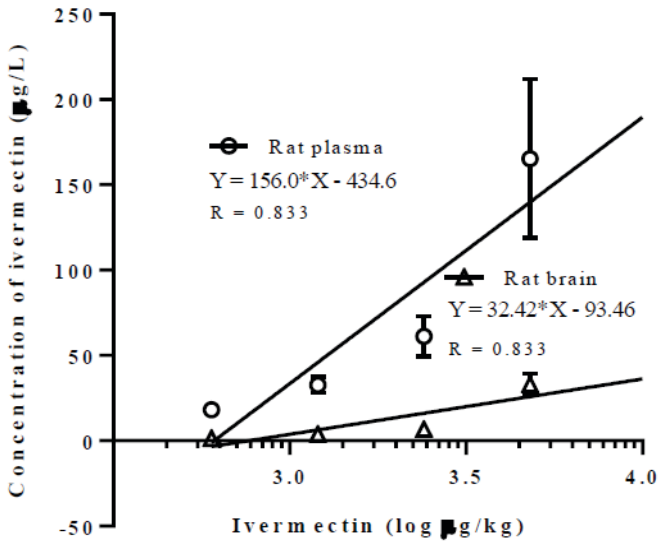

Figure 2: Linear regression analysis of dose-dependent increase in ivermectin concentration in plasma and brain of rats

Assessment of the coordination and balance

The Rota-rod test has been used to assess motor coordination and balance alterations in rodents (13). None of the treated or control rats fell off the rotating rod during the test. Also, none of the tested rats displayed visible signs of CNS depression, the righting reflex was fully preserved, walking on a flat static surface (after tail pinch test) was normal and all of the tested animals responded normally to external stimulation (approach response and touch response test).

Hematological and biochemical analyses

Determination of hematological parameters showed that the five-day treatment of rats with increasing doses of ivermectin (0.6-4.8 mg/kg) did not significantly affect the total number of leukocytes, but a dose of 0.6 mg/kg significantly increased the red blood cell count. In the other rats treated with ivermectin, there was an apparent increase in the number of erythrocytes compared to controls, but not to a significant value (Table 1). As with the number of erythrocytes, the concentration of hemoglobin in rats treated with 0.6 mg/kg was significantly increased compared to the controls. In the other treated groups of rats, this value did not differ either within groups or compared to control results (Table 1). Hematocrit was not significantly different in control and treated rats. However, MCV was reduced in all treated rats and reached a significant level in rats treated with ivermectin doses of 0.6, 1.2 and 2.4 mg/kg. In all ivermectin treated rats the MCH value was significantly reduced compared to the untreated control group (Table 1). However, the value of MCHC increased significantly only in rats treated with the lowest dose of ivermectin (0.6 mg/kg), while in other treated animals it was indistinguishable from control values.

In all rats treated for 5 days with ivermectin, a significant increase in the value of ALT was recorded, while the value of this enzyme did not differ between groups. On the other hand, the AST concentration increased only in rats treated with the highest tested dose of ivermectin. ALP was significantly reduced in rats treated with 0.6, 1.2 and 2.4 mg/kg, while in rats that received the highest dose (4.8 mg/kg), the value of ALP was only slightly reduced compared to the control. Gamma GT levels were higher than control in rats treated with 0.6 and 2.4 mg/kg, but significantly higher only in rats treated with the highest dose of ivermectin (4.8 mg/kg). Other biochemical parameters TP, TG, Creatinine and Urea did not differ significantly, both in relation to the control and between the treated groups (Table 2).

Ivermectin is extensively metabolized by cytochrome P450 enzymes (P450s, CYP) both *in vivo* and *in vitro* (7), therefore it was particularly important to examine the activity of this enzyme. The concentration of CYP in the plasma of treated rats increased proportionally with the dose of ivermectin administered (0.6, 1.2 and 2.4 mg/kg). From control 6.05±0.16 ng/ml, to 7.36±0.57, 8.11±0.43 and 8.15±0.30 ng/ml However, in rats that received the highest dose of ivermectin (4.8 mg/kg), the value of CYP remained similar to the control level (6.26±0.23 ng/ml) (Figure 1).

Liquid chromatography-tandem mass spectrometry assay of ivermectin in rat serum and brain tissue

We considered it important to determine ivermectin concentrations in plasma and brain of rats after the 5 daily treatments various oral doses of ivermectin. The selected doses used in humans at the time of COVID-19 infection were many times higher than the recommended antiparasitic dose of ivermectin (3, 6, 12 and 24x). Table 3 shows the mean values of the results. The concentration of ivermectin in plasma and brain tissue after 5 days treatment was proportional to the administered dose of the drug. Linear regression analysis shows that the increase in ivermectin concentrations in plasma and brain tissue is dose-dependent (Y=156.0*X-434.6, r=0.8338 and Y=32.42*X-93.46 r=0.7359) (Figure 2). Each two-fold increase in the dose of ivermectin (from 0.6 to 1.2 and from 1.2 to 2.4 mg/kg) produced an almost two-fold increase in plasma and brain drug concentrations. However, after administration of a dose of 4.8 mg/kg, the concentration recorded in the plasma was 2.5 times higher, while in the brain, almost 5 times higher than in rats that received twice the lower dose (2.4 mg/kg) (Table 3).

Gross and histopathological examination analysis of rat tissues

Gross pathology changes in the internal organs of rats treated with ivermectin were not observed. However, histopathological changes were noted in the majority of treated rats. Focal mononuclear infiltration of liver tissue was observed in rats of all treated groups, but intracellular edema and vacuolar degeneration of hepatocytes (Figure 3a) were more frequent in rats treated with the two highest doses of ivermectin, 2.4 and 4.8 mg/kg. Focal necrosis of hepatocytes and focal calcification were detected in the liver tissue of rats that received 4.8 g/kg of ivermectin. Tubular dilatation, intracellular edema and interstitial hemorrhage were observed in the kidney tissue of all treated rats. Glomerular sclerosis was observed in rats treated with ivermectin in doses of 1.2, 2.4 and 4.8 mg/kg (Figure 3b). Changes in brain tissue were found only in rats receiving the highest

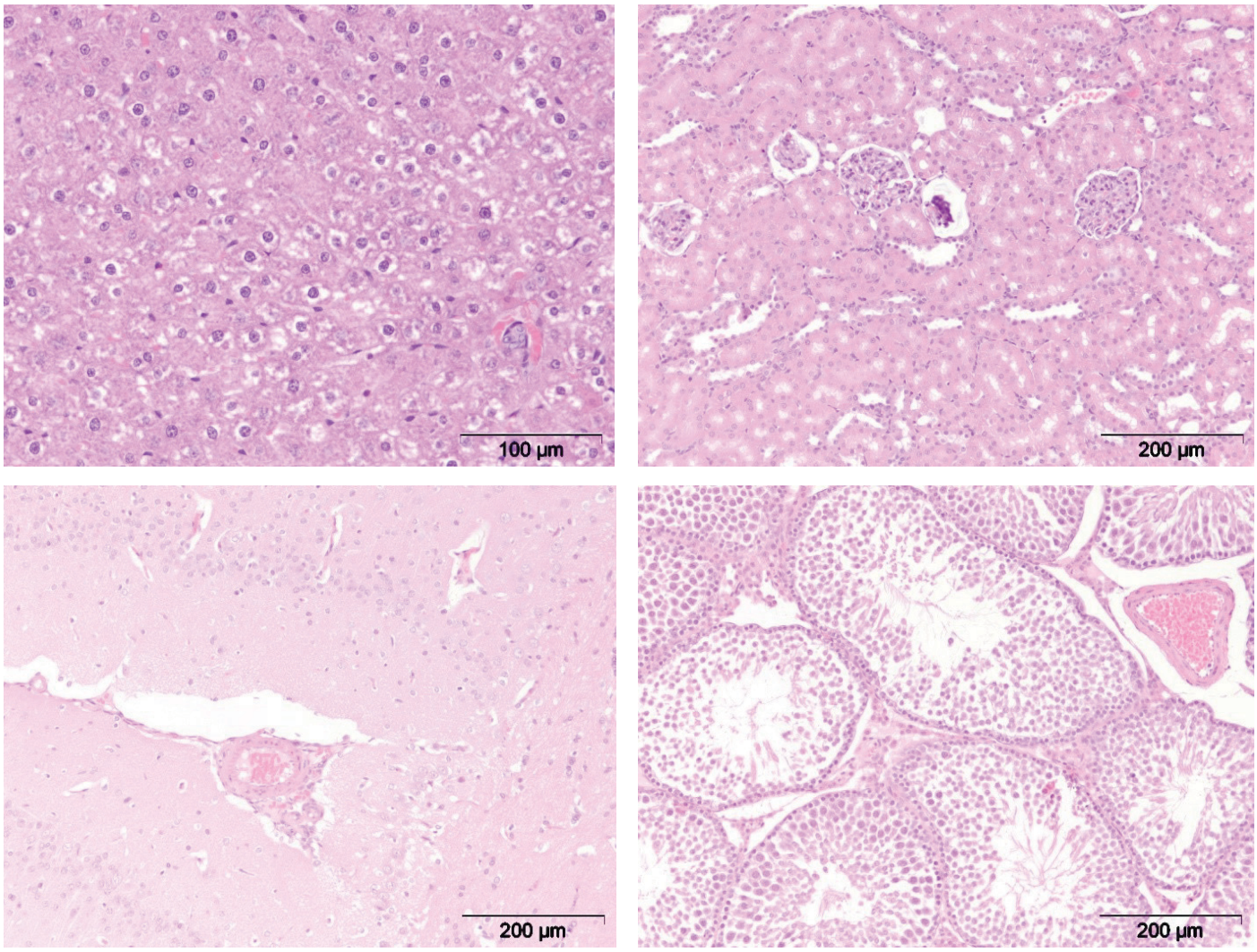

Figure 3: a) Intracellular edema and vacuolar degeneration of hepatocytes; b) Glomerular sclerosis 121 in the kidneys of rats; c) Focal and perivascular bleeding in the rat brain; d) Degeneration of the 122 epithelium of the seminiferous tubules of the testicles

tested dose of ivermectin (4.8 mg/kg). Focal bleeding as well as perivascular bleeding was observed (Figure 3c). Also, histopathological changes in testicular tissue were detected only in rats treated with the highest dose of ivermectin. These changes included epithelial degeneration of the seminiferous tubules of the testes and the epithelium of the epididymis (Figure 3d), reduction and absence of spermatogenesis was also observed.

Discussion

In this study, we examined the toxic effects of high oral doses of ivermectin after five days of administration in rats. The most commonly applied antiparasitic dose of ivermectin in human and veterinary medicine is 0.2 mg/kg of body weight (14,15). Based on data from the Oregon Poison Center (9), we applied oral doses of ivermectin of 0.6, 1.2, 2.4, and 4.8 mg/kg, which is 3, 6, 12, and 24 times higher than the therapeutic antiparasitic dose. During the fiveday treatment with various oral doses of ivermectin, no clinical symptoms of poisoning were noted. The oral LD_{50} values of ivermectin in rats are reported to be in the range of 42.8-52.8 mg/kg (2) and 10-50 mg/kg (16). In our study, rats received 3, 6, 12, or 24 mg/kg of ivermectin for a total of 5 days, which means that rats treated with the two highest doses received nearly ¼ and ½ the LD_{50} of ivermectin, but did not show any clinical symptoms. In addition, the Rota rod test did not show any disruption of CNS integration as a consequence of the neurotoxic effect of ivermectin even at these at high concentrations.

Hematological analyses indicated no changes in the number of leukocytes in the white blood cell differential count. Hematocrit values and hemoglobin concentrations were unchanged compared to control group, except in rats treated with ivermectin at a dose of 0.6 mg/kg where the hemoglobin concentration was significantly higher compared to the control. We emphasize that the number of erythrocytes was slightly increased in all treated rats, while MCV and MCH values were lower than in controls (Table 1). This finding indicates microcytosis in treated rats, which could be a consequence of ivermectin treatment, but this effect is not dose-dependent (at the concentrations tested) and did not differ between groups in relation to the dose of ivermectin received.

The analysis of biochemical parameters showed a significant increase in the level of ALT (not dose-dependent) and a significant dose-dependent increase in the level of gamma-GT (Table 2). The increase in the value of these two enzymes, which indicates liver tissue damage, even at the lowest test dose of ivermectin, is in agreement with the histopathological changes in the liver that we observed. These results are in in agreement with the hepatic disorders (hepatitis, hepatocellular injury, cholestasis, increased alanine aminotransferase and/or aspartate aminotransferase levels, abnormal liver function tests) observed in humans who received ivermectin as therapy against the SARS-CoV-2 (16). However, our results are not in agreement with the research of Dong et al. (18) where 14 daily intraperitoneal application of ivermectin in doses of 100 to 380 mg/kg surprisingly, did not lead to changes in liver enzyme values. On the contrary, when Wistar rats were treated intraperitoneally 4 times a week for 21 days in doses of 0.4 mg/kg and 4 mg/kg of body weight, an increase in ALT, GGT and AST values was recorded (19). These results are consistent with our findings. Remarkably, in our investigation, we noted histopathological changes in the kidneys of treated rats, despite the absence of increased concentrations of creatinine and urea in the blood. There are published data that ivermectin can cause glomerular and tubular dysfunctions in humans, determined after 5 days of treatment against onchocerciasis (20). Similar changes in the kidneys of rabbits were recorded by GabAllh et al. (21). In rabbits treated once a week with ivermectin 0.8 mg/kg for 8 weeks, congestion of renal blood vessels was recorded. The renal tubules showed severe degeneration as evidenced by vacuolation of cytoplasm, necrosis and desquamation of affected epithelium. The highest dose of ivermectin in our study caused degenerative changes in testicular tissue. Similar changes in the testicles of rabbits were described GabAllh et al. (21). In our study, histopathological changes in the brain including focal bleeding as well as perivascular bleeding were observed only in rats treated with 4.8 mg/kg of ivermectin. Degenerative changes in the rabbit brain after administration of therapeutic and double therapeutic doses for 8 weeks were also described by GabAllh et al. (21).

It was particularly important to examine cytochrome P-450 concentrations in rats treated with increasing doses of ivermectin administered in humans during the COVID-19 pandemic. Ivermectin is extensively metabolized by human liver microsomes by cytochrome P-450. The predominant isoform responsible for the biotransformation of this compound in the liver is cytochrome P-450 3A4 (7). Our results show that doses of ivermectin 3, 6, and 12 times higher than the therapeutic dose, lead to a dose-dependent increase in plasma concentrations of P-450 3A4 (Figure 1). However, a dose 24 times higher than the therapeutic did not increase serum enzyme concentrations further. Ivermectin is known to be both a substrate for and inhibitor of human P-450 enzymes (7). Based on our results, it is obvious that in very high doses, ivermectin did not cause an increase in the concentration of this enzyme, it remains at the control level which leads to an elevation in the concentrations of ivermectin in plasma and tissues.

Ivermectin concentrations recorded in the plasma of treated rats were compatible with the administered doses. A two-fold increase in the dose resulted in a two-fold increase in the concentration of the drug in the plasma. The highest dose tested showed an exception, with the plasma concentration being nearly three times higher compared to the preceding dose level. This result is in agreement with the finding that this highest dose of ivermectin does not increase

concentration of P-450 enzyme that metabolizes ivermectin and allows such an increase of drug level in plasma. On the other hand, tested doses 3, 6, 12, and 24 times higher than therapeutic, produced maximum plasma concentrations that were far lower than the *in vitro* IC50 value of ivermectin for SARS-CoV-2 virus. Caly et al. (22) reported that ivermectin inhibited SARS-CoV-2 *in vitro* causing a ~5000-fold reduction in viral RNA at 48h at concentrations of 5 μM. The concentration resulting in 50% inhibition (IC50) which they obtained, was 1750 μg/L, while we recorded a concentration of 165.317±46.450 μg/L, 24 hours after the last administration. Our results indicate that it is almost impossible to achieve an effective antiviral concentration of ivermectin, even a 24-fold higher than therapeutic dose produces a concentration in plasma 10 times lower than the IC50 for SARS-CoV-2. Furthermore, serious damage of the body is highly likely. Our findings are supported by the results of Buonfrata et al. (8). In order to treat SARS-CoV-2 infection, these authors administered ivermectin to humans orally in doses of 0.6 and 1.2 mg/kg, for 5 days. Serious side effects observed included visual impairment, abdominal pain, diarrhea, nausea & vomiting, arthralgia, dizziness, headache, and paranesthesia. However, log10 viral load reduction did not differ between untreated and ivermectin-treated humans.

The concentrations of ivermectin in the brain were consistent with the administered doses, and the observed increase in concentrations was directly proportional to the dose. Similar to plasma, doubling the dose produced a two-fold increase in the concentration of ivermectin in the brain, except at the highest dose tested (Table 3). The highest dose tested produced a fivefold increase in brain ivermectin concentrations compared to the previous dose. Such a high concentration of ivermectin in the brain is probably due to saturation of P-450 and the absence of increased activity of P-450 as well as insufficiency of the P-glycoprotein efflux transporters at the blood-brain barrier. However, the concentration of 33.033±6.313 μg/kg does not lead to clinical symptoms, but does damage brain tissue. This is in agreement with the data of Geyer et al. (23) who indicate that a therapeutic dose of ivermectin in mice 24 hours after p.o. administration produces a brain concentration of 2 μg/kg, but in MDR1-deficient knockout mice, the concentration of ivermectin was 127 μg/kg. Significant for comparison is the case of a man who received ivermectin p.o. and subcutaneously a dose of 12 mg against infection with *Strongyloides stercoralis*. Although the infection was significantly suppressed, the patient fell into a coma and died. The concentration of ivermectin detected postmortem in his brain was 30 μg/kg tissue and by excluding other potential causes of neurotoxicity, the authors of this clinical report suggest that ivermectin was the main cause (24). This concentration of ivermectin is lower than the concentration we detected, which obviously indicates that some people are more sensitive to the neurotoxic effects of ivermectin.

Conclusions

Ivermectin at the doses used in humans against the SARS-CoV-2 (3, 6, 12 and 24 times higher than the antiparasitic dose), causes changes in red blood cell counts and increases the levels of liver enzymes in treated rats, without visible clinical symptoms. Histopathological changes were recorded in the liver, kidneys and testicles of rats, and the highest dose tested led to bleeding in the brain tissue. Obviously, ivermectin somewhat stimulates the activity of the enzyme P-450 isoform 3A4, whose substrate it is, but the highest tested dose reduces its concentration in plasma to the control level. Notably, the concentrations of ivermectin recorded in plasma of treated rats, indicate that even high doses do not reach the *in vitro* IC50 value of ivermectin for SARS-CoV-2 reported in the literature. On the other hand, the concentrations of ivermectin in the brain approach the values that can manifest extremely toxic effects described in humans.

Acknowledgements

This work was supported by the Ministry of Science, Technological Development and Innovation of the Republic of Serbia (Contract number 451-03-47/2023-01/200143), Science Fund of the Republic of Serbia, #GRANT No, 7355 Project title-FARMASCA and Veterinary Specialist Institute Niš, Serbia.

Funding. The authors declare that no funds, grants, or other support were received during the preparation of this manuscript.

Competing interests. The authors have no relevant financial or non-financial interests to disclose.

Author contributions. VM, conceptualization, investigation, methodology, writing–original draft; DM, investigation, methodology; DjSM, investigation, methodology; NA, conceptualization, methodology; MP, conceptualization, methodology; JFA, investigation, methodology; MR, investigation, methodology; DM, investigation, methodology; VK conceptualization, methodology; SMT, conceptualization, methodology, supervision, writing–review and editing. All authors have contributed to the final version of the manuscript. All authors approved the final manuscript.

References

1. Prichard R, Ménez C, Lespine A. Moxidectin and the avermectins: consanguinity but not identity. Int J Parasitol Drugs Drug Resist 2012; 2: 134–53. doi: 10.1016/j.ijpddr.2012.04.001

2. Siegmund OH, ed. The Merck veterinary manual. 5th ed. Rathway: Merck, 1979.

3. Trailović SM, Varagić VM. The effect of ivermectin on convulsions in rats produced by lidocaine and strychnine. Vet Res Commun 2007; 31(7): 863–72. doi: 10.1007/s11259-007-0050-3

4. Trailovic SM, Ivanovic SR, Varagić VM. Ivermectin effects on motor coordination and contractions of isolated rat diaphragm. Res Vet Sci 2011; 91(3): 426–33. doi: 10.1016/j.rvsc.2010.09.016

5. Trailovic SM, Nedeljkovic JT. Central and peripheral neurotoxic effects of ivermectin in rats. J Vet Med Sci 2011; 73(5): 591–99. doi: 10.1292/jvms.10-0424

6. Edwards G. Ivermectin: does P-glycoprotein play a role in neurotoxicity? Filaria J 2003; 2(Suppl. 1): S8. doi: 10.1186/1475-2883-2-S1-S8

7. Rendic SP. Metabolism and interactions of Ivermectin with human cytochrome P450 enzymes and drug transporters, possible adverse and toxic effects. Arch Toxicol 2021; 95(5):1535–46. doi: 10.1007/s00204-021-03025-z

8. Buonfrate D, Chesini F, Martini D, et al. High-dose ivermectin for early treatment of COVID-19 (COVER study): a randomised, double-blind, multicentre, phase II, dose-finding, proof-of-concept clinical trial. Int J Antimicrob Agents 2022; 59(2): 106516. doi: 10.1016/j.ijantimicag.2021.106516

9. Temple C, Hoang R, Hendrickson RG. Toxic Effects from Ivermectin Use Associated with Prevention and Treatment of Covid-19. N Engl J Med 2021; 385(23): 2197–8. doi: 10.1056/NEJMc2114907

10. Collins AB, Zhao L, Zhu Z, et al. Impact of COVID-19 on male fertility. Urology 2022; 164: 33–9. doi: 10.1016/j.urology.2021.12.025

11. Whelan M, Kinsella B, Furey A, et al. Determination of anthelmintic drug residues in milk using ultra high-performance liquid chromatography-tandem mass spectrometry with rapid polarity switching. J Chromatogr A 2010; 1217(27): 4612–22. doi: 10.1016/j.chroma.2010.05.007

12. Simunovic S, Jankovic S, Baltic T, et al. Histamine in canned and smoked fishery products sold in Serbia. Meat Technol 2019; 60(1): 8–16. doi: 10.18485/meattech.2019.60.1.2

13. Jones BJ, Roberts DJ. The quantitative measurement of motor inco-ordination in naive mice using an accelerating rotarod. J Pharm Pharmacol 1968; 20(4): 302–4. doi: 10.1111/j.2042-7158.1968.tb09743.x

14. Brunton LL, Chabner BA, Knollmann BC. Goodman and Gilman's the pharmacological basis of therapeutics. 12th ed. New York: McGraw-Hill Education, 2011: 1456-7.

15. Riviere JE, Papich MG. Veterinary pharmacology and therapeutics. 10th ed. Hoboken: Wiley-Blackwell, 2018: 1101–27.

16. Lankas GR, Gordon LR. Toxicology. In: Campbell WC, ed. Ivermectin and abamectin. New York: Springer, 1989: 89–112.

17. Oscanoa TJ, Amado J, Romero-Ortuno R, Carvajal A. Hepatic disorders associated with the use of Ivermectin for SARS-CoV-2 infection in adults: a pharmacovigilance study in VigiBase. Gastroenterol Hepatol Bed Bench. 2022; 15(4): 426–9. doi: 10.22037/ghfbb.v15i4.2383

18. Dong Z, Xing SY, Zhang JY, Zhou XZ. 14-Day repeated intraperitoneal toxicity test of ivermectin microemulsion injection in Wistar rats. Front Vet Sci 2020; 7: 598313. doi: 10.3389/fvets.2020.598313

19. Utu-Baku AB. Effect of therapeutic and toxic doses of ivermectin (Mectizan) on total serum proteins and hepatic enzymes of Wistar albino rats. Int J Biol Chem 2009; 3(4): 142–7. doi: 10.3923/ijbc.2009.142.147

20. Burchard GD, Kubica T, Tischendorf FW, Kruppa T, Brattig NW. Analysis of renal function in onchocerciasis patients before and after therapy. Am J Trop Med Hyg. 1999; 60(6): 980-6. doi: 10.4269/ajtmh.1999.60.980

21. GabAllh M, El-mashad A, Amin A, Darweish M. Pathological studies on effects of ivermectin on male and female rabbits. Benha Vet Med J 2017; 32(1): 104–12. doi: 10.21608/bvmj.2017.31162

22. Caly L, Druce JD, Catton MG, Jans DA, Wagstaff KM. The FDA-approved drug ivermectin inhibits the replication of SARS-CoV-2 in vitro. Antiviral Res 2020; 178: 104787. doi: 10.1016/j.antiviral.2020.104787

23. Geyer J, Gavrilova O, Petzinger E. Brain penetration of ivermectin and selamectin in mdr1a,b P-glycoprotein- and bcrp- deficient knockout mice. J Vet Pharmacol Ther 2009; 32(1): 87–96. doi: 10.1111/j.1365-2885.2008.01007.x

24. Westerloo van DJ, Landman GW, Prichard R, Lespine A, Visser LG. Persistent coma in Strongyloides hyperinfection syndrome associated with persistently increased ivermectin levels. Clin Infect Dis 2014; 58(1): 143–4. doi: 10.1093/cid/cit656

Veliki odmerki ivermektina povzročajo toksične učinke pri podganah po kratkotrajnem peroralnem dajanju

V. Marjanović, D. Medić, D. S. Marjanović, N. Andrić, M. Petrović, J. Francuski Andrić, M. Radaković, D. Marinković, V. Krstić, S. M. Trailović

Izvleček: Protiglivični makrociklični laktoni (ML) so najpomembnejše učinkovine v sodobni farmakoterapiji parazitskih okužb. Vendar so med pandemijo covida-19 pri ljudeh proti okužbi z virusom SARS-CoV-2 uporabljali bistveno višje odmerke ivermektina od odobrenih antiparazitičnih odmerkov. Takšna uporaba je bila ustvarjena izključno na podlagi testov *in vitro*, vendar ni bila uradno odobrena v nobeni državi na svetu. Zato smo izvedli študijo na podganah, ki smo jih 5 dni peroralno zdravili z 0,6, 1,2, 2,4 in 4,8 mg ivermektina na kg telesne teže. Naša preiskava je pokazala, da ivermektin v povišanih odmerkih, ki se uporabljajo pri ljudeh proti virusu SARS-CoV-2 (3-, 6-, 12- in 24-krat večjih od antiparazitskega odmerka 0,2 mg/kg), povzroča spremembe v številu eritrocitov in zvišuje raven jetrnih encimov brez vidnih kliničnih simptomov. Histopatološke spremembe smo zabeležili v jetrih, ledvicah in testisih podgan, največji testirani odmerek pa je povzročil krvavitev v možganskem tkivu. Znano je, da ivermektin kot substrat nekoliko poveča koncentracijo encima P-450 izoforma 3A4, vendar največji testirani odmerek zmanjša njegovo koncentracijo v plazmi na kontrolno raven. Koncentracije ivermektina, zabeležene v plazmi zdravljenih podgan, kažejo, da tudi visoki odmerki ne dosežejo *in vitro* vrednosti IC50 ivermektina za SARS-CoV2, ki je navedena v literaturi. Po drugi strani pa se koncentracije ivermektina v možganih približujejo vrednostim, ki lahko povzročijo izjemno toksične učinke, opisane pri ljudeh.

Ključne besede: ivermektin; toksičnost; SARS-CoV-2; citokrom P-450; P-gp; histopatološke spremembe; podgane

Slovenian Veterinary Research
DOI 10.26873/SVR-1792-2023
UDC 599.322.21:591.422:611.018:611
Pages: 291–7

Original Research Article

Anatomical and Histological Features of Lingual Papillae on Tongue in Squirrel (*Sciurus vulgaris*)

Key words

light microscopy;
lingual papillae;
rodent;
squirrel;
taste bud

Burhan Toprak[1]*, Bahadır Kilinç[2]

[1]Yozgat Bozok University, Faculty of Veterinary Medicine, Department of Anatomy, 66100 Yozgat, Türkiye,
[2]Veterinary Control Central Research Institute, Pathology Laboratory, 06020 Ankara, Türkiye

***Corresponding author:** burhan.toprak@bozok.edu.tr

Abstract: This study examined the anatomical and histological features of lingual papillae in squirrels. Two adult male squirrel tongues were used as the material in the study. Three parts were detected in the tongue: apex, corpus, and radix. There was a median sulcus on the apex of the tongue and an intermolar prominence on the body of the tongue. Five types of papillae such as filiform, conical, fungiform, vallate, and foliate were observed on the tongues of the squirrels. Filiform papillae were located from the apex of the tongue to the root as the dominant papilla. Conical papillae were observed on the intermolar prominence, on the sides of the tongue root, and between the vallate papillae. The direction of this papillae was oriented caudomedially. Fungiform papillae were randomly distributed among the filiform papillae. These papillae were mushroom shaped and had slits that separated them from filiform papillae. Three vallata papillae, arranged in a triangle with the apex pointing backward, were found on the root of the tongue. These papillae were surrounded by a trench. Foliate papillae were observed like mucosal folds in the caudolateral part of the tongue. On light microscopic examination, lingual papillae were covered with stratified squamous epithelium and had connective tissues. There were varying degrees of keratinization on the epithelial surfaces of the papillae. Although taste buds were seen in the epithelial layer of the fungiform and vallate papillae, they were not observed in the epithelium of the grooves of the foliate papillae. The findings obtained in the study were compared with those obtained from the lingual papillae of other rodents, and similarities and differences were revealed.

Received: 15 June 2023
Accepted: 20 November 2023

Introduction

Rodents are an order that includes about half of the known mammals in the world. Of the 166-167 mammals recorded in Türkiye, 65 belong to the rodent order. One of the best known rodent species is the squirrel (*Sciurus vulgaris*), which is very common in the Anatolian part of Türkiye (1).

The tongue plays an important role in nutrition, along with the other organs located in the oral cavity. The morphological and histological features of the tongue in mammals are a reflection of the differences between the diets of living things (2). In the tongue mucosa, there are two types of papillae, mechanical and gustatory, according to their functions. Mechanical papillae are keratinized. In the gustatory papillae, the epithelial layer contains taste buds sensitive to taste (3)

To date, macroscopic, light microscopic, and scanning electron microscopic studies have been carried out on the distribution, types, and structures of lingual papillae in many mammalian species. Macroscopic and light microscopic properties of both mechanical and gustatory papillae found on tongues of many species belonging to the rodent order were investigated. Accordingly, the macroscopic, light microscopic and scanning electron microscopic structures of the papillae of the mouse (4-7), rat (8-11), guinea pig (12, 13), porcupine (14, 15), hamster (16), Japanese lesser flying squirrel (17), Jentink's flying squirrel (18), greater cane rat (19), American beaver (20), capybara (21), agouti (22), hazel dormouse (23), large bamboo rat (24) and paca (25) were examined.

In the detailed literature review, it was determined that the macroscopic and light microscopic structures of the fungiform and vallate papillae, which are gustatory papillae in squirrels, were examined (26, 27). However, no study has been found on mechanical papillae and foliate papillae on the tongue. This study was conducted to reveal the anatomical and histological features of the papillae on the tongue mucosa of squirrels and to determine the similarities and differences between the data obtained from this study and the data obtained from other rodent studies.

Materials and methods

Ethical Approval

This study was conducted with permission from the Turkish Ministry of Agriculture and Forestry Management (permission number: E-21264211-288.04-7695477). Ethical approval was obtained from the Research Ethics Committee of the Veterinary Control Central Research Institute on October 26, 2022 (decision number: 2022/29).

Animal

As the study specimens, two male squirrels (*Sciurus vulgaris*) sent to Etlik Veterinary Control Central Research Institute Pathology Laboratory were used. The oral cavities of the squirrels were carefully opened and tongue samples were removed from the oral cavity. Fresh tongue specimens were washed with physiological saline. Measurements were made with the help of a digital caliper from these tongues and macroscopic photographs (Canon IXUS75 7.1 megapixel) were viewed with a digital camera.

Light microscopy

Histological tissue samples were fixed in 10% formaldehyde solution for 24 h. Samples were taken from the apex, corpus and radix parts of the dorsal part of the fixed tongues and from the ventral part of the apex of the tongue. For light microscopic evaluation; sample washing, dehydration, paraffin saturation and embedding were performed with alcohol and xylol series on an automatic tissue tracking device (Leica ASP 300S). Sections of 5 µm thickness were obtained from the prepared paraffin blocks with a microtome (Shandon/finesse) and placed on slides. These slides were kept in an oven at 60°C for 40 min. Then, it was stained with the Hematoxylin-Eosin stain method with a fully automatic (Shandon/varistain Gemini) device. The obtained preparations were examined under a light microscope with attachment (Leica DM2500 LED). Necessary assessments were made and microscopic pictures of the sections were taken.

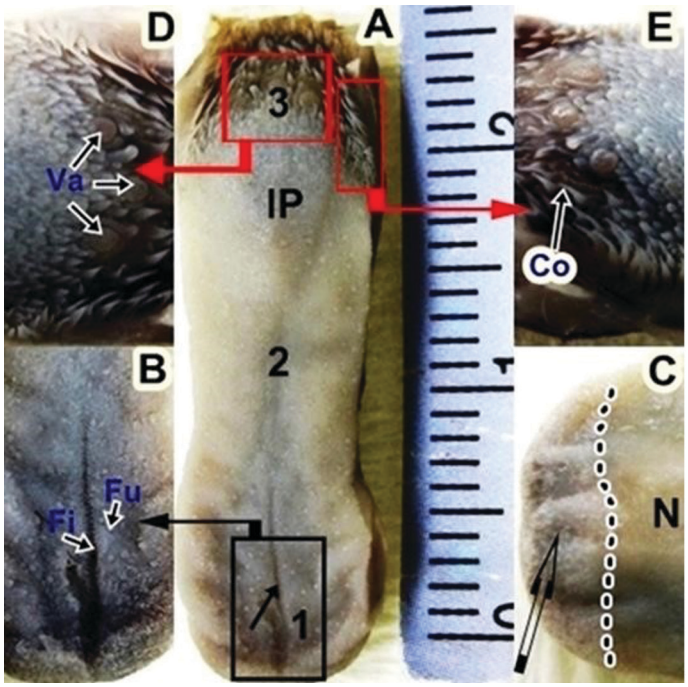

Figure 1: A: General macroscopic view of the tongue. 1: apex of tongue, 2: body of tongue, 3: root of tongue, arrow: median sulcus, IP: intermolar prominence. B: General macroscopic view from the dorsal part of the apex of the tongue. Fu: fungiform papillae, Fi: filiform papillae. C: General macroscopic view from the ventral part of the apex of the tongue. white arrow: filiform and fungiform papillae, N: nonpapillary part. D: General macroscopic view from the root of the tongue. Va: vallate papillae. E: Macroscopic view from the lateral part of the root of the tongue. Co: large conical papillae

Results

Macroscopic evaluation of the tongue

The squirrel's tongue was rectangular with an oval apex. A median sulcus was present at the apex of the tongue. A slightly prominent intermolar prominence was observed between the body and the root of the tongue. The length of the tongue was 28 mm on average, its width was 8 mm at the apex, 6 mm in the body and 9 mm at the root (Figure 1A). Five types of papillae on the tongue of squirrels were observed: filiform papillae (Figure 1B, C), conical papillae (Figure 1E), fungiform papillae (Figure 1B, C), vallate papillae (Figure 1D) and foliate papillae.

Filiform papillae

Filiform papillae were distributed on the dorsal surface of the tongue from the apex to the vallate papillae. Filiform papillae were observed as the predominant papilla type on the dorsal surface of the tongue. The tips of these papillae were caudally inclined (Figure 2A). These were also observed in the ventrolateral region of the apex of the tongue (Figure 1C). On light microscopic examination, it was determined that the filiform papillae were covered with stratified squamous epithelium. There was a varying degree of keratinized layer in the epithelial layer of these papillae (Figure 2B, C).

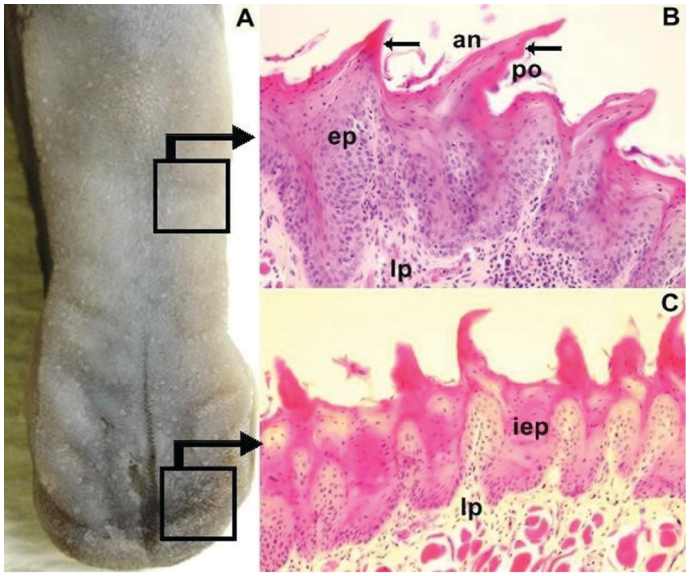

Figure 2: A: Macroscopic view of filiform papillae. B: Light microscopic view of filiform papillae on the body of the tongue. ep: epithelial layer, lp: connective tissue, an: anterior part of the filiform papilla, po: posterior part of the filiform papilla, arrows: keratin layer, H&E, 100 µm. C: Light microscopic view of the filiform papillae at the apex of the tongue. iep: interpapillary epithelial layer, lp: connective tissue, H&E, 200 µm

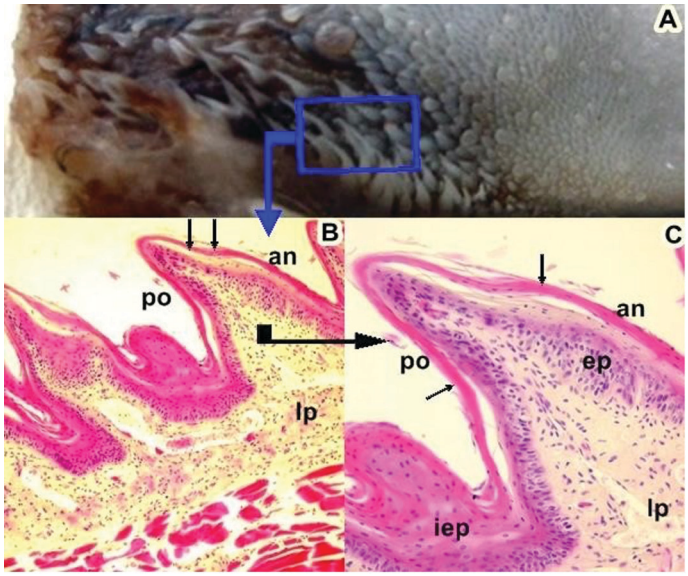

Figure 3: A: Macroscopic view of conical papillae. B: Light microscopic view of conical papillae. lp: connective tissue, an: anterior part of conical papilla, po: posterior part of conical papilla, arrows: keratin layer, H&E, 200 µm. C: Light microscopic view of a conical papilla. ep: epithelial layer, iep: interpapillary epithelial layer, lp: connective tissue, an: anterior part of conical papilla, po: posterior part of conical papilla, arrows: keratin layer H&E, 100 µm

Conical papillae

Conical papillae were detected on the intermolar prominence in the body of the tongue, on the side of the root part of the tongue and in the root part of the tongue. The conical papillae, which were on the side and behind the vallate papillae, were greater and their directions were also oriented caudomedially (Figure 3A). The conical papillae located in front of the vallate papillae and on the intermolar prominence were smaller and were directed caudally. On the microscopic examination, it was found that the conical papillae started with a thick root from the tongue mucosa and ended bluntly. The anterior and posterior parts of the conical papillae had the same thick keratin layer. The epithelial layer among the papillae was found to be thicker than the papillary epithelial layer (Figure 3B, C).

Fungiform papillae

Fungiform papillae were scattered among the filiform and conical papillae from the apex of the tongue to the vallate papillae. These papillae, round and resembling mushrooms were separated from the filiform papillae by a slit. Fungiform papillae were specially observed in the apex and body of the tongue. These papillae were not observed in the median sulcus in the middle of the apex of the tongue (Figure 4A). Fungiform papillae were also detected in the ventrolateral part of the apex of the tongue (Figure 1C). The average diameter of these papillae was around 0.34 mm. A weak keratinized layer was observed on the epithelial surface of the fungiform papillae on light microscopic examination (Figure 4B, C). Intraepithelial taste buds were observed in the dorsal epithelial layer of these papillae and their number was few. These taste buds were opened into the oral cavity through the taste pores. Dark and light-stained cells were observed in the taste buds (Figure 4D).

Vallate papillae

Three vallate papillae, arranged in a triangle with the apex pointing backward were found on the root of the tongue. They are surrounded by a circular trench that separates them from the rest of the tongue's surface. Conical papillae were present between and around these papillae. The average length of the vallate papillae was 0.96 mm, and the width was around 0.74 mm. (Figure 5A). On light microscopic examination, the taste buds of the vallate papillae were located intraepithelially in the trench-facing epithelial layer of the papillae. These taste buds were arranged perpendicular to the length of the epithelial layer and were observed in the epithelial layer up to half the trench (Figure 5B, C). Taste buds in the vallate papillae were observed to open into the papilla trenches through the taste pores. (Figure 5B). Dark and light-stained cells were detected in these taste buds (Figure 5D). While there was no keratinized layer on the epithelial surface of the vallate papillae, there was very weak keratinization on the epithelial surfaces facing the trench (Figure 5C).

Foliate papillae

Mucosal folds similar to those of foliate papillae were detected on the caudolateral sides of the root of the tongue. The number of these mucosal folds ranged from 10 to 14 (Figure 6A). On light microscopic examination, papillary protrusions and papillary clefts were quite evident. Taste

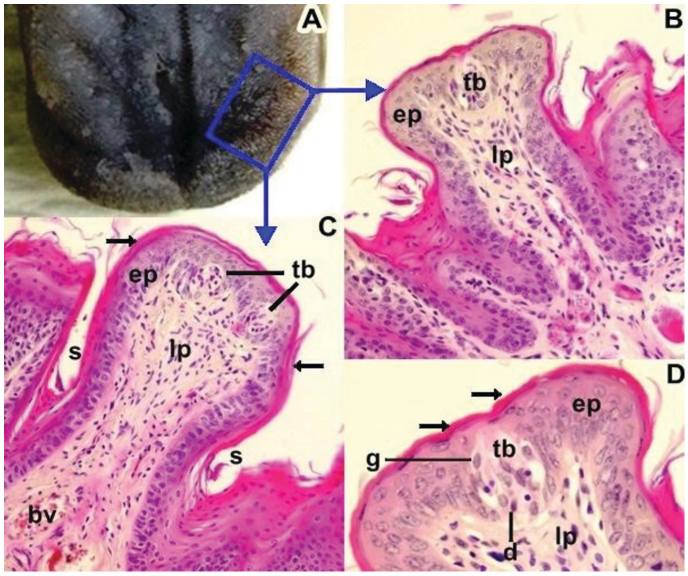

Figure 4: A: Macroscopic view of fungiform papillae. B: Light microscopic view of a fungiform papilla with one taste bud. ep: epithelial layer, lp: connective tissue, tb: taste bud, H&E, 100 µm. C: Light microscopic view of fungiform papilla with two taste buds. ep: epithelial layer, lp: connective tissue, s: papilla slits, bv: blood vessel, tb: taste buds, arrows: keratinized layer, H&E, 100 µm. D: Light microscopic view of a taste bud. ep: epithelial layer, lp: connective tissue, tb: taste bud, g: light-stained cell, d: dark-stained cell, arrows: keratinized layer, H&E, 50 µm

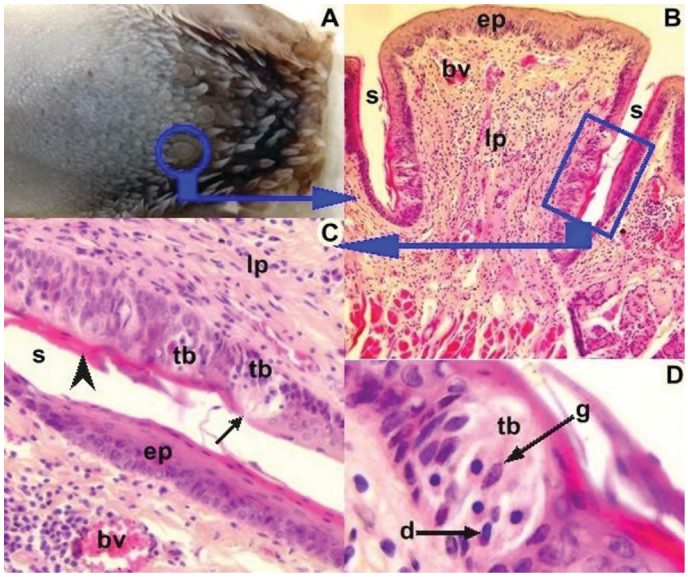

Figure 5: A: Macroscopic view of vallate papillae. B: Light microscopic view of a vallate papilla. ep: epithelial layer, lp: connective tissue, bv: blood vessel, s: trench of papilla, H&E, 200 µm. C: Light microscopic view of taste buds in the epithelial layer facing the trench in the vallate papilla. ep: epithelial layer, lp: connective tissue, s: trench of papilla, bv: blood vessel, tb: taste buds, arrow: taste pore, arrowhead: keratinized layer, H&E, 100 µm. D: Light microscopic view of a taste bud. tb: taste bud, g: light-stained cell, d: dark-stained cell, H&E, 50 µm

buds were absent in the epithelial layer facing the clefts and in the dorsal epithelium of the foliate papillae. A prominent keratinized layer was detected in the surface epithelial layer and in the epithelial layer facing the clefts of these papillae (Figure 6B, C).

Discussion

The median sulcus was detected on the apex part of the tongue in the squirrel, similar to what has been reported in the tongues of rats (8), WWCPS rat (11), porcupines (14, 15), Jentink's flying squirrel (18), agouti (22), hazel dormouse (23) and large bamboo rat (24). However, it has been reported that the median sulcus is absent in rodents such as guinea pigs (12), capybaras (21) and rock cavy (28). In this study, five types of tongue papillae filiform, conical, fungiform, vallate and foliate were detected on the tongue of the squirrel. The shape and distribution of these papillae were similar to the papillae found on the tongue of rats (8), Japanese lesser flying squirrel (17), Jentink's flying squirrel (18), hazel dormouse (23) and paca (25).

Filiform papillae were a common and abundant type of papillae on the tongue, extending from the apex to the root. The tips of these papillae were generally oriented in the caudal direction. The distribution of filiform papillae on the tongue in squirrels was similar to the distribution of filiform papillae found in the tongues of Wistar rat (10), guinea pig (12), Jentink's flying squirrel (18) and agouti (22). A weak keratinized layer was present on the epithelial surface of the filiform papillae on the tongue in squirrels, similar to reports of the filiform papillae in rats (8) and Jentink's flying squirrels (18).

Conical papillae on the tongue in squirrels were detected on the intermolar prominence located on the body of the tongue, on the sides of the root part of the tongue and on the root part of the tongue. The conical papillae located on the sides of the root part of the tongue were quite large and oriented caudomedially. Previos studies have reported that conical papillae are located in the middle of the root of the tongue in hazel dormouse (23) and on the intermolar prominence of the root of the tongue in rock cavy (28) and degu (29). The distribution of conical papillae on the tongues of Japanese lesser flying squirrel (17), Jentink's flying squirrel (18) and paca (25) were similar to our study findings. The presence of a thick keratinized layer detected on the epithelial surface of the conical papillae in this study was consistent with the expression of a keratinized layer on the surface of the conical papilla epithelium of tongues in the Jentink's flying squirrel (18) and rock cavy (28). It is considered that the large conical papillae on the tongue in squirrels are effective in sending the nutrients taken into the oral cavity to the pharynx.

Fungiform papillae were randomly distributed on the dorsal surface from the apex to the root of the tongue. These papillae were also detected in the ventrolateral part of the apex of the tongue. Some researchers reported that fungiform papillae were located on the apex and the body parts of the tongue in the rat (9), WWCPS rat (11), agouti (22), hazel dormouse (23), large bamboo rat (24), paca (25) and rock cavy (28). It has been reported that these papillae are

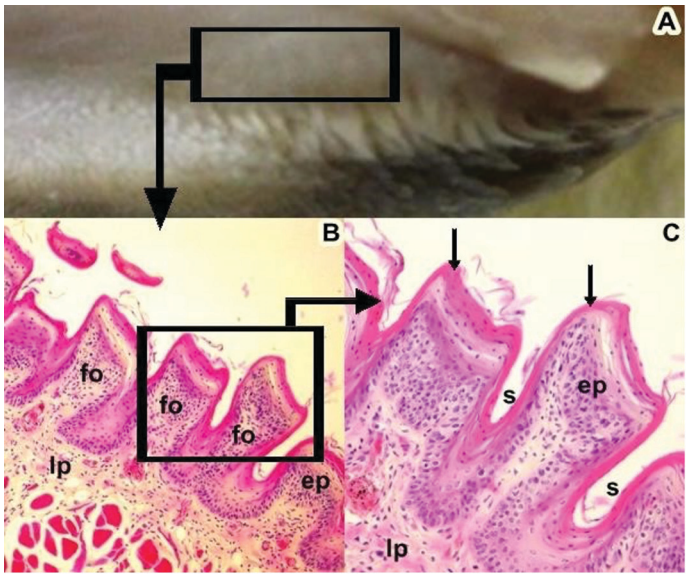

Figure 6: A: Macroscopic view of foliate papillae. B: Light microscopic view of foliate papillae. fo: foliate papillae folds, ep: epithelial layer, lp: connective tissue, H&E, 200 µm. C: Light microscopic view of two folds of foliate papillae. ep: epithelial layer, lp: connective tissue, s: grooves of papillae, arrows: keratinized layer, H&E, 100 µm

not found at the apex of the tongue in porcupines (14), they are located in the body and posterior third of the tongue and at the tip of the tongue and on the intermolar prominence in porcupines (15). It has been reported that there are no fungiform papillae on the tongue in degu (29). Contrary to the findings of this study, it has been reported that there are no fungiform papillae in the ventrolateral part of apex of the tongue in the hamster (16) and rock cavy (28). In this study, a few taste buds located intraepithelially in the dorsal region of the epithelial layer of the fungiform papilla were detected. One taste bud was observed in the fungiform papillae epithelial layer in mice (4), rat (8), Jentink's flying squirrel (18) and hazel dormouse (23). A few taste buds were detected in the epithelial layer of the fungiform papillae in guinea pig (12) and American beaver (20) and between 1 and 4 in large bamboo rats (24), and generally, 4-5 in porcupines (14). Dedection of several taste buds in the epithelial layer of the fungiform papillae in this study was similar to those reported in guinea pigs (12) and American beavers (20). The weak keratin layer detected on the fungiform papillae epithelial surface was consistent with findings in other rodent species (11, 12, 18, 22, 24, 26).

The number of vallate papillae on the root part of the tongue varies among rodent species. Accordingly, one vallate papilla was detected on the root part of the tongue in mice (7) and rats (8, 11). Two vallate papillae were observed on the root part of the tongue in the guinea pig (12), capybara (21), large bamboo rat (24), paca (25), rock cavy (28) and degu (29). Three vallate papillae were seen on the root part of the tongue in the Japanese lesser flying squirrel (17), Jentink's flying squirrel (18), American beaver (20), hazel dormouse (23) and squirrel (27). In agouti (22), there were four vallate papillae on the root of the tongue. In this study, three vallate papillae were detected on the root of the tongue, similar to those reported in the literature (17, 18, 20, 23, 27). In the squirrel, the taste buds of the vallate papillae were detected in the epithelial layer of the papillae facing the trench. These taste buds were opened to trench via taste pores. Taste buds of vallate papillae were detected in the epithelial layer on both walls of the trench in mice (7), WWCPS rats (11), guinea pigs (12, 13) and agouti (22). Taste buds of vallate papillae were observed in the epithelial layer on the interior wall of the trench in American beaver (20), Jentink's flying squirrel (18), hazel dormouse (23), large bamboo rat (24), squirrel (27) and degu (29). A weak keratinized layer was detected on the epithelium surface of vallate papillae in WWCPS rat (11), guinea pig (12), Jentink's flying squirrel (18), agouti (22) and large bamboo rat (24). A thick keratinized layer was observed on the epithelium surface of vallate papillae in guinea pigs (13), American beaver (20) and hazel dormouse (23). In this study, it was found that there was no keratinized layer on the surface of the epithelium of vallate papillae.

In the squirrel, mucosal folds similar to foliata papillae were detected in the caudolateral part of the tongue. The number of these mucosal folds ranged from 10 to 14. The number of foliate papillae mucosal folds were three in hazel dormouse (23) and four to six in mice (6). These mucosal folds were observed as five pairs of epithelial folds in the rat (9), WWCPS rat (11) and guinea pig (12). In the American beaver (20), 22-25 foliate mucosal folds were determined. Contrary to the reports that it is found caudolaterally between the body and root of the tongue in other rodent species, 170-200 foliate papillae were detected on the intermolar prominence in the dorsal part of the tongue in rats (8). In Jentink's flying squirrels (18), they were seen as mucosal folds in the dorsal part of the apex of the tongue. The absence of foliate papillae on the tongue of the large bamboo rat has been reported (24). In this study, contrary to the literature (6, 11, 12, 20, 23, 25, 28), taste buds were not observed in the epithelial layer facing the clefts of the foliate papillae mucosal folds. A prominent keratinized layer detected on the surface epithelium of foliate papillae in the squirrel was consistent with what has been reported in other rodent species (12, 23).

Conclusions

As a result, it was found that there were five types of lingual papillae, mechanical and gustatory, on the tongue of the squirrels. According to the comparison with other rodent species with lingual papillae, differences were detected, especially in conical and foliate papilla types, while other papilla types were found to have more similarities. It has been concluded that these similarities and differences can be due to the diet and nutrient selection of squirrels. It is considered that the findings of this study will contribute to the knowledge in the field of rodent anatomy and histology.

Acknowledgements

This study was conducted with permission from the Turkish Ministry of Agriculture and Forestry Management (permission number: E-21264211-288.04-7695477). Ethical Approval was obtained from the Research Ethics Committee of the Veterinary Control Central Research Institute on October 26, 2022 (decision number: 2022/29).

The availability of data and materials. Data sets analyzed during the current study are available from the corresponding author (BT) upon reasonable request.

Competing interests. There was no conflict of interest with regard to the authors reporting their findings.

Author contributions. This article was written by evaluating the anatomical and histological data planned by (BT). (BK) performed histological studies.

References

1. Karataş A. Türkiye'deki kemirici (Mammalia: Rodentia) türleri. Turk Hij Den Biyol Derg 2011; 68: 7–18.
2. Iwasaki S. Evolution of the structure and function of the vertebrate tongue. J Anat 2002; 202: 1–13. doi: 10.1046/j.1469-7580.2002.00073.x
3. König HE, Liebich HG. Veterinary anatomy of domestic animals. Textbook and Color Atlas.,7th edition. Thieme Verlag, Stuttgart- New York, 2020: 329.
4. Toprak B, Yılmaz S. Farelerde papilla fungiformislerin postnatal gelişimi üzerine işık ve taramalı elektron mikroskobik (SEM) incelemeler. FÜ Sağ Bil Derg 2003; 17: 183–8.
5. Toprak B. Light and scanning microscopic structure of filiform papillae in mice. Vet Arhiv 2006; 76: 555–62.
6. Toprak B, Yılmaz S. Investigations on postnatal development of the foliate papillae of the tongue by the light and scanning electron microscopy in the white laboratory mice. Revue Méd Vét 2007; 158: 479–82.
7. Toprak B, Yılmaz S. Light and scanning electron microscopic investigation of postnatal development of vallate papillae in the white laboratory mice. Atatürk Üniversitesi Vet Bil Derg 2016; 11: 131–37. doi:10.17094/avbd.04368
8. Davydova L, Tkach G, Tymoshenko A, et al. Anatomical and morphological aspects of papillae, epithelium, muscles, and glands of rats' tongue: Light, scanning, and transmission electron microscopic study. Interv Med Appl Sci 2017; 9: 168–77. doi: 10.1556/1646.9.2017.21
9. De Souza Reginato G, De Sousa Bolina C, Watanabe IS, Ciena AP. Three-dimensional aspects of the lingual papillae and their connective tissue cores in the tongue of rats: a scanning electron microscope study. ScientificWorldJournal 2014; 841879. doi: 10.1155/2014/841879.
10. Hutanu E, Damian A, Miclaus V, et al. Morphometric features and microanatomy of the lingual filiform papillae in the wistar rat. Biology (Basel) 2022; 11: 920. doi: 10.3390/biology11060920
11. Goździewska-Harłajczuk K, Klećkowska-Nawrot J, Barszcz K, et al. Biological aspects of the tongue morphology of wild-captive WWCPS rats: a histological, histochemical and ultrastructural study. Anat Sci Int 2018; 93: 514–32. doi: 10.1007/s12565-018-0445-y
12. Ciena AP, dos Santos AC, Vasconcelos BG, et al. Morphological characteristics of the papillae and lingual epithelium of guinea pig (Cavia porcellus). Acta Zool 2019; 100: 53–60. doi: 10.1111/azo.12230
13. Hussein Yousif N, Hashim Hazim N, Mahdi fathil N, Al-Hamoode SA. Histological study to the tongue for the guinea pig (Cavia porcellus) in Iraq. GSC Biol Pharm Sci 2022; 20: 226–33. doi: 10.30574/gscbps.2022.20.2.0329
14. Dinç G, Yilmaz S, Karan M, Aydin A, Atalar O. Study by light and scanning electron microscopy of the fungiform papillae on tongue of the porcupine (Hystrix cristata). FÜ Sağ Bil Vet Derg 2010; 24: 99–102.
15. Obead WF, Kadhim AB, Zghair FS. Macroanatomical investigations on the oral cavity of male porcupines (Hystrix cristata). J Pharm Sci & Res 2018; 10: 623–26.
16. Al-Alshemkhi A, Mohammed ZS, Hussein RM, Omran ZS, AL-Kraity WRH, Altaweel DA. Histological study of lingual papillae in male hamster, Mesocrictus auratus. Iran J Ichthyol 2022; (suppl. 1): 458-61.
17. Emura S. Morphology of the lingual papillae of the Japanese lesser flying squirrel and four-toed hedgehog. Okajimas Folia Anat Jpn 2019; 96: 23–6. doi: 10.2535/ofaj.96.23
18. Wihadmadyatami H, Saragih GR, Gunawan G, Mataram MBA, Kustiati U, Kusindarta DL. Morphological study of the lingual papillae of Jentink's flying squirrel (Hylopetes platyurus). Thai J Vet Med 2020; 50: 239–49.
19. Igado OO, Adebayo AO, Oriji CC, Aina OO, Oke BO. Macroscopic and microscopic analysis of the tongue of the greater cane rat (Thryonomys Swinderianus, Temminck). J Morphol Sci 2021; 38: 9-15. doi: 10.51929/jms.38.3.2021.
20. Shindo J, Yoshimura K, Kobayashi, K. Comparative morphological study on the stereo-structure of the lingual papillae and their connective tissue cores of the American beaver (Castor Canadensis). Okajimas Folia Anat Jpn 2006; 82: 127–38. doi: 10.2535/ofaj.82.127
21. Watanabe IS, Haemmerle CAS, Dias FJ, et al. Structural characterization of the capybara (Hydrochaeris hydrochaeris) tongue by light, scanning, and transmission electron microscopy. Microsc Res Tech 2013; 76: 141–55. doi:10.1002/jemt.22145
22. Ciena AP, Bolina CdS, de Almeida SRY, et al. Structural and ultrastructural features of the agouti tongue (Dasyprocta aguti Linnaeus, 1766). J Anat 2013; 223: 152–8. doi:10.1111/joa.12065
23. Wolczuk K. Dorsal surface of the tongue of the hazel dormouse Muscardinus avellanarius: scanning electron and light microscopic studies. Zool Pol 2014; 59: 35–47. doi:10.2478/zoop-2014-0004
24. Wannaprasert T. Morphological characteristics of the tongue and lingual papillae of the large bamboo rat (Rhizomys sumatrensis). Anat Sci Int 2018; 93: 323–31. doi:10.1007/s12565-017-0414-x
25. Beraldo-Massoli MC, Ribeiro PRQ, Vieira LG, et al. Morfologia da língua e características das papilas linguais de Cuniculus paca (Rodentia: Cuniculidae). Biotemas 2013; 26: 167–77. doi: 10.5007/2175-7925.2013v26n4p167
26. Ünsaldı E. Macroscopic and light microscopic structure of fungiform papillae on the tongue of squirrels (Sciurus vulgaris). Kafkas Univ Vet Fak Derg 2010; 16: 115–8. doi:10.9775/kvfd.2009.530
27. Ünsaldı E, Yılmaz S. Sincaplarda (Sciurus vulgaris) papilla vallata'nın makroskobik ve işık mikroskobik yapısı. FÜ Sağ Bil Vet Derg 2009; 23: 83–8.
28. Santos AC dos, Aro MM de, Bertassoli MB, et al. Morphological characteristics of the tongue of the rock cavy-Kerodon rupestris Wied, 1820 (Rodentia, Caviidae). Biosci J 2015; 1820: 1174–82.

29. Cizek P, Hamouzova P, Jekl V, Kvapil P, Tichy F. Light and scanning electron microscopy of the tongue of degu (Octodon degus). Anat Sci Int 2016; 92: 493–99 doi: 10.1007/s12565-016-0346-x

Anatomske in histološke značilnosti jezičnih papil na jeziku pri veverici (*Sciurus vulgaris*)

Burhan Toprak, Bahadır Kilinç

Izvleček: V tej študiji smo preučevali anatomske in histološke značilnosti jezičnih papil pri vevericah. V študiji smo uporabili dva jezika odraslih samcev veveric. Določili smo tri dele jezika: vrh, telo in koren. Na vrhnjem delu jezika je bila sredinska brazda, na telesu jezika pa medmolarna izboklina. Na jezikih veveric smo opazili pet vrst papil: nitaste, konične, gobaste, otočkaste in listaste. Nitaste papile so bile prevladujoče, prisotne od vrha do korena jezika. Konične papile so bile prisotne na intermolarnem izrastku, na straneh korena jezika in med otočkastimi papilami. Usmerjene so bile kavdomedialno. Gobaste papile so bile naključno razporejene med nitastimi papilami. Te papile so bile v obliki gobe z režami, ki so jih ločevale od filiformnih papil. Na korenu jezika so bile tri otočkaste papile razporejene v trikotnik z nazaj obrnjenim vrhom. Obdane so bile z jarkom. Listaste papile so bile v obliki gube sluznice v kavdolateralnem delu jezika. Pod svetlobnim mikroskopom so bile jezične papile pokrite z večskladnim ploščatim epitelijem, imele so vezivno tkivo. Na epitelijskih površinah papil so bile vidne različne stopnje poroženevanja. Čeprav so bile v epitelijski plasti gobastih in otočkastih papil vidne brbončice, jih v epiteliju žlebov listastih papil ni bilo opaziti. Ugotovitve, pridobljene v tej študiji, smo primerjali z ugotovitvami študij jezičnih papil drugih glodavcev ter prikazali podobnosti in razlike med njimi.

Ključne besede: svetlobna mikroskopija; jezične papile; glodavec; veverica; brbončica

Slov Vet Res
DOI 10.26873/SVR-1832-2024
UDC 591.432:599.723.12:616-072.1:616-089.8:616.24-002
Pages: 299–305

Case Report

Endoscopic and Surgical Intervention of Complete Esophageal Stricture in a One-month-old Thoroughbred Foal With *Rhodococcus equi* pneumonia

Key words

balloon dilation;
foal;
esophageal stricture;
esophagostomy;
pneumonia

Jungho Yoon[1,2], Ahram Kim[1], Jeonghun Lee[1], Young Beom Kwak[1], In-Soo Choi[2], Taemook Park[1]*

[1]Equine Clinic, Jeju Stud Farm, Korea Racing Authority, Namjo-ro 1660, Jeju-si, Jeju, 63346 Korea, [2]College of Veterinary Medicine, Konkuk University, Neungdong-ro 120, Gwangjin-gu, Seoul 05029, Korea

***Corresponding author:** taemook@kra.co.kr

Abstract: This case report describes a surgical and endoscopic approach for treating a complete esophageal stricture in a one-month-old Thoroughbred foal with *Rhodococcus equi* pneumonia. Clinical symptoms included coughing, nasal discharge, regurgitation, and lethargy. Endoscopic and ultrasonographic examinations revealed a complete esophageal obstruction caused by soft tissue stricture surrounding the esophageal lumen. The tube esophagostomy, combined anterograde retrograde esophageal assessment, and endoscopic balloon dilation were sequentially applied for the stricture lesion, along with the critical care for the secondary complications. After treatment, the foal was allowed to eat ground feed, chopped hay, and milk, and showed improved vitality. The foal was discharged on post-admission day 35.

Received: 7 August 2023
Accepted: 16 April 2024

Introduction

Esophageal stricture (ES) is a common disorder in horses usually caused by external or internal trauma of the esophageal wall leading to narrowing of the lumen (1, 2). The primary clinical sign is deglutition related to fibrosis and scar tissue formation (2). The impaired passage in the esophagus is manifested by ptyalism, coughing, dysphagia, and regurgitation with complications including aspiration pneumonia, esophageal diverticula, and inflammation (1, 3) . Three types of strictures are recognized, affecting the types of treatment and prognosis (1, 4) : type I, lesions involving the tunica muscularis and adventitia; type II, cicatrix or fibrous rings involving the mucosa and submucosa; type III, strictures involving all layers of the esophageal wall.

Along with the physical examination, several diagnostic tools, such as endoscopy, ultrasonography, and radiography, can be used for esophageal evaluation (4, 5). Surgical interventions and alternative therapies, such as balloon dilation, have been applied for existing strictures (1, 6) . The use of balloon dilation is most recently described in equine medicine, and it offers relatively safe and successful outcomes without complications in other methods (2, 5, 7) . On the other hand, the overall prognosis of ES is guarded, especially in foals less than one year of age, because of the high rate of recurrence and concurrent esophageal diseases (3, 6, 7).

Pneumonia caused by the intracellular bacterium *Rhodococcus equi* (*R. equi*) is a significant cause of disease and death in foals (8, 9) . The distribution of *R. equi* is worldwide, and infection occurs by the inhalation of dust contaminated with virulent *R. equi* (8, 9). It is unknown why some foals suffer *R. equi* infection with or without clinical findings, while some do not (10-12) . According to the epidemiological data in the US, clinical finding are observed in 10–20% of foals in endemic farms, but ultrasonographic evidence of

lung abscessation have been reported to vary between 30% and 60% (10-13). Moreover, extrapulmonary disorders are not such rare as was believed (10). Immunocompromised hosts are highly susceptible to *R. equi*, leading to opportunistic and complicated pneumonia with clinical signs, such as cough, fever, lethargy, and increased effort and rate of respiration (8).

This paper reports a case of complete ES in a one-month-old Thoroughbred foal with *R. equi* pneumonia. A tube esophagostomy was performed before balloon dilation 1) to use combined anterograde and retrograde esophageal endoscopy to assess the stricture lesion from both sides, 2) to use tube esophagostomy for enteral nutritional support, and 3) to make time for endoscopic balloon wire preparation. This article describes the sequential therapies and critical care process as well as the limitations of the case, expanding the current knowledge for ES and related considerations in horses.

Case Presentation

A one-month-old, 95 kg male Thoroughbred foal was referred for the clinical signs of coughing, nasal discharge, phlegm, regurgitation, and lethargy. According to the owner and referring veterinarian, the respiratory symptoms were recognized more than 10 days before presentation and became gradually aggravated despite receiving symptomatic treatment, including a nonsteroidal anti-inflammatory drug (NSAID; flunixin meglumine, 1.1 mg/kg, IV) and antibiotics (procaine penicillin G, 22,000 IU/kg, IM).

A physical examination of the horse revealed a heart rate of 84 beats/min, a body temperature of 38.8 °C, and a respiratory rate of 60 breaths/min with green-milky nasal discharge, mild depression, and bilateral crackling sound on lung auscultation. In the laboratory analysis, neutrophilia (12.47 × 10^9/L; reference range 2.3–9.5 × 10^9/L), hyperglycemia (114 mg/dL; reference range 65–110 mg/dL), hypocalcemia (10.8 mg/dL; reference range 11.5–14.2 mg/dL), elevation of total bilirubin (2.3 mg/dL; reference range, 0.5–2.3 mg/dL) and gamma-glutamyl transferase (35 U/L; reference range, 5–24 U/L), and insufficient passive immune transfer (IgG < 400 mg/dL; reference range, > 800 mg/dL).

On diagnostic endoscopy, a yellowish-white fluid, presumably a milky mixture, was visible in the upper respiratory tract and trachea (Figure 1A). Further esophagoscopy revealed a complete esophageal obstruction caused by soft tissue stricture surrounding the lumen (Figure 1B). Cervical ultrasonography confirmed the location and size of the stricture, which was located at the level of the 3rd cervical vertebra with a diameter of 1.1 cm and length of 2 cm (Figures 1C, D). The normal cervical esophagus is not visible on plain radiographs; however, using negative-contrast radiography with air insufflation, we could identify the esophagus. The absence of air shadows beyond the ES lesion confirmed a complete obstruction (Figure 1E). In ultrasonography and contrast radiography, there was no change in the diameter of the esophagus, and the most significant changes were observed in the mucosa and submucosa, while the adventitia remained intact (Figure 1C, D, E). Based on these findings, it was inferred to be a type II stricture. In thoracic radiography, the outline of the caudal vena cava and caudal silhouette of the heart were obscured by the caudoventral opacity, and multiple patchy opacities were observed in the entire lung (Figure 4A). Thoracic ultrasonography showed roughening of the pleural surface with multiple comet-tail artifacts. The subsequent laboratory microbiology analysis using trans-tracheal wash (TTW) fluid revealed a positive *R. equi* result among nine respiratory disease-causing agents (IDEXX Reference Laboratories, USA).

Based on the physical examination and imaging, complete ES with *R. equi* pneumonia was diagnosed. Owing to the difficulty of anterograde passage and feeding, tube esophagostomy was performed distal to the stricture to bypass the lesion for enteral nutritional supply and approach the stricture retrogradely. Under sedation and intravenous anesthesia (diazepam 0.1 mg/kg and ketamine 2.2 mg/kg), the foal was positioned in right lateral recumbency, and the surgical site was prepared aseptically. The flexible endoscope was first inserted anterogradely as a guide; the incision site was chosen around the level of the 3rd cervical vertebra. A linear skin incision, approximately 10 cm in length, was made ventral and parallel to the left jugular vein. The brachiocephalic and sternocephalic muscles were separated bluntly, and the carotid sheath was retracted to expose the esophagus. A 4 cm long longitudinal incision, approximately 3 cm distal to the stricture, was made through the esophagus using endoscopic transillumination as a guide for finding the lesion and incision site (Figures 2A, B). An endoscopy through an esophageal incision, the stricture lesion, and the remaining region distal to the stricture of the esophagus as well as the stomach were assessed endoscopically. After confirming no abnormalities except for the stricture site, the esophagostomy tube was inserted and secured to the skin with sutures and bandages (Figure 2C).

During the hospitalized period, the foal was treated with a nonsteroidal anti-inflammatory drug (flunixin meglumine, 1.1 mg/kg, IV, q12hr), antibiotics (ceftiofur, 2.2 mg/kg, IV, q24hr; azithromycin, 10 mg/kg, PO, q24hr; rifampin, 5 mg/kg, PO, q12hr), gastroprotectants (omeprazole, 4 mg/kg, PO, q24hr; ranitidine 6.6 mg/kg, IV, q8hr), and nebulization (fluticasone 2mg/kg, 10% acetylcysteine 3ml, gentamicin 2mg/kg, q12hr) with oxygen. For nutritional support, the foal received fluid (Hartmann's solution) and parenteral nutrition (OLIMEL® N9E, Baxter) under glucose monitoring until a tube esophagostomy was applied for nutritional supply. Because of the limited amount of mare's milk, commercial powdered goat's milk was supplied via the tube esophagostomy route. After the installation of an esophagostomy tube, feeding with milk was initiated at 1% of body weight

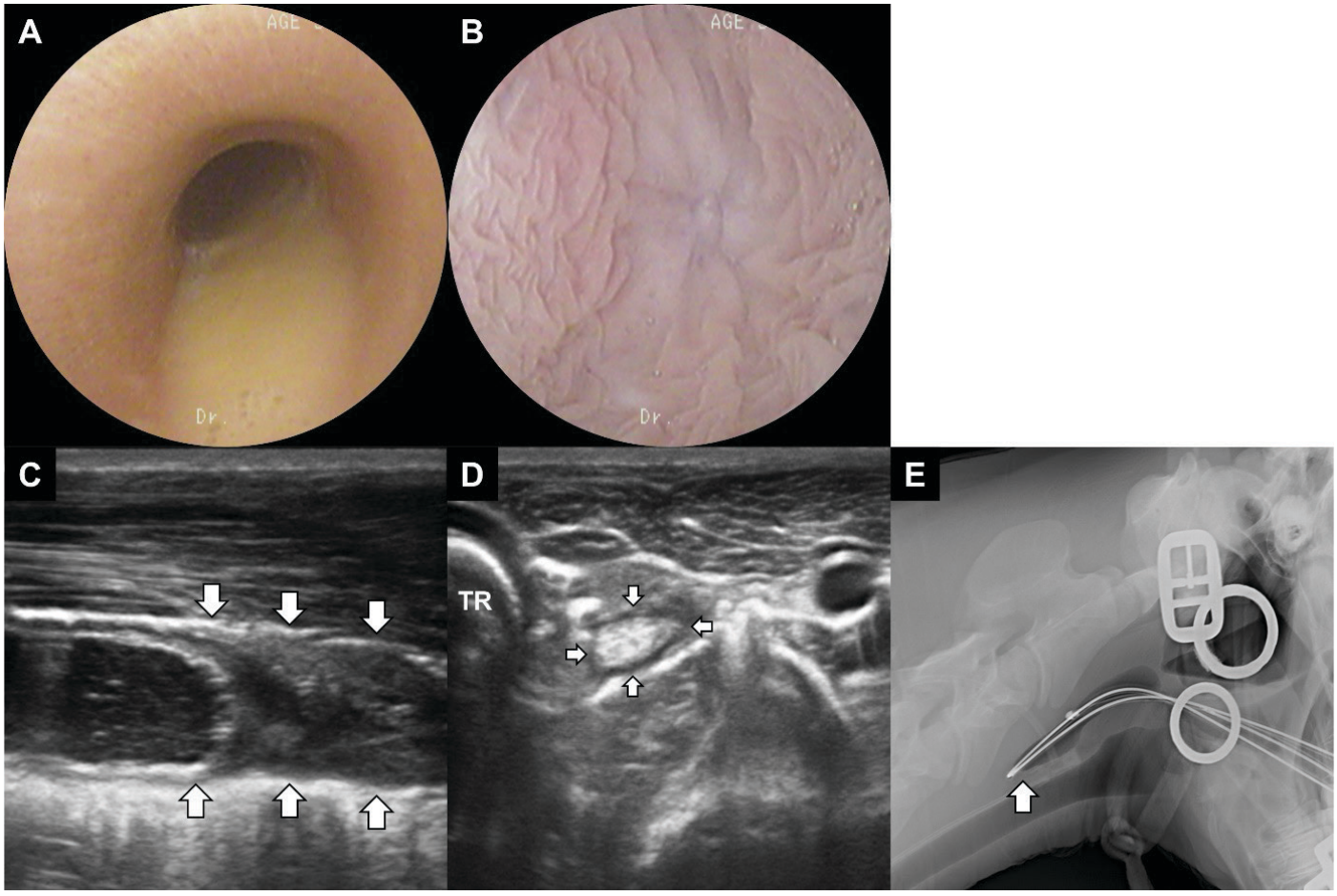

Figure 1: Endoscopic (A, B), ultrasonographic (C, D), and radiographic (E) images of the stricture lesion (white arrows) in the esophagus. (A) The trachea is filled with milky fluid. (B) The esophagus is entirely obstructed by the soft tissue stricture. (C, D) The longitudinal and transverse view of the stricture lesion on ultrasonography. TR indicates trachea. (E) Negative-contrast radiography through air insufflation was performed, confirming complete esophageal obstruction

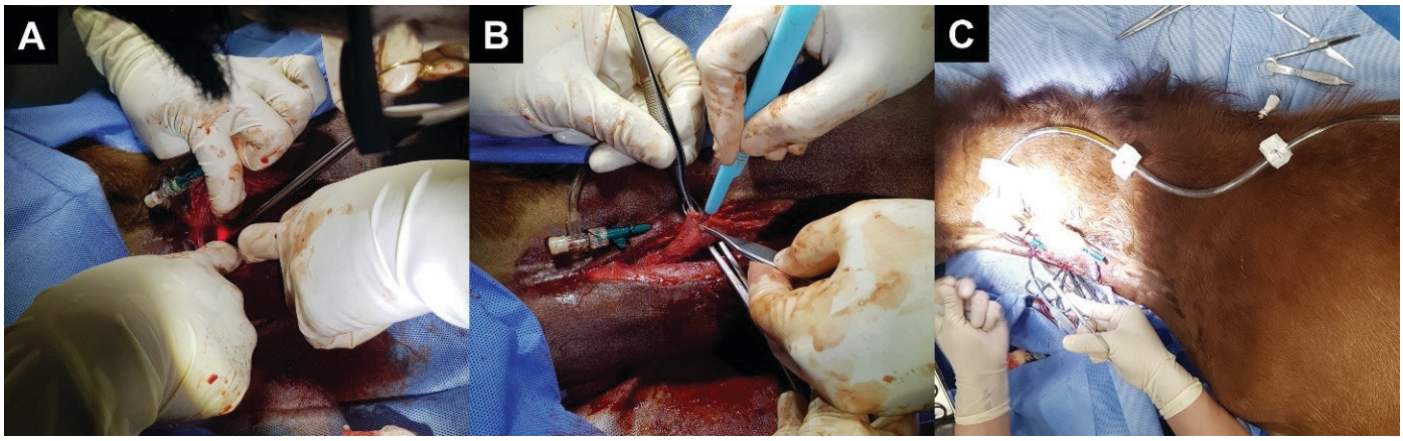

Figure 2: Surgical intervention for tube esophagostomy and retrograde assessment. (A) Endoscopic transillumination as a guide for finding lesions and the incision site. (B) Incision on the esophagus, approximately 3 cm distal to the stricture. (C) Esophagostomy tube application and securement for nutritional support

per day, and gradually increased over 10 days to 10% of body weight per day.

The complications during the treatment and enteral supply were diarrhea, fever, and weight loss. Despite the nutritional support, the foal lost 10% of body weight during the first week, but the diarrhea improved gradually, and the body weight soon increased slowly.

Seven days after presentation, endoscopic balloon dilation was performed using a controlled radial expansion wire-guided balloon catheter (CRE wire-guided dilator, Boston

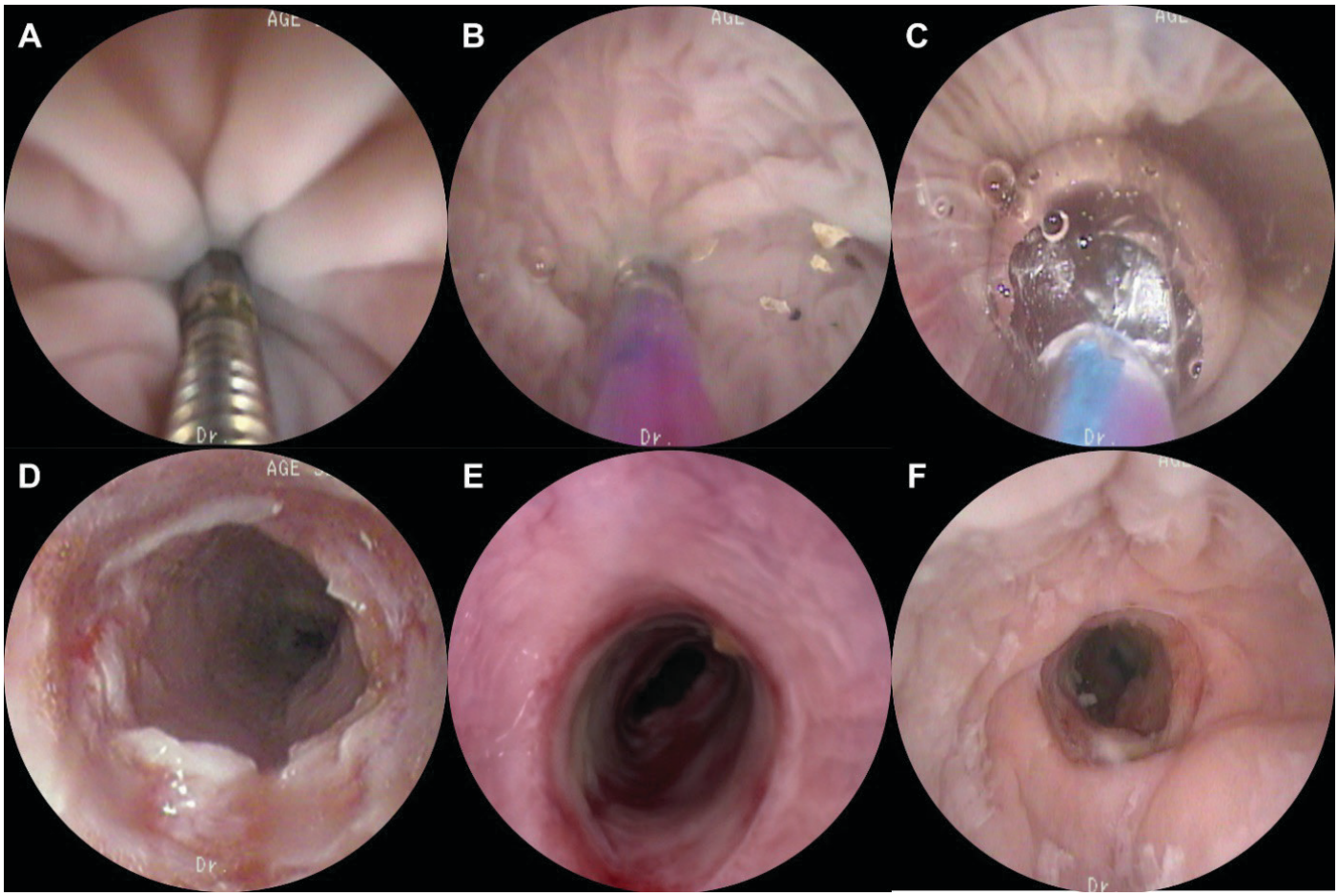

Figure 3: Endoscopic balloon dilation of the stricture lesion. (A) The stricture lesion was punctured using a biopsy wire for the balloon catheter placement. (B) The balloon catheter was placed into the stricture. (C) The balloon was inflated to reach the desired diameter stated by the manufacturer. (D) Widened esophageal lumen with mild bleeding immediately after the balloon dilation. (E) The stricture area six days post balloon dilation. (F) The stricture area 26 days post balloon dilation

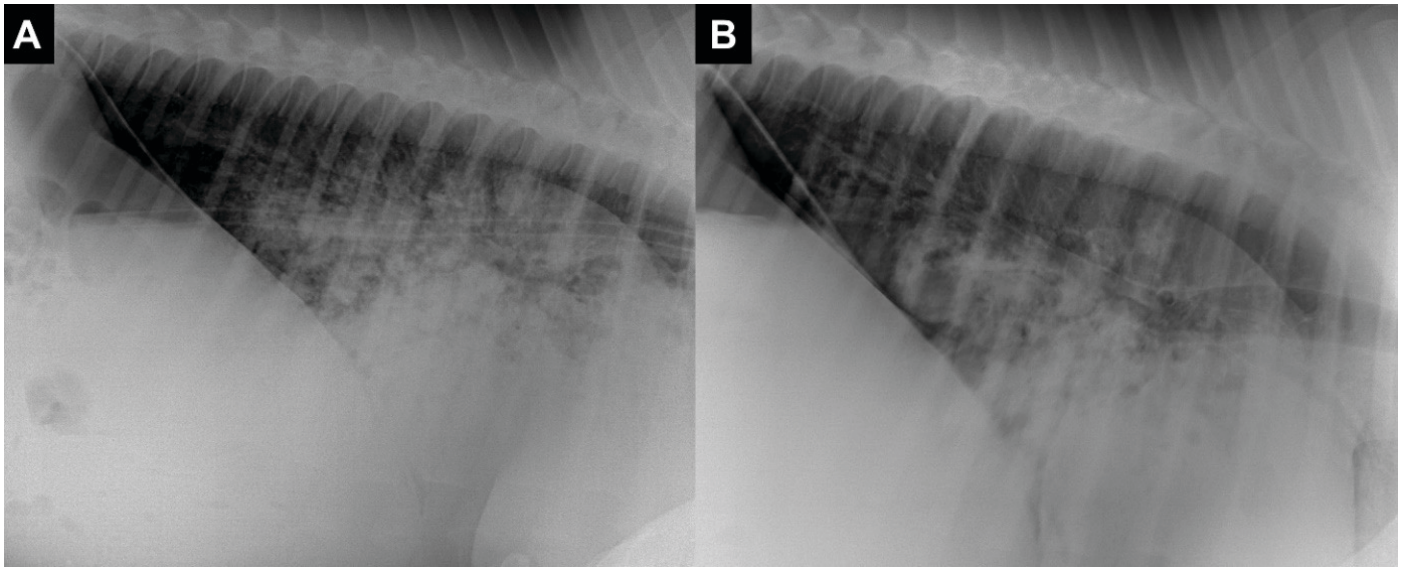

Figure 4: The radiographic image on pre- (A) and post-treatment (B) of the lung in this study. (A) The outline of the caudal vena cava and caudal silhouette of the heart were obscured due to the caudoventral opacity, and multiple patchy opacities were observed in the entire lung. (B) The patchy opacities in the lung and silhouette of the heart improved significantly after treatment (30 days post admission)

Scientific. Natick, MA, USA). The appropriate size of the balloon dilator was prepared based on the measured diameter and length of the stricture lesion. Initially, the stricture was punctured using a biopsy wire under visualization of the lesion with anterograde and retrograde esophagoscopy (Figure 3A). Subsequently, the balloon catheter was placed

into the stricture and inflated to reach the desired diameter according to the manufacturer's instructions (Figures 3B, C). The pressure and diameter of the balloon were maintained for 90 seconds with the high-pressure inflation device designed for balloon inflation and deflation (Encore 26 Inflator, Boston Scientific. Natick, MA, USA). After the procedure, the mucosa of the esophagus was closely evaluated (Figure 3D), and topical steroid injection (Triamcinolone, 1mg/site, total 6mg) into the submucosa was performed trans-endoscopically. The esophagostomy tube was removed, and a nasogastric tube was placed and secured for re-epithelialization and nutrition supply. The incision site of the tube esophagostomy was restored well without complications.

Six days after the first balloon dilation, the nasogastric feeding tube was removed, and the stricture lesion was assessed. The diameter of the stricture lesion was smaller than the adjacent normal tissue, and the scar tissue remained (Figure 3E). Subsequently, the foal was permitted to consume ground feed and chopped hay, in addition to commercial goat's milk formula, due to occasional coughing or regurgitation observed after the foal consumed a mass of grass. This dietary management was continued even after the foal was discharged. The second and third balloon dilation was also performed one week apart to widen the lesion, but it did not greatly affect the diameter. The diameter of the dilated lesion was maintained until discharge on post-admission day 35 (Figure 3F). The obscured heart silhouette and multiple patchy opacities in the lung radiography caused by aspiration and *R. equi* pneumonia were also improved (Figure 4B). On the other hand, in the long-term follow-up, the foal showed colic signs one month after discharge. The owner decided against further treatment and the foal was euthanized without referral for treatment or post-mortem necropsy.

Discussion

The primary causes of ES in equines include esophageal obstruction, trauma, nasogastric intubation, congenital defects, or complications following esophageal surgery (4, 6, 7). Strictures occur due to the formation of fibrous tissue and the deposition of collagen, which are stimulated by esophageal lesions (4, 6, 7). In human studies, peptic stenosis is identified as the most common cause of esophageal strictures, accounting for 70-75% of cases, resulting from gastric acid exposure (14-16). Other causes include the ingestion of caustic products, radiotherapy, foreign bodies, and infections (14-16). In this report, the precise cause of the ES is challenging to determine. However, considering that the lesion extensively covers a specific area of the esophagus and has progressed to complete obstruction, it is presumed that the lesion—potentially caused by trauma, impaction, peptic ulcer, or other factors—has developed into stenosis over a long period. Moreover, considering the horse's young age, the presence of a congenital lesion cannot be ruled out.

Despite the common occurrence of ES in horses and the several reports of successful applications of balloon dilation in stricture lesion in partial obstruction (5, 7, 17) , there are no reports on complete ES in equine cases. In humans, combined anterograde retrograde esophageal dilation (CARD) was used for complete ES through the gastrostomy tube and flexible endoscope (18, 19). Horses are suitable for applying CARD because the length of the equine neck is much longer than a human and the retrograde approach through esophagostomy is more straightforward than that through a gastrostomy. Therefore, CARD was applied in this case, and esophagostomy was used for the retrograde approach and nutritional support. This is the first case report regarding the application of CARD in equine species describing the sequence of surgical intervention and endoscopic dilation, post-operative care, and complications.

In general, the prognosis of ES in foals is poor (7, 20). The stricture and concurrent complications, including megaesophagus, aspiration pneumonia, and stricture recurrence, adversely affect the prognosis (4, 7, 20). In this study, the foal had *R. equi* pneumonia with insufficient passive immune transfer. The pneumonia caused by *R. equi* infection in Korea is assumed to be prevalent (21), aggravating the disease in immunocompromised foals. When the foals have symptoms of respiratory disease, the practitioners and owners often administer drugs targeting *R. equi* without conducting a thorough examination, leading to a delayed diagnosis of ES. In particular, foals less than one month old typically ingest mare's milk rather than solid food, and the symptoms caused by ES are not evident until the route is completely obstructed. The similarities of the respiratory signs caused by ES and an *R. equi* infection might result in a misdiagnosis and delay suitable treatment. Consequently, it is suggested that the practitioners include ES in a differential diagnosis of respiratory disease in foals for the early detection of ES to achieve a better prognosis. In addition, large-scale investigations regarding the *R. equi* epidemiology in Korea are warranted for managing the current situation of *R. equi* infections, which have never been conducted.

While it is difficult to attribute the impact of *R. equi* pneumonia directly on ES, it is evident that *R. equi* combined with complications such as aspiration pneumonia, nutritional deficiency, and stress caused by ES, worsened the patient's prognosis, highlighting the importance of critical care. To meet the primary nutritional needs resulting from complete esophageal obstruction, an esophagostomy was performed initially to create a bypass for nutrient delivery. Additionally, to prevent aspiration pneumonia and secondary infections commonly associated with ES, broad-spectrum, third-generation cephalosporin (ceftiofur) was administered. The pneumonia caused by biofilm-forming bacteria *R. equi* can exacerbate respiratory symptoms and

increase mortality rates in foals, so a combination of antibiotics (azithromycin, rifampin) targeting these pathogens was used. Considering that stimulation by gastric acid is a major contributing factor to ES (15, 16), antacids, including a proton pump inhibitor (omeprazole) and an H2 blocker (ranitidine), were administered throughout the period of hospitalization. Addressing pneumonia alongside ES is crucial for improving the survival rates of young foals, leading to the administration of nebulization containing antibiotics (gentamicin), steroid (fluticasone), and mucolytic agent (acetylcysteine) as well as intravenous NSAID (flunixin meglumine). Although TTW results did not identify significant pathogenic bacteria other than *R. equi*, a broad spectrum of medications was deemed necessary to counteract the potential lethality of infections and inflammations in immunocompromised young foal in this case. The horse's condition was closely monitored, with regular blood tests to detect any potential side effects.

Dilation of the esophagus is a relatively high-risk procedure, and there are no guidelines for clinicians in veterinary medicine on how to perform the practice safely. Although the authors referred to the guidelines for humans and previous animal case studies (4, 5, 7, 17, 22, 23) , the scarcity of resources available for complete ES in horses presents several limitations for optimal care, particularly for young foals. First, there is no grading system and treatment protocols to assess the condition of the ES beneficial for selecting a proper treatment to deal with the emergency. The degree of severity and progression could not be rated in the present case and consequently there were limitations to the process of the treatments for a favorable prognosis. Second, an in-depth examination, such as histopathology and cross-sectional imaging (CT), could not be included during the procedure to exclude malignancies, as in human protocols, because of the cost and lack of resources (22). Lastly, the lack of experience and knowledge by veterinarians and owners can result in a delayed diagnosis and mistreatment. Thus, regular education and system establishment for suitable care are necessary for the horse industry.

Conclusions

In conclusion, this is the first case report of complete ES in a one-month-old Thoroughbred foal with *R. equi* pneumonia. This paper described the sequential therapies and critical care process as well as the limitations of the case, expanding the current knowledge of ES and the related considerations in horses. The data will benefit practitioners and owners by contributing to a better understanding of ES in the foals.

Acknowledgments

The authors thank all KRA staffs who participated in this study.

Conflict of Interest. The authors declare no conflicts of interest..

Author contributions. Conceptualization: J Yoon, and T Park; Data curation: J Yoon, A Kim, YB Kwak, and J Lee; Formal analysis: J Yoon; Resources: A Kim, and J Lee; Supervision: I-S Choi, and T Park; Validation: J Yoon, I-S Choi, and T Park; Visualization: J Yoon; Writing-original draft: J Yoon; Writing-review & editing: J Yoon, YB Kwak, and T Park.

References

1. Auer JA, eds. Equine Surgery. 5th ed. St. Louis: Elsevier, 2018.
2. Southwood LL. Complications of esophageal surgery. In: Rubio-Martinez LM, eds. Complications in equine surgery. Hoboken: 2021: 254–64.
3. Chiavaccini L, Hassel D. Clinical features and prognostic variables in 109 horses with esophageal obstruction (1992–2009). J Vet Intern Med 2010; 24(5): 1147–52. doi: 10.1111/j.1939-1676.2010.0573.x
4. Waguespack RW, Bolt DM, Hubert JD. Esophageal strictures and diverticula. Compend Equine Contin Educ Vet 2007; 4: 194–207.
5. Nijdam P, Elmas C, Fugazzola M. Treatment of an esophageal stricture in a 1-month-old Miniature Shetland colt. Case Rep Vet Med 2017; 17(1): 3069419. doi: 10.1155/2017/3069419
6. Freeman DE. Surgery for obstruction of the equine oesophagus and trachea. Equine Vet Edu 2005; 17(3): 135–41.
7. Prutton J, Marks SL, Aleman M. Endoscopic balloon dilation of esophageal strictures in 9 horses. J Vet Intern Med 2015; 29(4): 1105–11. doi: 10.1111/jvim.13572
8. Bordin AI, Huber L, Sanz MG, Cohen ND. Rhodococcus equi foal pneumonia: update on epidemiology, immunity, treatment and prevention. Equine Vet J 2022; 54(3): 481–94. doi: 10.1111/evj.13567
9. Giguère S, Cohen MD, Chaffin MK, et al. Rhodococcus equi: clinical manifestations, virulence, and immunity. J Vet Intern Med 2011; 25(6): 1221–30. doi: 10.1111/j.1939-1676.2011.00804.x
10. Rakowska A, Marciniak-Karcz A, Bereznowski A, Cywinska A, Żychska M, Witkowski L. Less typical courses of Rhodococcus equi infections in foals. Vet Sci 2022; 9(11): 605. doi: 10.3390/vetsci9110605
11. Rakowska A, Cywinska A, Witkowski L. Current trends in understanding and managing equine rhodococcosis. Animals (Basel) 2020; 10(10): 1910. doi: 10.3390/ani10101910
12. Giguère S, Cohen ND, Chaffin MK, et al. Diagnosis, treatment, control, and prevention of infections caused by Rhodococcus equi in foals. J Vet Inter Med 2011; 25(6): 1209–20. doi: 10.1111/j.1939-1676.2011.00835.x
13. Chaffin MK, Cohen ND, Martens RJ. Evaluation of equine breeding farm management and preventative health practices as risk factors for development of Rhodococcus equi pneumonia in foals. J Am Vet Med Assoc 2003; 222(4): 476–85. doi: 10.2460/javma.2003.222.476
14. Hernández JM, Arias SP, Franz CAC, Mejía MV. Dilation of a proximal esophageal stricture by endoscopically and radiologically guided Balloon in a falabella foal. Rev Med Vet 2016; 31: 85–95.
15. Ferguson D. Evaluation and management of benign esophageal Strictures. Dis Esophagus 2005; 18(6): 359–64. doi: 10.1111/j.1442-2050.2005.00516.x
16. Egan JV, Baron TH, Adler DG, et al. Esophageal Dilation. Gastrointest Endosc 2006; 63(6): 755–60. doi: 10.1016/j.gie.2006.02.031

17. Chidlow HB, Robbins EG, Slovis NM. Balloon dilation to treat oesophageal strictures in five foals. Equine Vet Edu 2017; 29(11): 609–16. doi: 10.1111/eve.12538

18. Fowlkes J, Zald PB, Andersen P. Management of complete esophageal stricture after treatment of head and neck cancer using combined anterograde retrograde esophageal dilation. Head Neck 2012; 34(6): 821–5. doi: 10.1002/hed.21826

19. Bueno R, Swanson SJ, Jaklitsch MT, Lukanich JM, Mentzer SJ, Sugarbaker DJ. Combined antegrade and retrograde dilation: a new endoscopic technique in the management of complex esophageal obstruction. Gastrointest Endosc 2001; 54(3): 368–72. doi: 10.1067/mge.2001.117517

20. Craig DR, Shivy DR, Pankowski RL, Erb HN. Esophageal disorders in 61 horses: results of nonsurgical and surgical management. Vet Surg 1989; 18(6): 432–8. doi: 10.1111/j.1532-950x.1990.tb01120.x

21. Song KO, Yang HS, Son WG, Kimm JH. Pathologic characteristics for the Rhodococcus equi infection in foals in Jeju. Korean J Vet Res 2019; 59(3): 141–9. doi: 10.14405/kjvr.2019.59.3.141

22. Sami SS, Haboubi HN, Ang Y, et al. UK guidelines on oesophageal dilatation in clinical practice. Gut 2018; 67(6): 1000–23. doi: 10.1136/gutjnl-2017-315414

23. Tillotson K, Traub-Dargatz JL, Twedt D. Balloon dilation of an oesophageal stricture in a one-month-old Appaloosa colt. Equine Vet Edu 2003; 15(2): 67–71. doi: 10.1111/j.2042-3292.2003.tb00218.x

Endoskopska in kirurška obravnava popolne strikture požiralnika pri enomesečnem čistokrvnem žrebetu s pljučnico, povzročeno z *Rhodococcus equi*

J. Yoon, A. Kim, J. Lee, Y.B. Kwak, I. Choi, T. Park

Izvleček: V poročilu o primeru je opisana kirurška in endoskopska obravnava popolne strikture požiralnika pri enomesečnem čistokrvnem žrebetu s pljučnico, povzročeno z *Rhodococcus equi* (*Rhodococcus equi* pneumonia). Klinični simptomi so bili kašelj, izcedek iz nosu, regurgitacija in letargija. Endoskopska in ultrazvočna preiskava je pokazala popolno obstrukcijo požiralnika, ki jo je povzročila striktura mehkih tkiv okoli lumna požiralnika. Za zdravljenje strikture smo zaporedno izvedli cevno ezofagostomo, kombinirano anterogradno retrogradno oceno požiralnika in endoskopsko balonsko dilatacijo skupaj s kritično oskrbo sekundarnih zapletov. Po zdravljenju je žrebe lahko jedlo mleto krmo, rezano seno in mleko, njegova vitalnost pa se je izboljšala. Žrebe je bilo odpuščeno 35. dan po sprejemu.

Ključne besede: balonska dilatacija; žrebe; ezofagealna striktura; ezofagostoma; pljučnica

Table of Content